

**In compliance with the
Canadian Privacy Legislation
some supporting forms
may have been removed from
this dissertation.**

**While these forms may be included
in the document page count,
their removal does not represent
any loss of content from the dissertation.**

Synthesis and Self-Assembly of Polymers Containing Dicarboximide Groups by Living Ring-Opening Metathesis Polymerization

By

Jake Dalphond

Department of Chemistry
McGill University, Montréal

A thesis submitted to the Faculty of Graduate Studies and Research of McGill University
in partial fulfillment of the degree of Master of Science

Submitted October, 2002
© Jake Dalphond, 2002



National Library
of Canada

Bibliothèque nationale
du Canada

Acquisitions and
Bibliographic Services

Acquisisitons et
services bibliographiques

395 Wellington Street
Ottawa ON K1A 0N4
Canada

395, rue Wellington
Ottawa ON K1A 0N4
Canada

Your file *Votre référence*
ISBN: 0-612-88178-4
Our file *Notre référence*
ISBN: 0-612-88178-4

The author has granted a non-exclusive licence allowing the National Library of Canada to reproduce, loan, distribute or sell copies of this thesis in microform, paper or electronic formats.

L'auteur a accordé une licence non exclusive permettant à la Bibliothèque nationale du Canada de reproduire, prêter, distribuer ou vendre des copies de cette thèse sous la forme de microfiche/film, de reproduction sur papier ou sur format électronique.

The author retains ownership of the copyright in this thesis. Neither the thesis nor substantial extracts from it may be printed or otherwise reproduced without the author's permission.

L'auteur conserve la propriété du droit d'auteur qui protège cette thèse. Ni la thèse ni des extraits substantiels de celle-ci ne doivent être imprimés ou autrement reproduits sans son autorisation.

Canada

Abstract

DNA is remarkable because of its highly selective molecular recognition properties and self-assembly behavior. Recent attempts in generating biomimetic synthetic polymers have been flawed by a lack of structural control. To overcome this shortcoming, we generated molecular recognition polymers and copolymers containing a regioselective arrangement of thymine/uracil analogs via Ring-Opening Metathesis Polymerization (ROMP). The ROMP of *exo*-7-oxabicyclo[2.2.1]hept-5-ene-2,3-dicarboximide was found to fulfill the criteria for a living polymerization. This gave access to polymers with narrow molecular weight distribution and well-controlled architecture. Furthermore, the living character of the reaction allowed for the facile synthesis of diblock copolymers. We have synthesized diblock copolymers containing a small hydrophilic block bearing molecular recognition units and a longer hydrophobic block consisting of long pendant alkyl chains. These copolymers undergo self-assembly into nanoscale aggregates with surface localized multi-point hydrogen bonding sites. Finally, molecular recognition properties of monomers and polymers containing the thymine/uracil analogs were characterized by ¹H NMR and HPLC.

Résumé

L'ADN est doté de propriétés de reconnaissance moléculaire exceptionnelles ainsi qu'un potentiel pour l'auto-assemblage. La plupart des polymères synthétiques générés pour rivaliser les propriétés de l'ADN ne possèdent pas de structures bien définies. Nous avons utilisé la polymérisation par ouverture de cycle par métathèse (ROMP) afin d'inclure des unités de reconnaissance moléculaire (analogues de thymine et uracil) de façon régiosélective à l'intérieur de polymères et copolymères à blocs. La polymérisation de *exo*-7-oxabicyclo[2.2.1]hept-5-ene-2,3-dicarboximide par ROMP s'est révélé de nature *vivante*. Ceci nous permet donc d'obtenir des polymères possédant une étroite distribution de masses moléculaires ainsi qu'un accès facile à plusieurs copolymères à blocs. Nous avons synthétisé des copolymères à blocs munis d'une courte chaîne hydrophilique (dotée d'unités de reconnaissance moléculaires) et d'une longue chaîne hydrophobique. Ces copolymères s'auto-assemblent en nanosphères possédant une surface entièrement recouverte d'unités de reconnaissance moléculaire. Les propriétés de reconnaissance moléculaire des monomères et polymères ont été analysées grâce à la spectroscopie RMN ^1H et la chromatographie HPLC.

Acknowledgements

I would like to greatly acknowledge the support and enthusiasm of my research supervisor, Professor Hanadi F. Sleiman, who showed me that good ideas can go a very long way (and sometimes lead to a publication). I would also like to thank my labmates, Debbie Mitra, Felaniaina Rakotondradany, Mohammed Slim, Jean Bouffard (who contributed to the HLPC studies), and especially Hassan S. Bazzi for helping me with the many facets of my project. Thank you all for the good times we had in the lab.

Many thanks to the Eisenberg research group, especially Carl Bartels for the help with the DLS and Dr. A. Eisenberg for his great knowledge of polymer self-assembly. I would also like to acknowledge Dr. H. Vali and Jeannie for help with TEM studies.

I am grateful to my parents for supporting me, thank you for your words of encouragement and for the financial support. Many thanks go to my girlfriend, Carolina, for her patience and attention during those two years.

Contribution of the Authors

Authors of *Macromolecular Chemistry and Physics*, **2002**, 203, 1988:

Jake Dalphond

I carried out the monomer, polymer and copolymer synthesis and optimized the polymerization procedure. In addition, I carried out the polymer and copolymer characterization, which includes: DLS, FTIR, GPC, NMR, and TEM.

Hassan S. Bazzi

He initiated the project by studying the Ring-Opening Metathesis Polymerization of monomer **1** and **6**. He contributed in establishing that the polymers and copolymers could be obtained in a controlled manner. In addition, he helped in finding a proper solvent system for copolymer self-assembly.

Kenza Kahrim

As part of her summer project, she assisted Hassan S. Bazzi in synthesizing the monomers and polymers described in the paper.

Hanadi F. Sleiman

As my research supervisor, Professor Sleiman helped me plan every step of the project and helped in solving problems associated with every aspect of this work. Our biomimetic polymer would not exist without her precious advice.

Table of Contents

Abstract	II
Résumé	III
Acknowledgements	IV
Contribution of the Authors	V
Table of Content	VI
Glossary of Symbols and Abbreviations	IX
Chapter 1. Introduction	1
1.1 Ring-Opening Metathesis Polymerization	2
1.1.1 Alkene Metathesis Catalysts	2
1.1.2 Alkene Metathesis Mechanism	4
1.1.3 Living Character of the ROMP Reaction	6
1.1.4 Addition of Phosphine to ROMP Reactions	7
1.1.5 Second Generation ROMP Catalyst	8
1.1.6 Recent Advances in Biologically Relevant ROMP Polymers	10
1.2 Molecular Recognition in Polymer Assemblies	13
1.2.1 Supramolecular Chemistry	13
1.2.2 Hydrogen Bonding	14
1.2.3 DNA Properties	14
1.2.4 Synthetic Receptors	16
1.2.5 Monomeric Receptors	17
1.2.6 Polymeric Receptors	18
1.2.7 Modulation of Molecular Recognition Properties	20
1.2.8 Polymer Blends	21
1.2.9 Microenvironment Favoring Hydrogen Bonding	24
1.3 Self-Assembly of Asymmetric Block Copolymers	25
1.3.1 Spherical Crew-Cut Micelles	26
1.3.2 Multiple Crew-Cut Morphologies	27
1.3.3 Thermodynamic Considerations	29
1.3.4 Large Compound Micelles	30
Chapter 2. Purpose of Research	32
2.1 Research Goals	32
2.2 Target Monomers	33
2.3 Synthetic Strategy of Monomers	34
2.3.1 Synthesis of Exo-7-oxabicyclo[2.2.1]hept-5-ene-2,3-dicarboximide and N-methyl and N-phenyl analogs	34
2.3.2 Synthesis of Exo-N-butyl-7-oxabicyclo[2.2.1]hept-5-ene-2,3-dicarboximide and Exo-N-decyl-7-	34

oxabicyclo[2.2.1]hept-5-ene-2,3-dicarboximide	
2.4 Synthetic Strategy of Polymers and Diblock Copolymers	35
2.4.1 Homopolymer General Synthesis	35
2.4.2 Diblock Copolymer General Synthesis	35
2.5 Self-Assembly Studies	36
2.6 Molecular Recognition Studies	
2.6.1 Monomer and Complementary Molecules	37
2.6.2 Polymer and Complementary Molecules	38
3. Experimental Procedures	40
3.1 General Considerations	40
3.2 Monomer Synthesis	41
3.3 Polymer Synthesis	43
3.4 ROMP Kinetic Experiment	48
3.5 Self-Assembly Studies	48
3.6 Hydrogen Bonding Studies	49
3.7 Guest Synthesis	51
3.8 Attempted Synthesis	51
4. Results and Discussions	55
4.1 Monomer synthesis	55
4.2 Polymer Synthesis and Characterization	58
4.2.1 Biomimetic Homopolymer	58
4.2.2 Biomimetic Block Copolymer	60
4.3 Self-Assembly Studies of the Biomimetic Copolymer	62
4.3.1 Self-Assembly in THF-Water Solvent System	62
4.3.2 TEM Staining Experiments	64
4.3.3 Self-assembly in Other Solvent Systems	65
4.4 Molecular Recognition Properties	67
4.4.1 Molecular Recognition between Monomer and Guest Molecules	67
4.4.2 Molecular Recognition between Polymers and Guest Molecules	69
4.4.2.1 Direct NMR Characterization	69
4.4.2.2 Indirect NMR Characterization	72
4.4.2.3 Indirect HPLC Characterization	77
4.5 Additional Polymer Systems	80
4.5.1 Synthesis and Behavior of N-Methyl Containing Polymers	80
4.5.2 Synthesis and Behavior of N-Phenyl Containing Polymers	81
4.5.3 Synthesis and Behavior of N-Alkyl Containing Polymers	85

5. Conclusion	89
6. References	91
Appendices I: Publication	99

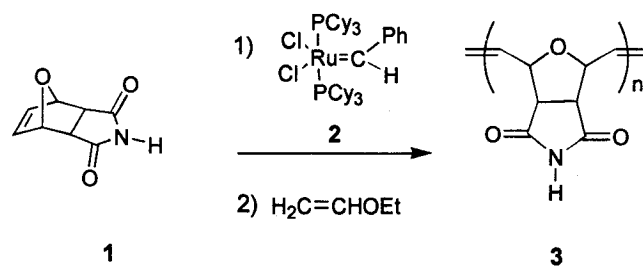
Glossary of Symbols and Abbreviations

- 2,6-DAP: 2,6-diaminopyridine
- A: adenine
- Å: angstroms
- Ac: acetyl
- ADMET: acyclic diene metathesis
- Bu: butyl
- °C: degree Celsius
- C: cytosine
- Ca.: approximately
- CHCl₃: chloroform
- CH₂Cl₂: dichloromethane
- Da: daltons
- DLS: dynamic light scattering
- DMF: dimethyl formamide
- DMSO: dimethyl sulfoxide
- DNA: deoxyribonucleic acid
- e.g. : for example
- Equiv.: equivalents
- Et: ethyl
- FTIR: Fourier transform infra-red
- G: guanine
- GPC: gel permeation chromatography
- HPLC: high performance liquid chromatography
- i.e.: that is
- Kcal: kilocalory
- k_i: rate of initiation
- k_p: rate of propagation
- LCM: large compound micelles
- Me: methyl
- Mes: mesityl

Min.: minute
Mmol: millimole
 M_n : average number molecular weight
Mol: mole
N: normal
Nm: nanometer
NMR: nuclear magnetic resonance
P4VP.MeI: poly(4-vinylpyridinium methyliodide)
PAA: poly(acrylic acid)
PDI: polydispersity index
Ph: phenyl
PR₃: phosphine ligand
PS: polystyrene
ROMP: ring-opening metathesis polymerization
T: thymine
TEM: transmission electron microscopy
THF: tetrahydrofuran
TMS: tetramethylsilane
U : uracil
vs.: versus

Chapter 1. Introduction

The ring-opening metathesis polymerization (ROMP) currently occupies a central role as an efficient method to generate functional polymers of narrow molecular weight distribution.^{1,2} In particular, with the development of highly active and functional group-tolerant ruthenium catalysts (e.g., Grubbs catalyst **2**¹), the scope of this reaction has recently been extended to biologically relevant polymers with increasingly complex functionalities, such as carbohydrates,^{3,4} peptides,⁵ nucleic acid bases,⁶ antitumor compounds⁷ and oligonucleotides.⁸ Importantly, due to the living nature of the ROMP reaction, this method has also been employed to give efficient access to a wide range of block copolymers.⁹ When containing asymmetric blocks of different solubility, these polymers can undergo self-organization into nanometer-scale micellar aggregates of spherical, lamellar, cylindrical, vesicular and other morphologies, with the functional blocks located in segregated domains.¹⁰



Equation 1: ROMP of monomer **1**

A particularly attractive molecule for incorporation into ROMP polymers and block copolymers is *exo*-7-oxabicyclo[2.2.1]hept-5-ene-2,3-dicarboximide **1**. (Equation 1) As a monomer, this molecule has shown antitumor activity, and its N-substituted derivatives are potent phosphatase inhibitors.^{11,12} Furthermore, addition polymers of this molecule have also exhibited significant antitumor activity, and have been demonstrated to be less cytotoxic than monomer **1**.¹¹

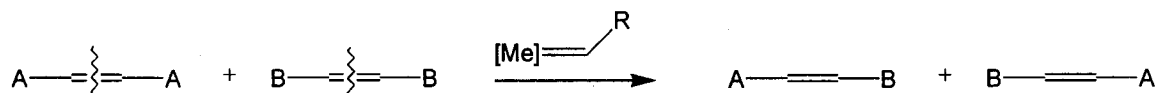
Importantly, the dicarboximide moiety in **1** possesses the same specific hydrogen-bonding characteristics as the nucleic acid bases thymine and uracil,^{13,14} making the unit well-suited for molecular recognition with complementary molecules. For instance, the dicarboximide unit can selectively bind adenine, and thus has the potential to bind to nucleic acids.^{15,16}

Monomer **1** has been previously polymerized using non-living methods.^{11,17} However, the synthesis of poly(**1**) using a living polymerization method as not yet been reported. A living polymerization of monomer **1** would result in polymers with controlled molecular weights and narrow molecular weight distributions, thus providing biologically relevant polymers with precisely known compositions and architectures.

The synthesis and self-assembly of ROMP block copolymers containing biologically active units could lead to novel polymers that would efficiently interface with biological systems. Here are presented the successful synthesis of monomer **1**, and a wide variety of polymers and copolymers incorporating this molecular recognition unit, their self-assembly into nanoscale morphologies, as well as exploratory studies on their molecular recognition properties.

1.1 Ring-Opening Metathesis Polymerization

1.1.1- Alkene Metathesis Catalysts



Equation 2

The alkene metathesis reaction involves the cleavage of C=C double bonds, followed by the formation of new alkene bonds. (Equation 2) Early work in this field was based on ill-defined, catalytically active mixtures of transition-metal chlorides, oxides and

oxychlorides with the need of cocatalysts such as R_4Sn ($R = Ph, Me, Et, Bu$), SiO_2 , Al_2O_3 , and $EtAlCl_2$ (e.g. WCl_6/Bu_4Sn , $WOCl_4/EtAlCl_2$, MoO_3/SiO_2 , Re_2O_7/Al_2O_3). Promoters were also often added to these mixtures (e.g. O_2 , $EtOH$ or $PhOH$).¹⁸

In the late 1980s and early 1990s, the research groups of R. Schrock and R. Grubbs pioneered the field by introducing highly active and well-defined metathesis catalysts bearing an alkylidene functionality.^{1,19} (Chart 1) The Grubbs catalyst **2** is based on a ruthenium alkylidene, while the Schrock catalyst **4** is based on molybdenum. These metal alkylidenes are structurally similar to $(CO)_5W(=CPh_2)$, the first reported isolable alkylidene based metathesis catalyst, which exhibited rather low activity.²⁰ These modern catalysts are quite advantageous by being highly active, thus eliminating the need for complex mixtures and cocatalysts. In addition, they can mediate various other metathesis reactions such as acyclic diene metathesis (ADMET) and ring closing metathesis.^{21,22} Both catalysts can be used to generate a wide range of polymers with narrow molecular weight distribution.^{1,2,19} Although the Schrock catalyst is known to be highly active, it lacks the functional group tolerance that distinguishes the Grubbs catalyst.

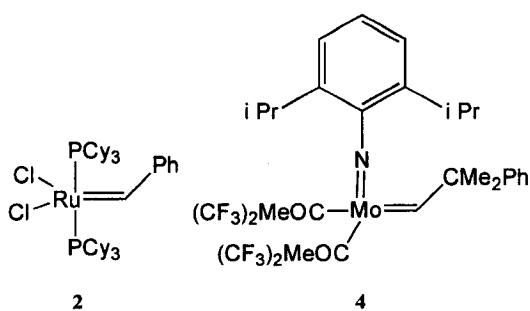
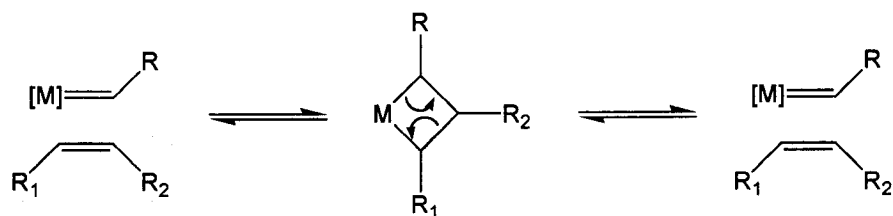


Chart 1

1.1.2- Alkene Metathesis Mechanism

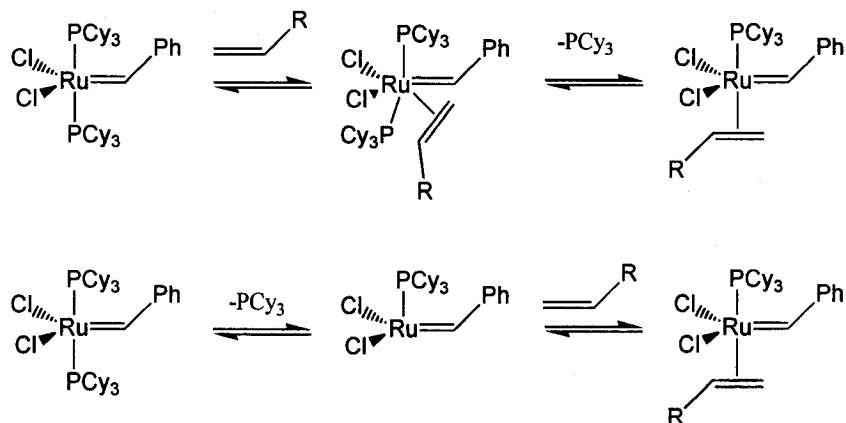


Scheme 1: Chauvin's mechanism

The general alkene metathesis mechanism was first proposed by Chauvin in 1970.²³ (Scheme 1) It involves the coordination of an olefin to the catalyst followed by a [2+2]cycloaddition leading to a metallacyclobutane intermediate, and a subsequent retro[2+2] reaction, thus forming a new alkene bond. The ring-opening metathesis polymerization (ROMP) reaction follows the same mechanistic trends. The main difference resides in the retro[2+2] reaction step, which leads to a progressive polymer chain growth.

Recently, Grubbs et al. elucidated the mechanistic details regarding the nature of the initiation step in ROMP using Grubbs ruthenium alkylidene catalyst.²⁴ For a number of years, the debate was based on the nature of the intermediate involved in the initiation step. Was the pathway associative or dissociative, thus favoring either an 18-electron intermediate or a 14-electron intermediate? The associative pathway involves binding of an olefin, generating a coordinatively saturated species (18-electron), followed by phosphine dissociation. On the other hand, the dissociative substitution proceeds by initial phosphine loss, thus generating a 14-electron species, with a subsequent olefin binding. (Scheme 2) Although an 18-electron intermediate seemed more likely, the group of Grubbs elegantly established that the initiation step was dissociative. This implied that

the intermediate was a 14-electron species and that the phosphine exchange played a major role in affecting the initiation rate of ROMP reactions.

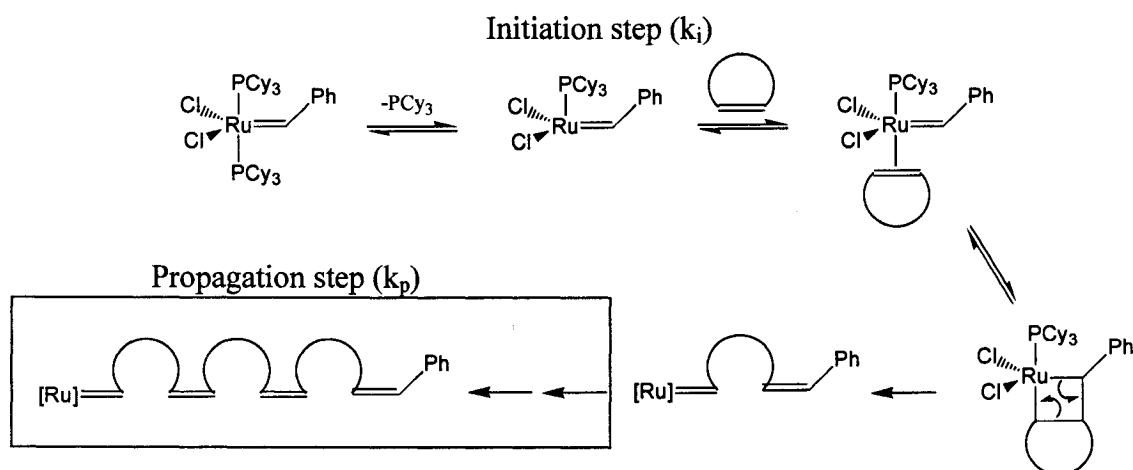


Scheme 2: ROMP mechanism: associative and dissociative initiation step

It was established that the rate determining step in the initiation process, which involves the initial substitution of phosphine with the olefinic substrate, was phosphine dissociation. In addition, phosphine dissociation is independent of phosphine concentration in solution. Both the entropy and enthalpy of activation were positive, strengthening the evidence for a dissociative pathway. Polymer chain propagation is carried out once the olefin binds to the 14-electron species. (Scheme 3) A [2+2]cycloaddition leads to the formation of a metallacyclobutane and the polymer chain is extended by the retro[2+2] reaction (or cycloreversion). Typically, only a few catalytic turnovers are carried out before the 14-electron active species returns to its resting state by coordinating free phosphine. Therefore, a catalyst that has an equal affinity for free phosphine and olefins will tend to carry out less catalytic turnovers than a catalyst with a high olefin affinity.

The investigation of the ROMP mechanism is crucial in increasing the efficiency of current catalyst, obtaining better control on the polymer end-result, as well as being

able to design and especially understand the behavior of the next-generation Grubbs catalysts. The objective of such studies is to design new metathesis catalysts with superior activity, stability and selectivity.



Scheme 3: The ROMP mechanism

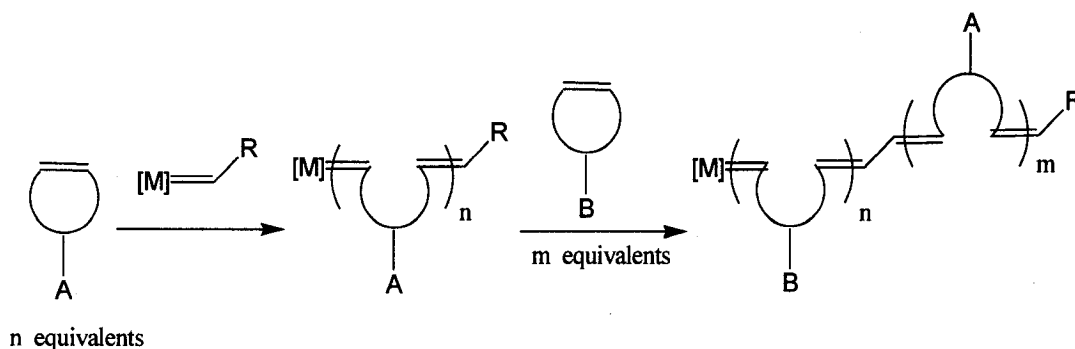
1.1.3- Living Character of the ROMP Reaction

The Grubbs catalyst offers many advantages as a catalyst for ring-opening metathesis polymerization. In addition to its functional group tolerance, it generally yields polymers with exceptionally low molecular weight distributions.^{1,2} This small polydispersity can be attributed to the living character of the ROMP reaction.

The living character of the ROMP reaction is due to the near absence of chain termination processes.²⁵ In order to obtain a living system that generates polymeric chains with an approximately equal number of repeating units, the rate of initiation (k_i) must be greater than the rate of propagation (k_p).²⁵ Under such conditions, all polymer chains will begin growing soon after the monomer is exposed to the catalyst (i.e. all chains start propagating at the same time), and chain growth (i.e. propagation) will be much slower. While most conventional polymerization methods such as free radical

polymerization involve rapid chain termination,²⁶ most polymerization initiated with the Grubbs catalyst will exhibit slow termination rates. A faster rate of initiation (vs. propagation) coupled to a slow rate of termination constitute the main characteristics of a living polymerization.

A living polymerization is necessary for generating well-defined diblock copolymers. The copolymerization using ROMP is a two-step, sequential procedure. (Scheme 4) Once the first monomer is entirely consumed, the second monomer is added and the polymerization continues, leading to the formation of a diblock copolymer with a well-defined and controlled architecture. This can only be achieved if the catalyst remains living throughout the entire reaction.

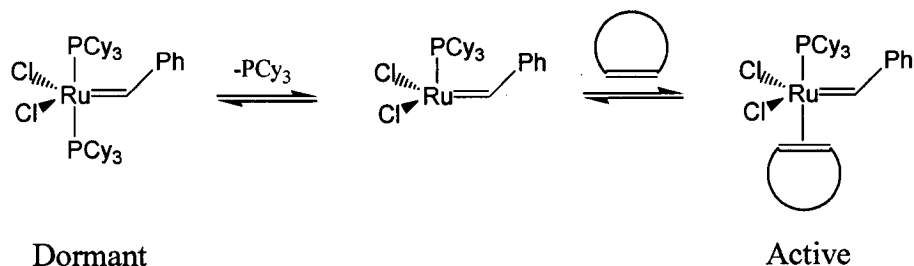


Scheme 4: Formation of a ROMP diblock copolymer

1.1.4- Addition of Phosphine to ROMP Reactions

By clearly identifying the mechanism in which the initiation step proceeds during ROMP reactions, it is possible to modulate the rate of propagation by adding excess phosphine to the system. The addition of phosphine in the reaction mixture does not affect the rate of initiation (k_i) (it is independent of $[PR_3]$). However, it will significantly slow down the propagation step by decreasing the number of catalytic turnovers that could occur before the active species returns to its resting state by re-coordinating free

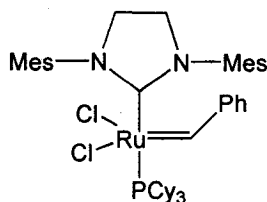
phosphine. (Scheme 5) Consequently, this will reduce the rate of propagation versus the rate of initiation.²⁷ The kinetic control allows for the generation of polymers with narrow molecular weight distribution; the smaller polydispersity index is most noticeable for monomers with high cyclic strain.



Scheme 5: Grubbs catalyst dormant/active species

1.1.5- Second Generation ROMP Catalyst

The classical Grubbs catalyst **2** has proven to be quite versatile and efficient for a wide range of monomers bearing different types of functionality such as alcohols, acids and ketones. Unfortunately to obtain a well-behaved system, these monomers are required to possess rings with a high degree of cyclic strain. This can be a limiting factor when designing functional monomers. The relief of cyclic strain acts as the reaction driving force, generating polymers with narrow molecular weight distribution. Low strain cycles, such as cyclooctene, cannot be polymerized in a controlled manner using the classical, first generation Grubbs catalyst **2**.²⁸ On the other hand, the Schrock catalyst **4** has been shown to be more active although less tolerant to air, moisture and various functional groups.^{19,29}



5

Recently, the research groups of Grubbs and Hermann synthesized a new ruthenium based metathesis catalyst **5** designed to rival the metathesis activity of the molybdenum based Schrock catalyst while retaining the remarkable stability and functional group tolerance characteristic of the benzylidene Grubbs catalyst **2**.^{22,30} This novel catalyst, containing a strong electron-donating N-heterocyclic carbene, was prepared from the classical Grubbs catalyst. A very high level of metathesis activity was observed for this second generation Grubbs catalyst. It is capable of ring-opening metathesis polymerization on monomers with low cyclic strain, which are otherwise inactive when exposed to the first generation Grubbs catalyst.^{28,31}

Initially, it was believed that the high level of activity obtained from this catalyst was due to a strong trans-effect caused by the N-heterocyclic carbene. The electron donating ligand was thought to enhance trans-phosphine dissociation, thus increasing the metathesis activity of the catalyst. In fact, phosphine dissociation is much slower for the second generation catalyst **5** compared to the first generation catalyst **2**.²⁴

The high activity level of this new catalyst was shown to be attributed to preferential olefin coordination.²⁴ The strong electron donating ligand leads to an electron rich metal center that will tend to bind to π -acidic olefins to reduce its electron density. The σ -donating phosphine dissociates quite slowly, but upon dissociation the active species that carries out the ROMP remains active for a longer period of time before returning to its resting state by reCOORDINATING free phosphine. This is due to improved selectivity for binding π -acidic olefins in the presence of phosphine. Consequently, olefin coordination followed by chain propagation can occur many times before the catalyst eventually returns to its passive state. This new feature greatly enhances the metathesis activity of the catalyst, but also greatly influences the molecular weight distributions of

the generated polymers. The slower rate of initiation and faster rate of propagation leads to polymers with larger molecular weight distribution.

As previously mentioned, in order to obtain a well-behaved and living polymer system, the rate of initiation (k_i) must be greater than the rate of propagation (k_p). In this particular case, initiation is slowed down due to slow phosphine dissociation and chain propagation is accelerated due to the catalyst affinity for binding olefins. Consequently, this leads to an unfavorable k_i/k_p ratio and polymers with broader molecular weight distributions are usually obtained.²⁴

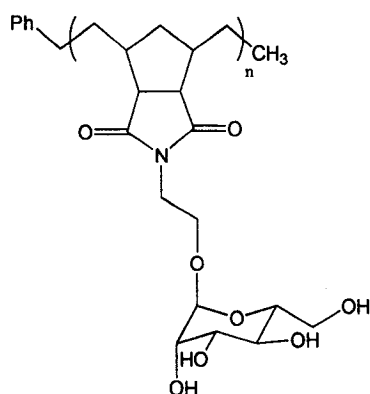
The high metathesis activity of the new catalyst can be useful if one plans to carry out the ROMP of low strain cyclic monomers, which would otherwise fail using the classical Grubbs catalyst **2**. In addition, certain amine containing monomers will quench the catalyst, resulting in an aborted polymerization. However, the second generation catalyst **5** can tolerate a wider array of functionalities due to its higher olefin affinity.³² In contrast, catalyst **5** is of little use for high-strain monomers bearing many different functional groups, which can be polymerized in a controlled manner using the first generation Grubbs catalyst **2**.

1.1.6- Recent Advances in Biologically Relevant ROMP Polymers

Ring-opening metathesis polymerization has been increasingly used to generate a wide range of biologically relevant polymers and copolymers. This method provides an appealing alternate synthetic procedure to the simple, yet mostly uncontrolled free radical polymerization. Well-behaved polymers of different length can be easily obtained by varying the monomer to initiator ratio. ROMP polymers with pendant biomolecules such as carbohydrates, peptides and anti-tumour drugs containing different functionalities have been generated.³⁻⁸ While the highly active but oxophilic Schrock catalyst would degrade

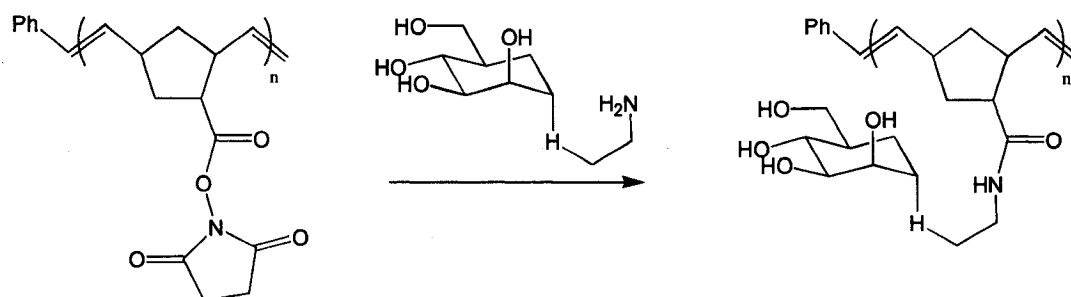
in such conditions, the Grubbs catalyst tolerates the presence of a wide range of functionalities. In addition, the living nature of the catalyst allows for the facile generation of diblock and triblock copolymers.^{5,9,33}

This polymerization method has been used by Kiessling and coworkers to generate a variety of synthetic carbohydrates.³ These neoglyopolymers can act as multivalent arrays and can bind strongly to the protein concanavalin A. Additional flexibility of the multivalent ligands is obtained through hydrogenation of the polymer backbone by post-polymerization processes. (Scheme 6)



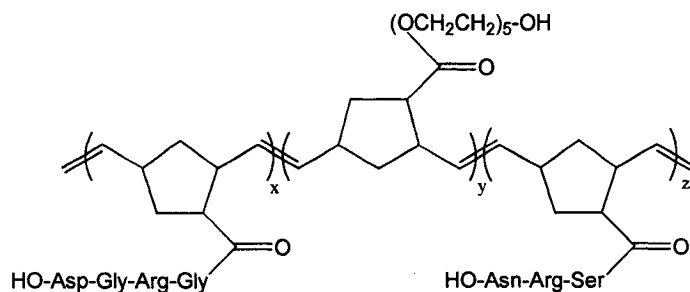
Scheme 6: Synthetic carbohydrate by ROMP

Over the course of many years, the group of Kiessling has studied multivalent receptors containing chelating biological units. Through the creation of new ROMP copolymers, they have demonstrated the efficiency and versatility of the ROMP method for the rapid generation of polymeric units with different binding affinities. In addition, a general methodology for the preparation of precursors to biologically active polymers have been developed.³⁴ It consists of the polymerization of a functional monomer bearing a labile activated ester, followed by a post-polymerization coupling with an amine functionalized biomolecule. (Equation 3) ROMP is at the heart of this method that leads to ready access to a library of new biopolymers.



Equation 3: Biopolymer precursor

Recently, synthetic oligopeptides as multivalent receptors were generated by Gibson³⁵ and Grubbs⁵. Interestingly, Grubbs reported the synthesis of a triblock copolymer bearing peptide sequences that are known to inhibit the adhesion of cell to fibronectin, thus leading to potential drug therapy applications. (Scheme 7)



Scheme 7: Grubbs triblock peptide polymer

The multivalent effects that are intrinsic to the polymeric architectures can be extended to well-known pharmaceutical drugs. In its polymeric form, a simple drug may offer many advantages compared to its monomeric counterpart such as: longer retention time, lower toxicity, greater specificity and enhanced permeability in cancerous cells.³⁶ However, typical polymeric drugs suffer from low degrees of drug loading as well as a lack of control of the polymer architecture and composition.³⁷ Nguyen et al. recently reported that well-established drugs could be easily attached to highly strained norbornene rings and polymerized to generate well-defined biomacromolecules.⁷ These

novel polymeric drugs were made possible due to the high functional group tolerance of the classical Grubbs catalyst. Furthermore, this polymerization strategy allows for the generation of block copolymers. It could be possible to combine many different drugs on the same polymeric chain. This would rival the actual treatments involving various drugs in order to optimize therapeutic effects. It is of note that even penicillin, the first antibiotic, was successfully incorporated into ROMP polymers, thus confirming the versatility, flexibility and ease of use of the ROMP reaction (using the Grubbs catalyst) to generate a variety of novel synthetic bioactive and biologically relevant polymers.³⁸

1.2 Molecular Recognition in Polymer Assemblies

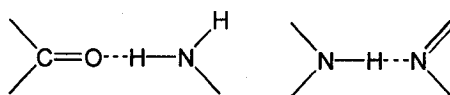
1.2.1- Supramolecular Chemistry

Supramolecular chemistry relies on a variety of weak interactions. It can be defined as the chemistry of multicomponent molecular assemblies, with molecular units held together by means of non-covalent forces. The desired complementarity is based on non-covalent interactions such as hydrogen bonding, π -stacking and hydrophobic/hydrophilic interactions.³⁹ Multi-point hydrogen bonding plays a crucial role in providing complementarity between guest and host molecules, which can lead to molecular recognition.

There is a distinct advantage in using weak non-covalent forces in complex assemblies. Sequence mismatch (i.e. structural errors), which can arise from improper pairing between non-complementary guest and host, may occur during the assembly of multicomponent systems. However, the reversible nature of non-covalent interactions allows the process of error correction. As the size and complexity of assembled structures increase, error correction processes will assume greater importance.

1.2.2- Hydrogen Bonding

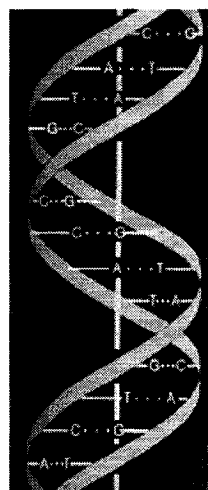
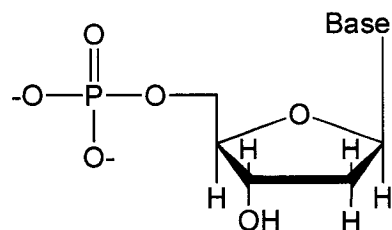
The intrinsic directionality of hydrogen bonds makes them ideal for achieving complementarity in supramolecular chemistry. Conventional hydrogen bonding involves neutral species that form a non-covalent bond via a donor group A-H and an acceptor group that contains lone-pair electrons, such as nitrogen, oxygen, fluorine and to a lesser extent, sulfur. The bond energy of a single hydrogen bond is quite small, between 2 to 5 kcal/mol. The bond length between donor and acceptor is approximately 1.7 to 2.0 Å. In comparison, a single C-C bond has an energy of 80 kcal/mol and a bond length of 1.5 Å.⁴⁰ Studies on biologically relevant molecules such as purines, pyrimidines, nucleosides and nucleotides have given us the precise nature of the particular molecular recognition motifs involving nitrogen and oxygen and their characteristics. Importantly, throughout this thesis, particular recognition patterns will be mentioned such as hydrogen bonding between an amine and a carboxylic acid functionality and between an imide and an imidazole. (Scheme 8)



Scheme 8: Biologically relevant hydrogen bonding motifs

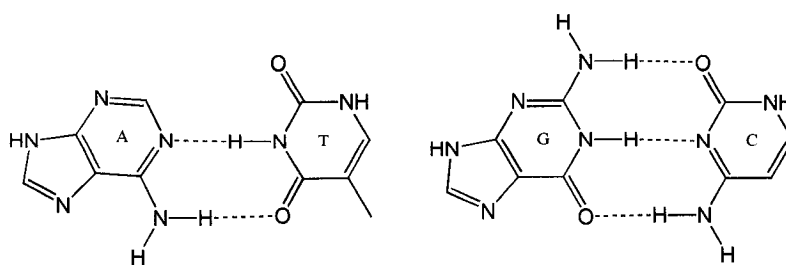
1.2.3- DNA Properties

The most selective hydrogen bonding interactions are present in biological systems. DNA or deoxyribonucleic acid consists of macromolecules with a sugar backbone held together by a phosphate ester linkage (at the 3' and 5'-positions). In addition, each sugar ring has a base attached at the 1'-position. DNA will tend to form a double helix (in aqueous media), thus exposing its hydrophilic backbone while hiding the hydrophobic bases within the structure. (Scheme 9)



Scheme 9: DNA and the double helix

Molecular recognition is an essential component of the structure and function of DNA. As the double helix forms, the hydrophobic bases start to associate via molecular recognition and are held together by multi-point hydrogen bonding. These interactions are referred as the Watson-Crick base pairing and provide one of the important stabilizing factors that leads to the helical structure of two DNA strands.⁴¹ The DNA bases consist of the complementary pair thymine (T) and adenine (A) and the complementary pair guanine (G) and cytosine (C). (Scheme 10) The presence of molecular recognition in DNA leads to an important phenomenon known as the cooperative effect. When the first four bases of two complementary DNA strands start to associate via hydrogen bonding, these act as a driving force to encourage the next base pairs to bind.⁴²



Scheme 10: Watson and Crick base pairing

Such information storage and processing has not yet been achieved in synthetic systems. However, molecular recognition using directed multi-point hydrogen bonding is becoming an important aspect of supramolecular chemistry using small molecules, synthetic polymers as well as copolymers.^{14,43,44}

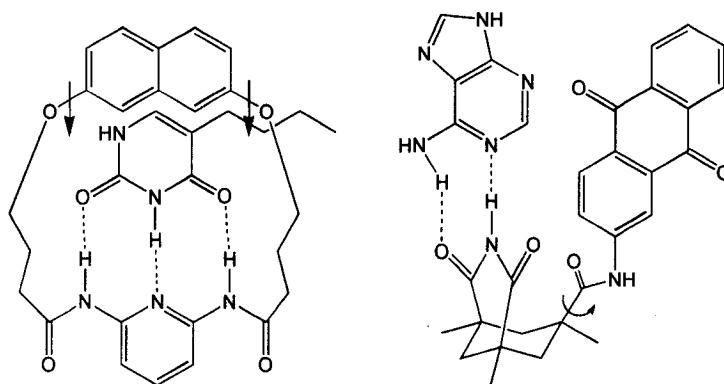
1.2.4- Synthetic Receptors

Based on the remarkable efficiency of molecular recognition in natural processes, it was envisioned that it could serve as a powerful tool for forming self-assembled systems. These systems could be designed to host particular multi-point hydrogen bonding patterns, thus leading to the binding of complementary guest molecules and perhaps lead to a self-assembled morphology. Multi-point hydrogen bonding is used for molecular recognition purposes due to the low energy, and most importantly low selectivity of a single hydrogen bond. For instance, adenine and thymine rely on a two-point hydrogen bonding motif to recognize each other while guanine and cytosine rely on three.

Recently, synthetic receptors of monomeric and polymeric nature containing recognition motifs have been created for many different purposes. For instance, monomeric receptors can be considered simple models in search of synthetic DNA. On the other hand, synthetic polymers may not be as defined as naturally occurring DNA but may offer many different advantages such as: ease of synthesis, stability in many different environments and wide range of potential variations that can lead to specific applications, such as biosensing and drug-delivery.^{45,46}

1.2.5- Monomeric Receptors

Early work by Rebek and Hamilton demonstrated that the classical Watson-Crick base pairing could inspire the creation of molecules that would efficiently bind nucleic acids.^{47,48} The simple receptors possess a molecular recognition site, such as a dicarboximide, which behaves like a thymine or uracil, and a π -stacking surface. In a similar way to DNA, this biomimetic approach combines two weak interactions, hydrogen bonding and π -stacking. (Scheme 11) Upon binding between the host and guest molecule, the ^1H NMR signals of the hydrogen bonding atoms shift downfield while the signals for the aromatic peaks shift slightly upfield, indicating the presence of hydrogen bonding and π - π interactions.

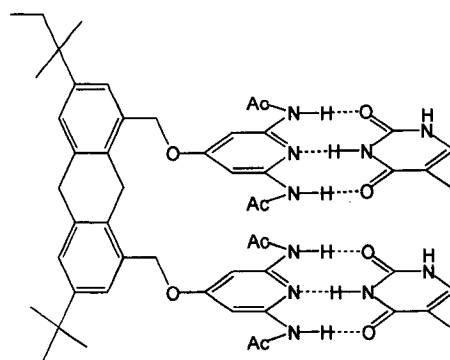


Scheme 11: Synthetic receptor a) Hamilton b) Rebek

This very same strategy was applied in the synthesis of thymine receptors. In 1991, Rebek et al. described a system that exploited base pairing with the eventual goal of promoting catalysis involving thymine.¹³ The proposed system, while more complex than examples previously mentioned, contains multi-point hydrogen bonding as well as π -stacking. The main difference arises from the nature of the π -stacking, which is precisely located at the molecular recognition sites, in a very similar way to base pairing and stacking interactions present in the DNA double helix. (Scheme 12) It is important to

note that the acylated diaminopyridine derivative was included in the design of this receptor, thus greatly increasing the binding constant with thymine.⁴⁹

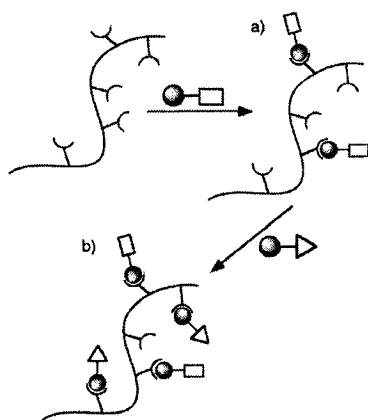
While monomeric receptors can be of interest, if one plans on mimicking DNA, polymers will be required. Polymers can present many advantages over their monomeric counterparts, such as the possibility of cooperative effects through the effective use of multivalent binding.⁵⁰



Scheme 12: Thymine receptor

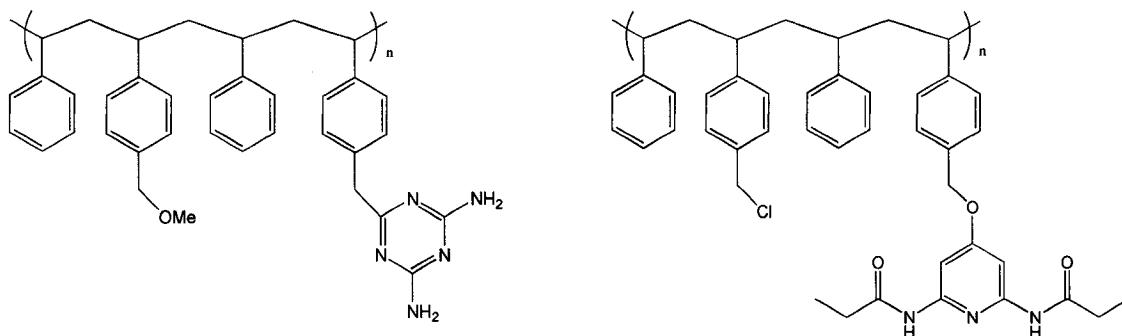
1.2.6- Polymeric Receptors

Synthetic limitations, prohibitive costs and overall lack of stability of natural nucleic acids in the biological environment have lead to the concept of synthetic DNA. Tailoring of nanostructures generated with synthetic polymers and copolymers using weak interactions and molecular recognition can be obtained by using Nature's tools as an inspiration. Rotello and coworkers have provided, over the past years, many examples of polymeric receptors that, upon exposure to guest molecules such as the thymine analog, butyluracil, undergo morphological rearrangement. (Scheme 13) This approach can be perceived as non-covalent functionalization of polymer chains or "Plug and Play" polymers.^{14e}



Scheme 13: Non-covalent polymer modification

The approach is based on random copolymers containing molecular recognition sites that are added in a post-polymerization process. The polymers are obtained in a straightforward fashion, using free-radical polymerization of styrene and chlorostyrene monomers. The first generation of copolymers is based on triazine units, while the second generation is based on diaminopyridine derivatives.^{14e,51} (Scheme 14)



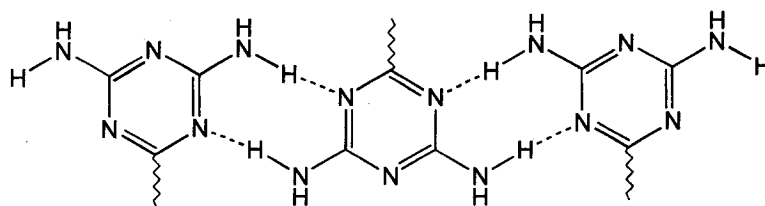
Scheme 14: Rotello's molecular recognition random copolymers

In addition to guest binding, self-assembly can occur upon mixing two complementary polymer systems. The group of Rotello observed such behavior when combining a copolymer bearing diaminopyridine units with a copolymer bearing complementary thymine units.^{14d} Giant vesicles with hollow cores were obtained in

CHCl₃. Hydrogen bonding interactions created phase separated domains, thus leading to a self-assembled morphology. These vesicles, although very stable, were easily disrupted at high temperatures. This indicates that hydrogen bonding provides the necessary interactions for forming these morphologies.

1.2.7- Modulation of Molecular Recognition Efficiency

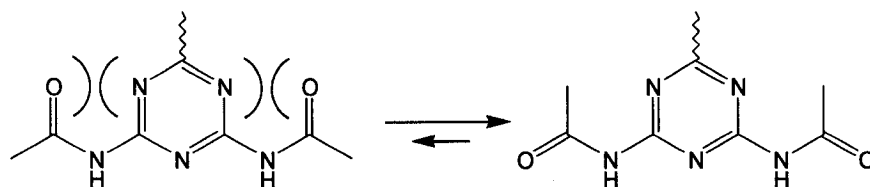
Due to the presence of two types of binding sites, diaminotriazine based copolymers display a greater tendency to form micellar aggregates. The considerable intramolecular interactions can be attributed to the self-complementary nature of diaminotriazine. (Scheme 15) Fortunately, molecular recognition interactions can be modulated by the inclusion of functionalities that decrease the tendency for self-association while increasing the binding efficiency with complementary guests.



Scheme 15: Self-complementarity of diaminotriazine

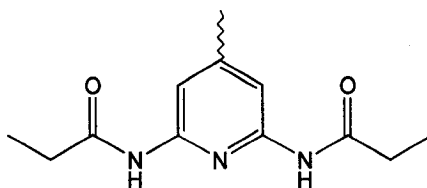
While synthetically accessible, diaminotriazine is limited by its lower level of selectivity. On the other hand, bis-acetyl-2,6-diaminopyridine (and propionyl derivatives), possess a single binding site that tends to form stronger hydrogen bonds due to the increased acidity of the amide protons. However, acylation of the diaminotriazine should be avoided, because it leads to a receptor site with unfavorable orientation of the carbonyl groups. The nitrogen lone pair is in close proximity to the lone pair of the carbonyl group. (Scheme 16) Consequently, the carbonyl could repel guest molecules

attempting to bind, thus leading to considerable decrease in binding efficiency of the three-point hydrogen bonding motif.⁴⁹



Scheme 16: Hydrogen bonding motif in acylated diaminotriazine

On the other hand, intramolecular interactions are considerably reduced with the inclusion of bis-propionyl-2,6-diaminopyridine units into polymers.⁵² (Scheme 17) The micellar structure adopted by the polymer is less rigid and polymer unfolding more facile. This in turn favors polymer rearrangement, which is necessary for proper guest binding via molecular recognition.

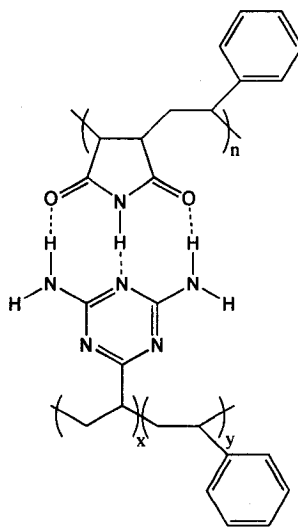


Scheme 17: bis-propionyl-2,6-diaminopyridine unit

1.2.8- Polymer Blends

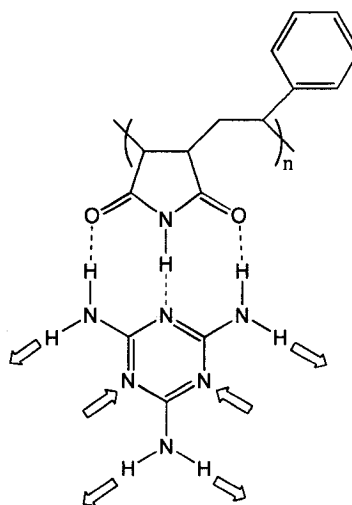
In 1995, Meijer and coworkers proposed a polymeric system that made use of molecular recognition to create novel polymer blends.^{14b} Although no morphologies were observed upon mixing of two complementary polymers, a homogeneous material with new properties was obtained. (Scheme 18) A styrene random copolymer bearing diaminotriazine functionalities and an alternating copolymer of maleimide/styrene were first dissolved in a strong hydrogen bonding solvent (DMSO) to favor necessary polymer unfolding. The new material was then obtained by coprecipitation in water, generating a

polymer with a single glass transition temperature, an indication that a miscible blend was formed.



Scheme 18: Hydrogen bonded polymer blend

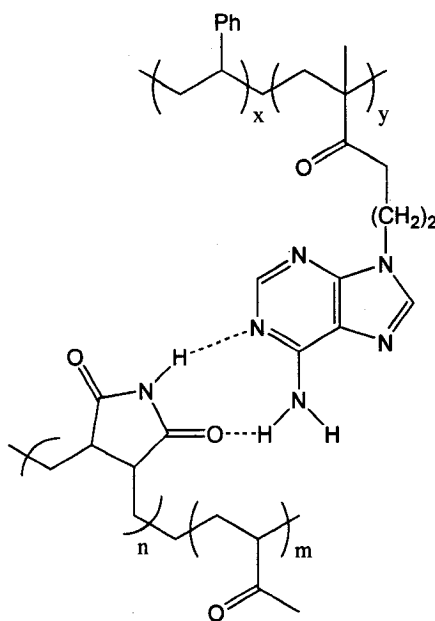
Surprisingly, even melamine, known to be insoluble in most organic solvents, could be solubilized by the maleimide/styrene copolymer due to the strong interactions generated by the presence of multi-point hydrogen bonding. A total of 9 binding interactions per melamine unit could be envisioned, leading to a strong polymer solvating



Scheme 19: Solubilizing melamine

effect. (Scheme 19, white arrows indicate additional hydrogen bonding interactions with the polymer)

In addition, Cowie et al. recently confirmed that different polymer blends could be created using Watson-Crick base pairing.⁵³ (Scheme 20) DNA bases were found to play a significant role in blend formation between incompatible polymers, but did not lead to any considerable increase in miscibility when compared to single-site hydrogen bonding. In general, polymer miscibility is promoted through the use of simple secondary interactions such as coulombic attractions,⁵⁴ ion-dipole interactions,⁵⁵ and single site hydrogen bonding.⁵⁶ Polymer blends aimed for simple commercial application generally rely on non-specific interactions for simplicity, ease of synthesis and for less constraining steric requirements. However, blend formation using the Watson-Crick base pairing



Scheme 20: Cowie's polymer blend

demonstrates that DNA-like molecular recognition between polymers is achievable in synthetic systems and can be a tool to promote higher organization within the bulk in polymers blends. This can serve as a powerful method for the design of new materials

with distinct properties. In order to optimize such organization, these materials will most probably require a polymerization method that generates very well-defined polymers (with a controlled architecture and narrow molecular weight distribution) capable of site selective binding.

1.2.9- Microenvironment Favoring Hydrogen Bonding

Molecular recognition not only relies on selective hydrogen bonding but on various non-covalent interactions. By combining multi-point hydrogen bonding and hydrophobic/hydrophilic interactions, many natural systems can perform molecular recognition in hydrogen bonding solvents. Normally, hydrogen bonding solvents such as water, DMSO and THF will inhibit binding due to their competitive nature (they may act as hydrogen bonding donors or acceptors).

While many synthetic receptors will bind guest molecules in non-hydrogen bonding solvents^{47,48} such as CHCl_3 , CH_2Cl_2 , toluene and benzene, natural systems (e.g. DNA) can readily undergo molecular recognition in water. To achieve hydrogen bonding in protic media, additional electrostatic and/or stacking interactions are necessary. Hydrophilic/hydrophobic interactions can play a crucial role in molecular recognition, as demonstrated by Asanuma and coworkers.¹⁵ This research group recently shown that selective binding in aqueous media was possible between nucleic acid bases and a complementary polymer insoluble in water. It was postulated that the selective adsorption between poly(vinyldiaminotriazine) and uracil in the presence of other non-complementary bases was achieved by combining multi-point hydrogen bonding with the hydrophobic microenvironment created by the coil nature of the polymeric chains.

Similar work was reported by Nowick and coworkers using non-polymeric receptors capable of hydrogen bonding in water.⁵⁷ This was achieved by shielding the

host-guest dyad, consisting of thymine and adenine, within a sodium dodecylsulfate micelle. The hydrophobic nature of the core prevented the disruption of molecular recognition by water molecules. This demonstrates that molecular recognition can be mediated in different environments, including competitive hydrogen bonding solvents. It can be assumed that a polymer designed for molecular recognition can be insoluble (or partially soluble) and still perform selective binding. In addition, copolymers offer the possibility for the creation of microenvironments whether they are in the bulk or as self-assembled micelles.

1.3 Self-Assembly of Asymmetric Block Copolymers

Asymmetric diblock copolymers have the potential to self-assemble into nanoscale aggregates. Self-assembly is often promoted through the combination of copolymer design and the clever use of selective solvent systems. By dissolving a block copolymer in a solvent which is selective for only one block, colloidal particles may be formed as a result of the aggregation of the insoluble block. Many examples in the literature are based on amphiphilic block copolymers where the corona (or shell) forming block is considerably longer than the block forming the core of the micellar structure. In aqueous media, these polymers tend to form simple star micelles when the corona forming block is hydrophilic.⁵⁸

However, when the core forming block is large and the corona relatively short, the aggregates are referred as *crew-cut*.^{10,59} The method of preparation of crew-cut aggregates differs greatly from the star micelle system. For the crew-cut system, the diblock copolymer has a relatively short soluble block (which forms the corona). This implies that the major fraction of the copolymer is insoluble in a selective solvent for the corona. Therefore, a single solvent cannot lead to polymer self-assembly. A common

solvent for both blocks must be initially used for proper polymer unfolding. Water is then slowly added to the copolymer solution. As the solvent becomes worse for the core forming block, self-assembly begins by the segregation of the hydrophobic block within the core of the micellar structure. This results in a wide range of nanoscale aggregates of great interest, especially in the field of drug delivery and DNA transfection.^{16,60}

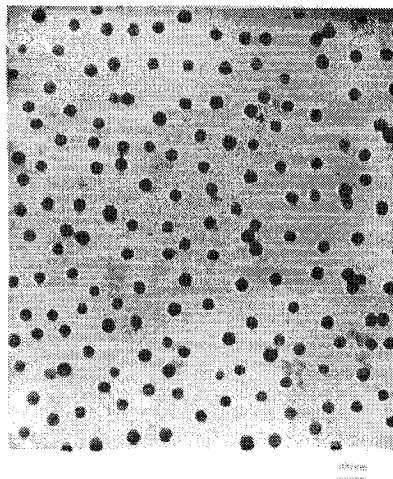
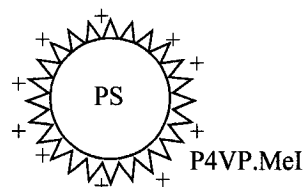
Eisenberg et al. have reported over the course of recent years that asymmetric block copolymers can self-assemble into crew-cut aggregates of various morphologies such as: spheres, rods, lamellae, reverse micelles as well as large compound micelles or LCM.^{10b,61} These morphologies can be generated by varying many conditions such as: copolymer composition,⁶¹ copolymer polydispersity,⁶² presence of ions (and pH),⁶³ presence of homopolymer,⁶⁴ and solvent system.⁶⁵

1.3.1- Spherical Crew-Cut Micelles

Many amphiphilic diblock copolymers can be used for creating crew-cut aggregates in aqueous media. Poly(styrene) is typically included into these copolymers as the core-forming block, mainly due to its hydrophobic nature. In addition, styrene can be polymerized in a controlled fashion by anionic polymerization, a requirement for creating diblock copolymers.⁶⁶ The hydrophilic corona-forming block can either be positively or negatively charged through the use of poly(4-vinylpyridinium methyl iodide) or poly(acrylic acid).^{59,61,63} In addition, neutral poly(ethylene glycol) can also act as the corona-forming block.⁶⁷ It is worth noting that the majority of polymeric drug-delivery systems rely on the biocompatibility of poly(ethylene glycol).⁶⁸

One of the first examples of crew-cut micelles was reported using PS(933)-b-P4VP.MeI (82).⁵⁹ The block copolymer was dissolved in DMF (a common solvent for both blocks), water was added in a dropwise fashion and the solution dialyzed against

water to remove the DMF and kinetically freeze the morphology for observation under transmission electron microscopy. The micelles exhibited a very narrow size distribution with diameters ranging from 40-65 nm. (Scheme 21) The electron density being approximately the same for both blocks, one cannot visually discern the presumably thin



Scheme 21: Crew-cut spherical micelles

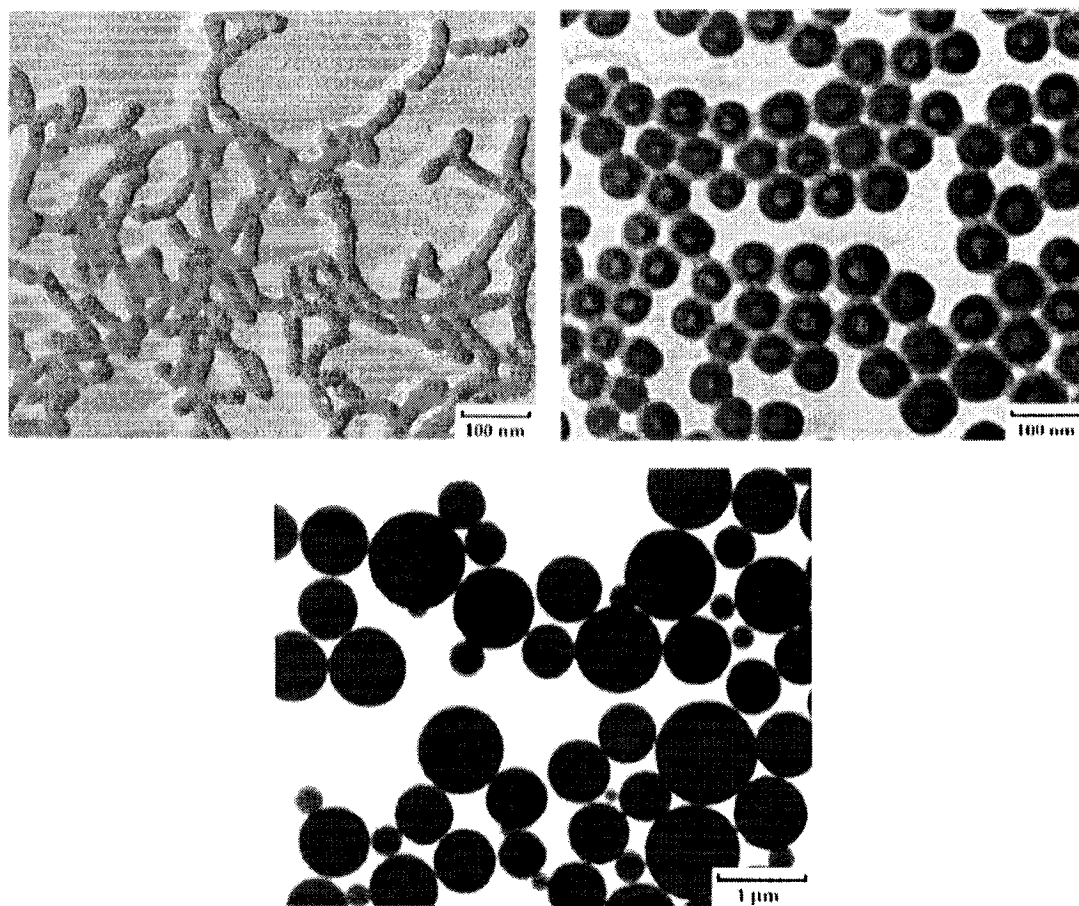
corona from the PS core. This is the simplest morphology one can obtain with crew-cut systems.

1.3.2- Multiple Crew-Cut Morphologies

It quickly became apparent that, unlike star-micelles which adopt a spherical morphology over a very broad range of copolymer composition, crew-cut aggregates generated a panoply of intriguing morphologies that could be beneficial for many applications including drug delivery research.⁶⁰ Crew-cut aggregates tend to adopt various morphologies based on different criteria such as polymer composition and preparation conditions. Interestingly, there is a clear relation between the length of the corona forming block, poly(acrylic acid) for instance, and the morphology of the aggregates. As the length of the PAA block decreases, in a PS-b-PAA copolymer, the

crew-cut morphology changes from spherical to rod-like to lamellar or vesicular and eventually to large compound micelles.^{10,59,63} (scheme 22)

In addition, many morphologies have been observed to coexist. As water is being progressively added to the copolymer solution, the morphological phase diagram is being crossed. As a result of this water addition, the solvent environment becomes hostile to the core-forming block (poly(styrene) for example) and the aggregates change morphology (from spheres, to rods, to vesicles) in response to this *stimulus*. The presence of multiple morphologies can be attributed to a rapid crossing of stability regions in the copolymer phase diagram.⁶¹



Scheme 22: a) rodlike micelles from PS(180)-b-PAA(15) b) vesicles from PS(410)-b-PAA(20) c) compound micelles from PS(200)-b-PAA(4)

1.3.3- Thermodynamic Considerations

Block copolymers consisting of poly(styrene) and poly(acrylic acid) can adopt a wide range of morphologies as crew-cut polymers. With a high PAA content, the obtained aggregates tend to be spherical and micelle-like. The different morphologies have a direct relation with the length of the hydrophilic PAA block. Unlike star micelles, crew-cut micelles have a rather low density of coronal chains as well as a low degree of stretching in the core. From a thermodynamic point of view, the structure of the aggregates is controlled by mainly two contributions to the free energy of micellization. The factors are: the repulsive interactions between the corona chains and the stretching entropy of the core forming block.⁶¹

The importance of chain-chain repulsion at the corona surface has been demonstrated by inducing morphological changes of the crew-cut aggregates by protonating the coronal PAA block or by adding monovalent or divalent ions.⁶³ By decreasing chain repulsion at the corona, larger aggregates can be formed. In fact, this holds true by simply varying the copolymer composition. As the length of the PAA block decreases, the size of the crew-cut aggregates may increase due to lower repulsion (electronic and steric) between the PAA chains. This size increase results in greater PS chain stretching and a decrease of entropy. At one point, morphological changes occur to counter the unfavorable PS chain stretching. By switching to a different morphology, the system reduces the thermodynamic penalty of elongation by creating a structure bearing a PS core with a lower degree of chain stretching.

Based on this behavior, it is apparent that the degree of stretching of the core-forming block can significantly dictate the morphology of the aggregates. This can be experimentally proven by varying different parameters such as: the copolymer

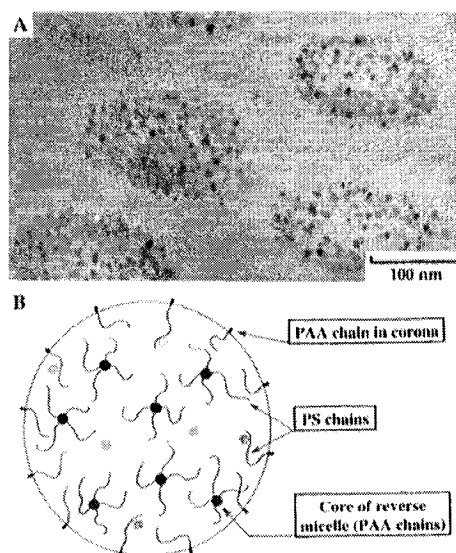
composition (previously mentioned) and the nature of the common solvent during aggregate formation. By using a common solvent that has a higher affinity for the PS chains, swelling of the PS core will increase during the formation of the self-assembled aggregates. When a polymer chain is exposed to a solvent for which it has a high affinity, it tends to uncoil upon solvation. Therefore, as the solvent content increases within the PS core, the core expands (due to chain uncoiling) and morphological changes occur to reduce PS chain elongation. The initial morphology is of spherical nature (higher core elongation) and changes to rod and finally to vesicle (smaller core elongation).

This solvent-polymer interaction is not only valid for the PS core but can be of importance at the corona level by influencing the degree of repulsion between the coronal chains. If a solvent with a higher affinity for PAA is chosen, it may partially shield the polymer's negative charge. By reducing the level of repulsion between the PAA chains of the corona, larger aggregates may be formed. Consequently, this will once gain lead to PS chain elongation in the core, thus leading once again to a morphological rearrangements into rods or vesicle to reduce the PS chain elongation. It is obvious that various factors can affect the morphology of crew-cut systems. One can take advantage of the thermodynamics by tailoring polymeric systems to form specific nanoscale morphologies.

1.3.4- Large Compound Micelles

Large compound micelles or LCM generated with PS-b-PAA and isolated in aqueous solution possess a hydrophilic surface which renders them stable in water.⁶¹ They are typically obtained by reducing the length of the PAA block to a very considerable extent (eg. PS(200)-b-PAA(4)). They consist of large spherical aggregates with highly polydisperse size distribution. The interior consists of a large number of

reverse micelles, with a small hydrophilic core and large hydrophobic corona. In other words, a LCM consists of a hydrophobic matrix with domains of hydrophilic material. In addition, the shell of a LCM is hydrophilic, due to surface localized PAA blocks. This complex structure was revealed by staining experiments using CsOH.⁶¹ (Scheme 23) The darkened regions are a result of the high electron density of cesium ions associated with the carboxylic acid functionality of the PAA block. Combined to the extensive library of morphologies, this demonstrates the versatility of crew-cut aggregates for the design of novel functional nanoaggregates.



Scheme 23: TEM staining experiments on LCM

Chapter 2. Purpose of Research

2.1 Research Goals

Our research objective is focused on using living ring-opening metathesis polymerization (ROMP) to synthesize a variety of novel polymers and copolymers, which are designed to reproduce some of the properties of DNA. These polymers contain analogues of the nucleic acid bases thymine and uracil at each repeating unit. In addition, asymmetric block copolymers incorporating the nucleic acid analogues were generated to promote self-assembly into nanoscale morphologies. The self-assembled aggregates contain molecular recognition units, and thus could undergo morphological changes by the inclusion of complementary molecules or by the disruption of the molecular recognition patterns. Furthermore, they should be capable of selective binding with nucleic acids.

The monomer of interest, *exo*-7-oxabicyclo[2.2.1]hept-5-ene-2,3-dicarboximide, is a thymine/uracil analog that contains a hydrogen bonding pattern of acceptor-donor-acceptor (ADA). It can be readily obtained by a Diels-Alder reaction between maleimide and furan. The polymerization of this monomer can be accomplished by living ROMP using the well-established 1st generation Grubbs catalyst **2**. Polymer characterization includes ¹H, ¹³C NMR spectroscopy, gel permeation spectroscopy (GPC) and infra-red spectroscopy (FTIR).

In order to increase the solubility of the polymers of the thymine/uracil analog, monomers containing solubilizing groups have been designed. Integrating them with the thymine/uracil analog monomer will lead to diblock copolymers with novel properties. It is expected that in certain solvent conditions, these copolymers will tend to self-assemble

and form nanoscale morphologies. These will be characterized by dynamic light scattering (DLS) and transmission electron microscopy (TEM).

These polymers are anticipated to interact with complementary molecules which carry the donor-acceptor-donor (DAD) hydrogen bonding pattern. This can lead to the development of biosensors based on molecular recognition interactions. Probing these properties can be achieved by making use of NMR spectroscopy, as well as HPLC.

2.2 Target Monomers

A variety of monomers based on the *exo*-7-oxabicyclo[2.2.1]hept-5-ene-2,3-dicarboximide have been synthesized. (Chart 2) They possess different solubility in common organic solvents such as DMSO, THF, CH_2Cl_2 and CHCl_3 . Monomers **6** and **9** contain pendant alkyl chains and have been designed to confer greater solubility in non-hydrogen bonding solvents when incorporated into various diblock copolymers.

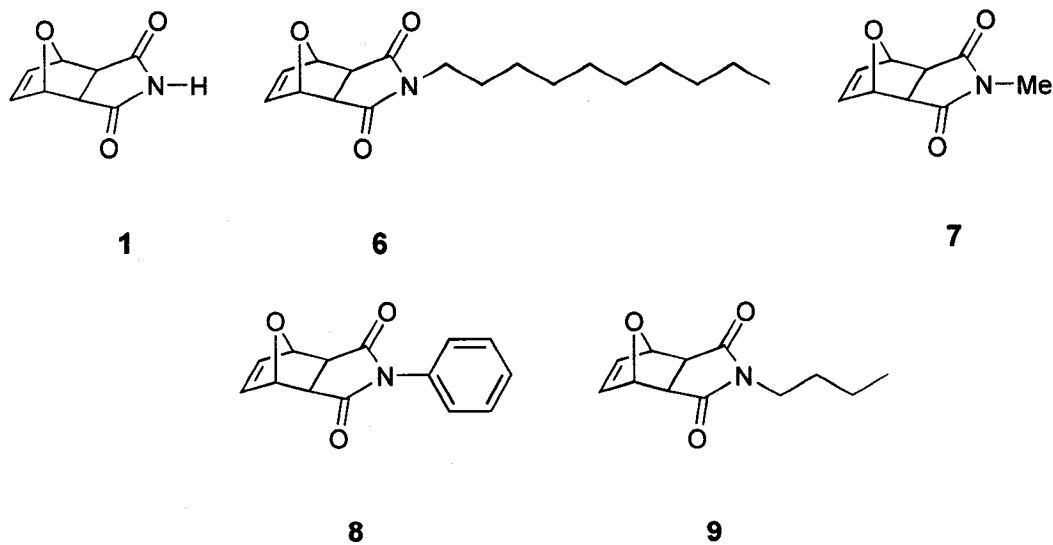
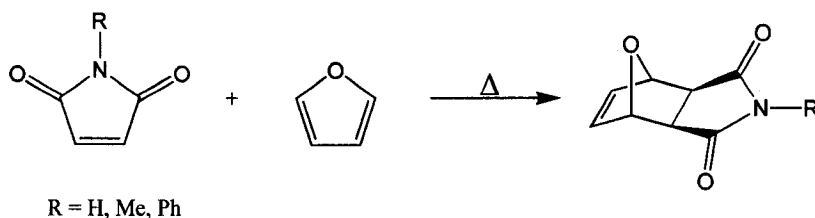


Chart 2

2.3 Synthetic Strategy of Monomers

2.3.1- Synthesis of Exo-7-oxabicyclo[2.2.1]hept-5-ene-2,3-dicarboximide and N-methyl and N-phenyl analogs

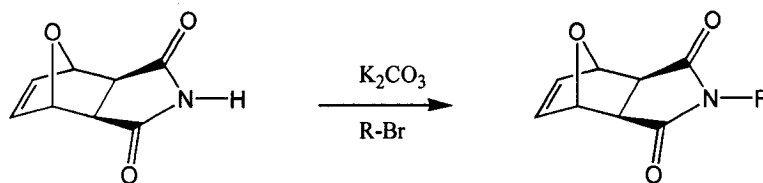
These monomers were obtained in their pure *exo* isomer (thermodynamic product) in a single step reaction via a high temperature Diels-Alder reaction between furan and the corresponding maleimide. (Equation 4)



Equation 4

2.3.2- Synthesis of Exo-N-butyl-7-oxabicyclo[2.2.1]hept-5-ene-2,3-dicarboximide and Exo-N-decyl-7-oxabicyclo[2.2.1]hept-5-ene-2,3-dicarboximide

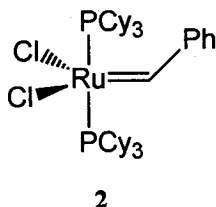
The alkylated monomers were synthesized by deprotonation of the *exo*-7-oxabicyclo[2.2.1]hept-5-ene-2,3-dicarboximide and subsequent reaction with alkylbromide (butyl or decyl). (Equation 5)



Equation 5

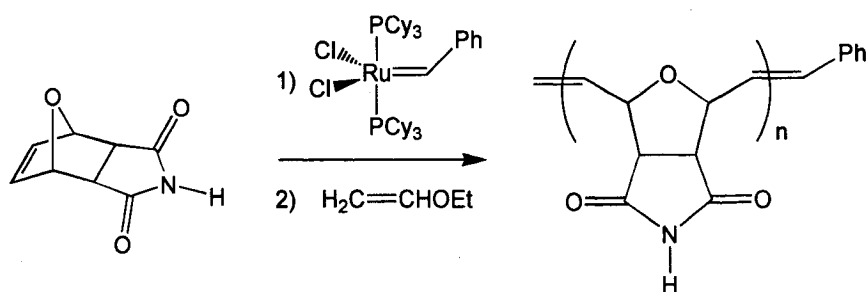
2.4 Synthetic Strategy of Polymers and Diblock Copolymers

The polymers and copolymers were obtained by Living Ring-Opening Metathesis Polymerizations (ROMP) using the Grubbs catalyst **2**.



2.4.1- Homopolymer General Synthesis

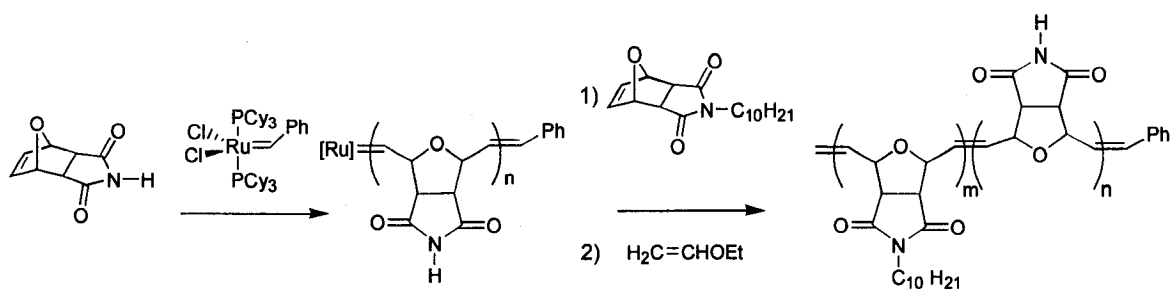
Homopolymers can be obtained using the previously mentioned monomers. Synthesis involves a simple ROMP polymerization procedure. (Equation 6) It is of note that the reactions are carried out under inert atmosphere (N₂), in either THF or CH₂Cl₂.



Equation 6

2.4.2- Diblock Copolymer General Synthesis

Copolymers are generated by a slightly more complex procedure which involves addition of the first monomer to the catalyst, followed by a subsequent addition of a second monomer to the living polymer chain. (Scheme 24) In order to prevent premature chain termination, the monomer addition is carried out under inert atmosphere.



Scheme 24: Diblock copolymer synthesis

2.5 Self-Assembly Studies

Following polymer and copolymer synthesis, the next objective of this research project is to evaluate the self-assembly behavior of various diblock copolymers. Analysis can be achieved using different experimental techniques.

Initially, conditions leading to self-assembly of the diblock copolymers must be surveyed. The first step consists in finding a common solvent for both polymer blocks. This will allow for proper polymer chain solvation and unfolding (in our case, THF is the best solvent). At that point, a non-solvent for one block may be added, such as water or methanol, in a dropwise fashion until turbidity becomes apparent, indicating the onset of aggregation. The next step involves the detection of spherical or non-spherical aggregates in solution using dynamic light scattering (DLS). If positive results are obtained, the final step is a direct observation of the aggregates by transmission electron microscopy (TEM). In order to yield satisfying results, it is preferable that a proper correlation exists between DLS measurements and TEM observations.

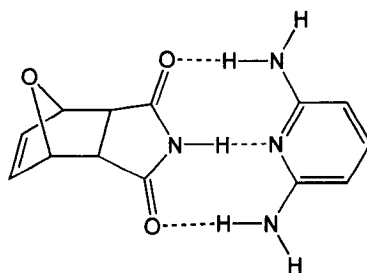
Upon detection of nanoscale aggregates, staining experiments can be carried out to determine if segregated domains exist within these aggregates. We believe that our system can be preferably stained at either the hydrophobic block (pendant alkyl chains)

using a solution of uranium acetate or at the hydrophilic block (thymine analog) using an aqueous solution of cesium hydroxide.

2.6 Molecular Recognition Studies

2.6.1- Monomer and Complementary Molecules

The purpose of this research project is to synthesize novel polymers and copolymers, which are capable of self-assembly and molecular recognition. It can be envisioned that the polymer's multi-point hydrogen bonding properties can be used to modulate the nanoscale morphologies and perhaps trap biologically relevant molecules via molecular recognition. Consequently, there is a need to establish that the polymers are capable of molecular recognition. The monomer of interest is *exo*-7-oxabicyclo[2.2.1]hept-5-ene-2,3-dicarboximide (monomer **1**) and has been incorporated into copolymers leading to self-assembled morphologies. This monomer is a thymine/uracil analog which is capable of three-point hydrogen bonding and can bind with a complementary molecule such as 2,6-diaminopyridine. (Scheme 25) In order to probe if molecular recognition is possible, experiments were conducted at the monomer level for simplicity, while preliminary studies were carried out using the polymers (with a lesser level of success that will be discussed later).

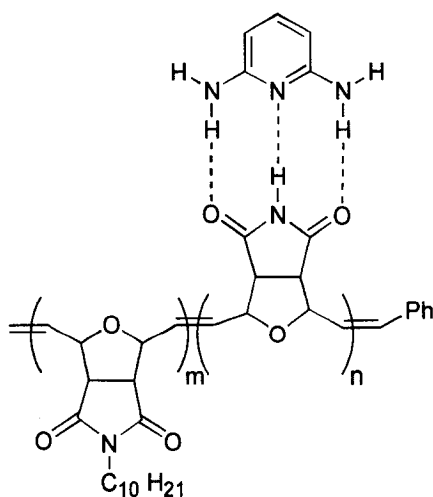


Scheme 25: Hydrogen bonded dyad

The characterization of the dyad formation in a non-hydrogen bonding solvent (CHCl_3) was carried out using ^1H NMR spectroscopy. Obvious downfield shifts were observed when the monomer was exposed to different guests such as 2,6-diaminopyridine, bis-propionyl-2,6-diaminopyridine and undecyl-diaminotriazine, in a 1:1 ratio. In addition to the obvious NMR shift of the imide proton (of the monomer), solubility of the monomer was significantly increased in aprotic solvents upon binding to complementary guest molecules.

2.6.2- Polymer and Complementary Molecules

Ideally, 2,6-diaminopyridine would strongly interact with copolymers containing the dicarboximide units via hydrogen bonding. (Scheme 26) Unfortunately, we believe that many complications arose from the micellar nature of the diblock copolymers in non-hydrogen bonding solvents such as CHCl_3 and CH_2Cl_2 . ^1H NMR spectroscopy provided no direct evidence of hydrogen bonding due to the absence of the polymer's imide signal in the spectra. In non-hydrogen bonding solvents, it is expected that the hydrogen-bonding moieties are hidden within a micellar structure, thus forming the core of the



Scheme 26: Molecular recognition with the copolymer

aggregates. The core which consists of the poly(1) block is not solvated by the deuterated solvent, consequently it is not apparent in the NMR spectra. Similar complications have already been reported by a research group working on copolymer micelles.⁶⁹

Indirect measurements of molecular recognition properties of the polymers were attempted based on previously published procedures.¹⁵ The method takes advantage of the lack of solubility of the hydrogen bonding polymers in certain solvents. It is based on selective adsorption which is driven by molecular recognition (such behavior is expected from our polymer system). In addition, it is believed that the hydrophobic environment created by the polymer chains might also play a significant role in enhancing the recognition properties of the insoluble polymer.

¹H NMR and HPLC experiments were conducted where the polymer was suspended in benzene-d₆ and THF/water (17% v/v water content) respectively. These solutions contained complementary and non-complementary nucleic acid bases that could bind to the polymeric substrate. Upon exposure to the polymer, the solution could be particularly depleted of complementary guest molecules if selective adsorption occurred. Unfortunately, the HPLC experiments did not lead to any significant adsorption of any of the various guest molecules in solution, while similar experiments using ¹H NMR generated some interesting but inconclusive results. It is worth noting that the NMR experiment demonstrated the possible presence of selective adsorption of complementary nucleic acid bases upon exposure to the insoluble polymer. However, an NMR experiment using toluene (as a guest molecule) displayed what seemed like an excessively high level of adsorption, thus leading to uncertainty on the validity of the results.

Chapter 3. Experimental Procedures

3.1 General

Material

Reagents were purchased from Aldrich and used as received. The Grubbs catalyst **2** was obtained from Strem Chemicals. Deuterated solvents were obtained from Cambridge Isotope Laboratories and used without further purification. Tetrahydrofuran (THF) was freshly distilled from sodium/benzophenone, dichloromethane (CH₂Cl₂) was freshly distilled from CaH₂. All polymerization reactions were carried out under a dry nitrogen atmosphere using standard Schlenk techniques.

Characterization

¹H NMR and ¹³C NMR spectra were recorded on a Varian M300 spectrometer operated at 300.076 MHz and 75.459 MHz respectively. Chemical shifts are reported in ppm relative to the deuterated solvent resonances. IR spectra were recorded on an Avatar 360 FT-IR spectrophotometer in the range of 4000 and 400 cm⁻¹ with a resolution of 2 cm⁻¹. GPC spectra were recorded using a Waters 510 pump equipped with two polystyrene-packed Styragel columns (HR4 and HR1, 7.8 X 300 mm) in series and in-line Waters 2410 refractive index detector. THF was used as the eluent at a flow rate of 0.6 mL/min, and the instrument was calibrated with polystyrene standards from Aldrich. TEM images were recorded on a JEOL 2000FX electron microscope operating at 80 kV, using 400 mesh carbon coated grids purchased from Electron Microscopy Sciences. DLS experiments were performed on a Brookhaven Instruments Corporation system equipped with a BI-200SM goniometer, a BI-9000AT digital correlator and a Compass 315-150 CW laser light source from Coherent Inc. operating at 532 nm (150 mW).

3.2 Monomer Synthesis

Synthesis of exo-7-oxabicyclo[2.2.1]hept-5-ene-2,3-dicarboximide 1

Monomer **1** was prepared according to literature methods.⁷⁰ Maleimide (5.3g, 54 mmol) and furan (7.3 g or 8 ml, 107 mmol) were dissolved in 50 ml of dry diethyl ether in a heavy-walled flask equipped with a Teflon seal. The mixture was sealed under reduced pressure and stirred at 90°C overnight. A white solid precipitated from solution upon cooling and was isolated by vacuum filtration and washed with diethyl ether. No further purification step was required (yield 97%). ¹H NMR spectroscopy reveals that the isolated product is pure exo.¹⁷ ¹H NMR (DMSO-d₆): δ 11.40 (s, 1H, NH), 6.52 (s, 2H), 5.10 (s, 2H), 2.83 (s, 2H). ¹³C NMR (DMSO-d₆): δ 178.4, 137.1, 81.0, 49.2.

Synthesis of exo-N-decyl-7-oxabicyclo[2.2.1]hept-5-ene-2,3-dicarboximide 6

Monomer **6** was prepared following a modification of literature procedure.⁷¹ Monomer **1** (1g, 6 mmol) and bromodecane (1.3g, 6 mmol) were dissolved in anhydrous DMF (50 ml). Potassium carbonate (4g, 40 mmol) was added to the reaction mixture at 50°C and stirred for 1.5h under N₂. The resulting mixture was poured in water (100 ml) and extracted (4x) with ethyl acetate (200 ml). The organic phase was collected, dried over MgSO₄ and evaporated to yield a yellow oil. Silica gel chromatography (5%MeOH / CH₂Cl₂) yielded a beige oil that quickly solidified (yield 65%). ¹H NMR (CDCl₃): δ 6.45 (s, 2H), 5.20 (s, 2H), 3.40 (t, 2H), 2.77 (s, 2H), 1.48 (m, 2H), 1.18 (m, 14H), 0.81 (t, 3H). ¹³C NMR (CD₂Cl₂): δ 176.59, 136.83, 81.29, 47.76, 39.11, 32.24, 29.85, 29.82, 29.64, 29.47, 27.91, 27.00, 23.04, 14.24. (C₁₈H₂₇NO₃) (305.41): Calcd. C 70.78, H 8.91, N 4.59; Found: C 70.49, H 9.25, N 4.62.

Synthesis of exo-N-methyl-7-oxabicyclo[2.2.1]hept-5-ene-2,3-dicarboximide 7

Monomer **7** was prepared according to literature methods.⁷² N-methylmaleimide (5.0 g, 46 mmol) and furan (6.2 g or 6.5 ml, 94 mmol) were dissolved in 25 ml of dry diethyl ether in a heavy-walled flask equipped with a Teflon seal. The mixture was sealed under reduced pressure and stirred at 90°C for 5 h. A white solid precipitated from solution upon cooling and was isolated by vacuum filtration and washed with diethyl ether. No further purification step was required (yield 50%). ¹H NMR spectroscopy reveals that the isolated product is pure exo.¹⁷ ¹H NMR (CDCl₃): δ 6.51 (s, 2H), 5.27 (s, 2H), 2.97 (s, 3H), 2.85 (s, 2H). ¹³C NMR (CDCl₃): ¹³C NMR (CDCl₃): δ 176.36, 136.65, 81.05, 47.80, 25.23.

Synthesis of exo-N-phenyl-7-oxabicyclo[2.2.1]hept-5-ene-2,3-dicarboximide 8

Monomer **8** was prepared following a modification of literature procedure.⁷² N-phenylmaleimide (7.8 g, 45 mmol) and furan (6.2 g or 6.5 ml, 94 mmol) were dissolved in 50 ml of dry diethyl ether in a heavy-walled flask equipped with a Teflon seal. The mixture was sealed under reduced pressure and stirred at 90°C for 4 h. A white solid precipitated from solution upon cooling and was isolated by vacuum filtration and washed with diethyl ether. No further purification step was required (yield 92%). ¹H NMR spectroscopy reveals that the isolated product is pure exo.¹⁷ ¹H NMR (DMSO-d₆): δ 7.44 (m, 4H), 7.17 (d, 2H), 6.59 (s, 2H), 5.23 (s, 2H), 3.07 (s, 2H). ¹³C NMR (DMSO-d₆): δ 176.38, 137.25, 132.70, 129.66, 129.15, 127.49, 81.51, 48.24.

*Synthesis of *exo*-N-butyl-7-oxabicyclo[2.2.1]hept-5-ene-2,3-dicarboximide 9*

Monomer **9** was prepared following a modification of literature procedure.⁷¹ Monomer **1** (1.5 g, 9 mmol) and bromobutane (1.2g, 9 mmol) were dissolved in anhydrous DMF (50 ml). Potassium carbonate (6g, 54 mmol) was added to the reaction mixture at 50°C and stirred for 1.5h under N₂. The resulting mixture was poured in water (100 ml) and extracted (4x) with ethyl acetate (200 ml). The organic phase was collected, dried over MgSO₄ and evaporated to yield a yellow oil. Silica gel chromatography (5%MeOH / CH₂Cl₂) yielded a yellow oil that quickly solidified (yield 73%). ¹H NMR (CDCl₃): δ 6.50 (s, 2H), 5.27 (s, 2H), 3.47 (t, 2H), 2.83 (s, 2H), 1.57 (m, 2H), 1.31 (m, 2H), 0.91 (t, 3H). ¹³C NMR (CDCl₃): δ 176.38, 136.67, 81.16, 47.72, 39.13, 30.04, 20.34, 14.08.

3.3 Polymer Synthesis

Synthesis of polymer 3 (monomer 1: initiator 2 - 20:1)

A solution of catalyst **2** (0.015g, 0.018 mmol) in THF (2.5 ml) was sonicated for 5 min. The catalyst solution was transferred to monomer **1** (0.060g, 0.36 mmol, 20 equiv.) in THF (2.5 ml). Initiation was apparent by the change of color from purple to brown. The reaction mixture was vigorously stirred for 10 min. and quenched with ethyl vinyl ether (600 equiv). The resulting light gray polymer was purified by precipitation in methanol (yield 80%). ¹H NMR (DMSO-d₆): δ 11.20 (s, br, NH), 5.89 (s, br), 5.66 (s, br, cis), 4.86 (s, br, cis), 4.44 (s, br, trans) ¹³C NMR (DMSO-d₆): δ 178.30, 131.78, 80.51, 53.99. IR (KBr); 3207 (NH), 3080, 2864, 2767, 1775 and 1712 (C=O), 1344, 1272, 1182, 1037, 972, 892, 755, 633. GPC (THF, polystyrene standards): a peak at M_n= 4217 Da (calculated M_n= 3404 Da) and PDI= 1.05. (trans 80%, determined by ¹H NMR).

Synthesis of polymers 3a and 3b (monomer 1: initiator 2 - 10:1; monomer 1: initiator 2 - 15:1)

Polymers **3a** and **3b** were obtained following the same procedure as for polymer **3**. The only variation resides in the monomer to initiator ratio. For polymer **3a**: monomer **1** (0.030g, 0.18 mmol, 10 equiv.). For polymer **3b**: monomer **1** (0.045g, 0.27 mmol, 15 equiv.). GPC analysis of **3a** (THF, polystyrene standards): a peak at $M_n = 2091$ Da (calculated $M_n = 1754$ Da) and PDI= 1.20. GPC analysis of **3b** (THF, polystyrene standards): a peak at $M_n = 2938$ Da (calculated $M_n = 2579$ Da) and PDI= 1.11.

Synthesis of polymer 10 (monomer 6: initiator 2 - 60:1)

Polymer **10** was obtained following the same procedure as for polymer **3** using monomer **6** (0.334g, 1.095 mmol, 60 equiv.) in CH_2Cl_2 . The resulting beige polymer was purified by precipitation in methanol (yield 67%). ^1H NMR (CDCl_3): δ 6.08 (s, br, trans), 5.79 (s, br, cis), 5.10 (s, br, cis), 4.45 (s, br, trans), 3.45 (s, br), 3.31 (s, br), 1.54 (s, br), 1.25 (s, br), 0.87 (t, br). ^{13}C NMR (CDCl_3): δ 175.81, 131.10, 81.24, 53.64, 52.54, 39.21, 32.10, 29.77, 29.73, 29.52, 29.41, 27.90, 27.07, 22.90, 14.35. IR (KBr): 2924, 2854, 1776 and 1701 (C=O), 1437, 1397, 1367, 1267, 1162, 1138, 1035, 968, 918, 770, 722, 635. GPC (THF, polystyrene standards): a peak at $M_n = 22161$ Da (calculated $M_n = 18404$ Da) and PDI= 1.08. (trans 71%, determined by ^1H NMR).

Synthesis of copolymer 11 (monomer 1: monomer 6: initiator 2 - 20:60:1)

A solution of catalyst **2** (0.015g, 0.018 mmol) in THF (2.5 ml) was sonicated for 5 min. The catalyst solution was transferred to monomer **1** (0.060g, 0.36 mmol, 20 equiv.) in THF (2.5 ml) and vigorously stirred for 10 min. At that point, half of the reaction mixture

was removed from the Schlenk flask, and a solution of monomer **6** (0.167g, 0.548 mmol, 30 equiv.) in THF (2.5 ml) was added. The reaction mixture was stirred for an additional 10 min. and quenched with ethyl vinyl ether (600 equiv). The resulting solution was concentrated by evaporation and precipitated in methanol, yielding a white polymer (yield 71%). ^1H NMR (C_6D_6): δ 6.70 (s, br, trans), 5.86 (s, br, cis), 5.26 (s, br, cis), 4.41 (s, br, trans), 3.45 (s, br), 2.96 (s, br), 1.59 (s, br), 1.28 (s, br), 0.93 (s, br). ^{13}C NMR (C_6D_6): δ 175.31, 131.33, 81.35, 52.68, 39.50, 32.34, 30.05, 29.81, 29.61, 28.19, 27.73, 23.17, 14.47. IR (KBr): 3195 (NH), 2923, 2855, 1775 and 1705 (C=O), 1437, 1398, 1364, 1269, 1163, 1137, 1037, 969, 918, 773, 721, 638. GPC (THF, polystyrene standards): the homopolymer gave a peak of $M_n = 3632$ (calculated $M_n = 3404$ Da) and a PDI = 1.09, the copolymer peak $M_n = 37992$ Da (calculated $M_n = 21704$ Da) and PDI = 1.09. (trans 85%, determined by ^1H NMR)

Synthesis of polymer 17 (monomer 7: initiator 2 - 20:1)

Polymer **17** was obtained following the same procedure as for polymer **3** using monomer **7** (0.065g, 0.365 mmol, 20 equiv.) in THF. The resulting white polymer was purified by precipitation in methanol (yield 61%). ^1H NMR (CDCl_3): δ 6.05 (s, br, trans), 5.78 (s, br, cis), 4.98 (s, br, cis), 4.49 (s, br, trans), 3.35 (s, br), 2.97 (s, br). GPC (THF, polystyrene standards): the homopolymer gave a peak of $M_n = 4262$ (calculated $M_n = 3524$ Da) and a PDI = 1.10 (trans 74%, determined by ^1H NMR).

Synthesis of polymer 18 (monomer 7: initiator 2 - 80:1)

Polymer **18** was obtained following the same procedure as for polymer **3** using monomer **7** (0.260g, 1.460 mmol, 80 equiv.) in CH_2Cl_2 . The resulting white polymer was purified

by precipitation in methanol (yield 91%). $^1\text{H NMR}$ (CDCl_3): δ 6.05 (s, br, trans), 5.78 (s, br, cis), 4.98 (s, br, cis), 4.49 (s, br, trans), 3.35 (s, br), 2.97 (s, br). (trans 74%, determined by $^1\text{H NMR}$).

Synthesis of polymer 19 (monomer 8: initiator 2 - 20:1)

Polymer **19** was obtained following the same procedure as for polymer **3** using monomer **8** (0.088g, 0.364 mmol, 20 equiv.) in THF. The resulting grayish beige polymer was purified by precipitation in methanol (yield 64%). $^1\text{H NMR}$ (DMSO-d_6): δ 7.41 (s, br), 7.29 (s, br), 6.03 (s, br, trans), 5.79 (s, br, cis), 5.07 (s, br, cis), 4.64 (s, br, trans), 3.51 (s, br). GPC (THF, polystyrene standards): a peak at $M_n = 2897$ Da (calculated $M_n = 4924$ Da) and PDI= 1.26. (trans 77%, determined by $^1\text{H NMR}$).

Synthesis of copolymer 20 (monomer 8: monomer 1: initiator 2 - 40:20:1)

A solution of catalyst **2** (0.015g, 0.018 mmol) in CH_2Cl_2 (2.5 ml) was sonicated for 5 min. The catalyst solution was transferred to monomer **8** (0.177g, 0.736 mmol, 40 equiv.) in CH_2Cl_2 (2.5 ml) and vigorously stirred for 10 min. A solution of monomer **1** (0.165g, 0.365 mmol, 20 equiv.) in minimum amounts of THF (1 ml) was added. The reaction mixture was stirred for an additional 10 min. and quenched with ethyl vinyl ether (600 equiv). The resulting solution was concentrated by evaporation and precipitated in methanol, yielding a white polymer (yield 76%). $^1\text{H NMR}$ (DMSO-d_6): δ 11.21 (s, br, NH), 7.45-7.28 (phenyl, br), 6.03 (s, br, trans), 5.90 (s, br, trans), 5.79 (s, br, cis), 5.68 (s, br, cis), 5.09 (s, br, cis), 4.87 (s, br, cis), 4.65 (s, br, trans), 4.45 (s, br, trans), 3.52 (s, br).

Synthesis of polymer 21 (monomer 9: initiator 2 - 60:1)

Polymer **21** was obtained following the same procedure as for polymer **3** using monomer **9** (0.241g, 1.095 mmol, 60 equiv.) in THF. The resulting tacky light brown polymer was purified by precipitation in methanol (yield 39%). ¹H NMR (CDCl₃): δ 6.07 (s, br, trans), 5.79 (s, br, cis), 5.01 (s, br, cis), 4.46 (s, br, trans), 3.47 (s, br), 3.32, 1.55 (m, br), 1.32 (m, br), 0.94 (m, br). GPC (THF, polystyrene standards): a peak at M_n = 16258 Da (calculated M_n = 13364 Da) and PDI= 1.20. (trans 82%, determined by ¹H NMR).

Synthesis of copolymer 22 (monomer 1: monomer 9: initiator 2 - 20:150:1)

A solution of catalyst **2** (0.015g, 0.018 mmol) in THF (2.5 ml) was sonicated for 5 min. The catalyst solution was transferred to monomer **1** (0.060g, 0.36 mmol, 20 equiv.) in THF (2.5 ml) and vigorously stirred for 10 min. At that point, half of the reaction mixture was removed from the Schlenk flask, and a solution of monomer **9** (0.302g, 1.35 mmol, 75 equiv.) in THF (2.5 ml) was added. The reaction mixture was stirred for an additional 40 min. and quenched with ethyl vinyl ether (600 equiv). The resulting solution was precipitated in hexanes, yielding a white fluffy polymer (86%). ¹H NMR (CDCl₃): δ 6.07 (s, br, trans), 5.79 (s, br, cis), 5.01 (s, br, cis), 4.46 (s, br, trans), 3.47 (s, br), 3.32 (s, br), 1.56 (s, br), 1.29 (m, br), 0.93 (t, br). GPC (THF, polystyrene standards): the homopolymer gave a peak of M_n = 3572 (calculated M_n = 3404 Da) and a PDI = 1.09, the copolymer peak M_n = 83681 Da (calculated M_n = 36554 Da) and PDI= 1.14. (trans 79%, determined by ¹H NMR)

3.4 ROMP Kinetic Experiment

NMR monitoring of the ROMP of 1

Monomer **1** (0.020g, 0.12 mmol, 10 equiv.) and catalyst **2** (0.010g, 0.012 mmol) were weighed and transferred to an NMR tube under inert atmosphere. Degassed THF-d₈ was cooled to -30°C to prevent any premature polymerization, and then added to the above reagents. ¹H NMR spectra were immediately recorded at 5 min. intervals for 90 min (-5°C, inert atmosphere). Monomer conversion values were obtained by integration of the vinyl peaks of the polymer and monomer. The average molecular weight of the formed polymer was determined by end-group analysis of the vinyl peak of the polymer vs. the phenyl signal of the polymer chain.

3.5 Self-Assembly Studies

Sample preparation-THF/water

Copolymer **11** was dissolved in distilled THF (1 mg / ml) and distilled water was added in a dropwise fashion until turbidity was observed, indicating the onset of aggregation. Turbidity was observed at 17% water content (v/v).

Sample preparation- THF/methanol

Copolymer **11** was dissolved in distilled THF (1 mg / ml) and methanol was added in a dropwise fashion until turbidity was observed, indicating the onset of aggregation. Turbidity was observed at 50% methanol content (v/v).

Transmission electron microscopy sample preparation

The turbid solution was deposited dropwise directly onto copper coated carbon grids (400 mesh). The grids were allowed to dry overnight before direct observation by TEM.

TEM staining experiments

TEM grids with deposited turbid solution were allowed to dry for one hour, then exposed to CsOH 0.1N (or uranium acetate 2% in water) for approximately one minute, and gently washed with distilled water.

3.6 Hydrogen Bonding Studies

Monomer 1 binding studies with 2,6-diaminopyridine 12

Monomer 1 (100 mg, 0.604 mmol) was mixed with 2,6-diaminopyridine (67 mg, 0.604 mmol) in CHCl₃ (25 ml), and stirred at 40°C for 1h. The solvent was removed under vacuum and the solid dissolved in CDCl₃. The hydrogen bonding was confirmed by ¹H NMR. Monomer 1: ¹H NMR (CDCl₃): δ 8.12 (s, 1H, NH), 6.51 (s, 2H), 5.31 (s, 2H), 2.87 (s, 2H). 2,6-diaminopyridine: ¹H NMR (CDCl₃): δ 7.22 (d, 1H), 5.90 (d, 2H), 4.08 (br, 4H) Hydrogen bonded dyad: ¹H NMR (CDCl₃): δ 9.38 (s, 1H, NH, downfield shift of 1.26), 7.21 (d, 1H), 6.52 (s, 2H), 5.85 (d, 2H), 5.31 (s, 2H), 4.56 (br, 4H, downfield shift of 0.48), 2.87 (s, 2H).

Monomer 1 binding studies with bis-propionyl-2,6-diaminopyridine 13

Monomer 1 (10 mg, 0.060 mmol) was mixed with bis-propionyl-2,6-diaminopyridine (10 mg, 0.060 mmol) in CHCl₃ (20 ml), and refluxed for 1h. The solvent was removed under vacuum and the solid dissolved in CDCl₃. The hydrogen bonding was confirmed by ¹H

NMR. Monomer 1: ^1H NMR (CDCl_3): δ 8.12 (s, 1H, NH), 6.51 (s, 2H), 5.31 (s, 2H), 2.87 (s, 2H). Propionyl-2,6-diaminopyridine: ^1H NMR (CDCl_3): 7.78 (br, 3H), 7.69 (br, NH), 2.60 (m, 2H), 1.26 (m, 3H). Hydrogen bonded dyad: ^1H NMR (CDCl_3): δ 9.51 (s, 1H, NH, downfield shift of 1.39 ppm), 8.20 (br, 2H, downfield shift of 0.51), 7.91 (br, 2H), 7.71 (br, 1H), 6.53 (s, 2H), 5.22 (s, 2H), 2.92 (s, 2H), 2.50 (m, 2H), 1.25 (m, 3H).

Monomer 1 binding studies with undecyl-diaminotriazine 14

Monomer 1 (10 mg, 0.060 mmol) was mixed with undecyl-diaminotriazine (16 mg, 0.060 mmol) in CHCl_3 (25 ml), and refluxed for 2h. The solvent was removed under vacuum and the solid dissolved in CDCl_3 . The hydrogen bonding was confirmed by ^1H NMR. Monomer 1: ^1H NMR (CDCl_3): δ 8.12 (s, 1H, NH), 6.51 (s, 2H), 5.31 (s, 2H), 2.87 (s, 2H). undecyl-diaminotriazine: ^1H NMR (CDCl_3): 3.52 (br, 4H), 2.72 (m, 2H), 1.61 (m, 2H), 1.25 (m, 16H), 0.87 (t, 3H). Hydrogen bonded dyad: ^1H NMR (CDCl_3): δ 11.35 (s, 1H, NH, downfield shift of 3.23), 6.52 (s, 2H), 5.79 (s, 4H, downfield shift of 2.27), 5.31 (s, 2H), 2.89 (s, 2H), 1.68 (br, 2H), 1.24 (br, 16H), 0.87 (br, 3H).

HPLC binding studies

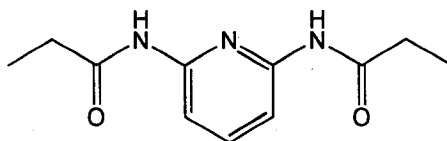
Stock solutions (2.91 mmol per litre) of each guest molecules (C, T, A, caffeine) were prepared using (THF- 17% water (v/v)) as the solvent. 0.25 ml of each stock solution (0.73 μmol of each guest molecule) were combined in one vial. HPLC injection of the guest mixture provided initial relative peak integrations based on caffeine (the internal standard). HPLC studies were conducted on a HP series 1100, equipped with a C18 column, running at 0.800 ml/min. A solvent gradient was used as the eluent: 10% MeOH-90% H_2O for the first 7 min. followed by 100% MeOH. 5 mg (29 μmol) of polymer 3

was then suspended in the guest solution and centrifuged for 30 min. The polymer was removed and the guest containing solution was injected again, and peak integration was evaluated and compared with the initial values.

3.7 Guest Synthesis

Synthesis of bis-propionyl-2,6-diaminopyridine 13

The guest was synthesized following literature procedures.⁴⁹ Crystallization from diethyl ether (and minimum amounts of CHCl_3) was required. Light yellow crystals were obtained. (yield 29%) ^1H NMR (CDCl_3): 7.78 (br, 3H), 7.69 (br, NH), 2.60 (m, 2H), 1.26 (m, 3H).



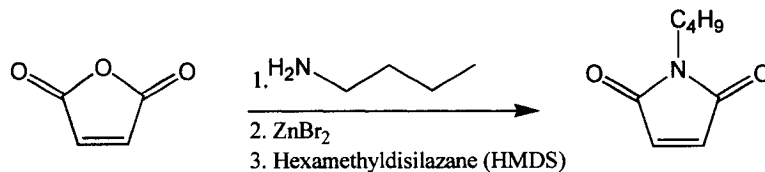
13

3.8 Attempted Synthesis

Synthesis of monomer 9 using N-butylmaleimide

a) Synthesis of N-butylmaleimide (equation 7)

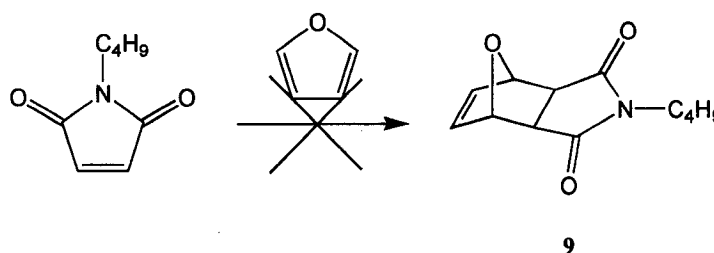
N-butylmaleimide was synthesized according to a literature procedure.⁷⁴ The procedure was scaled up 6 times. Purification was carried out using column chromatography (SiO_2) with hexanes/EtOAc (7:3). The product was isolated as a light yellow oil. (yield 33%) ^1H NMR (CDCl_3): 6.65 (s, 2H), 3.49 (t, 2H), 1.55 (m, 2H), 1.30 (m, 2H), 0.91 (t, 3H).



Equation 7

b) Diels-Alder reaction between furan and N-butylmaleimide (equation 8)

Preparation of monomer **9** was attempted according to literature methods.⁷⁰ N-butylmaleimide (704 mg, 3.2 mmol) and furan (217 mg or 0.25 ml, 3.2 mmol) were dissolved in 10 ml of dry diethyl ether in a heavy-walled flask equipped with a Teflon seal. The mixture was sealed under reduced pressure and stirred at 90°C overnight. Very little product was obtained after evaporation of the solvent (it remained soluble in diethyl ether). NMR analysis revealed that it was not the desired product.

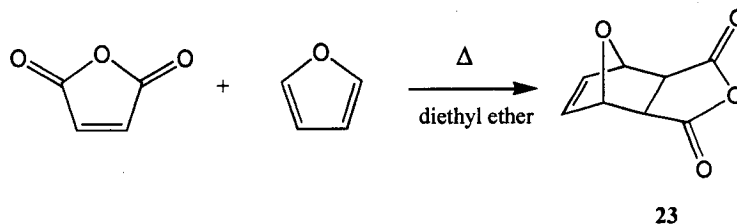


Equation 8

Synthesis of monomer 9 using oxanorbornene anhydride

a) Synthesis of oxanorbornene anhydride **23** (equation 9)

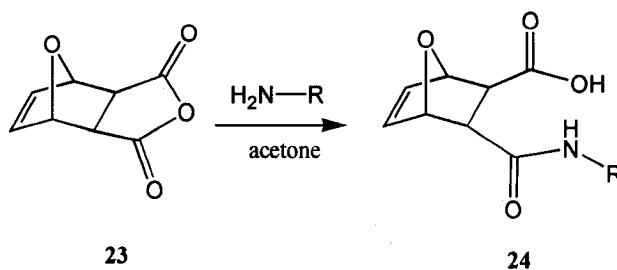
Maleic anhydride (20g, 204 mmol) and furan (28 ml, 408 mmol) were dissolved in diethyl ether. The reaction mixture was refluxed overnight. A white solid precipitated out of solution and was washed with diethyl ether. (yield 68%) ¹H NMR (DMSO-d₆): 6.55 (s, 2H), 5.32 (s, 2H), 3.29 (s, 2H). NMR revealed that only the *exo* isomer was formed.¹⁷



Equation 9

b) Ring opening of **23** and nucleophilic substitution (equation 10)

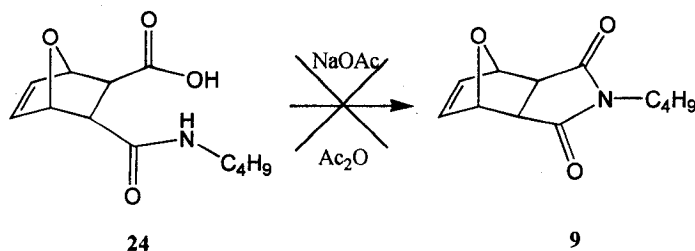
Oxanorbornene anhydride **23** (5g, 30 mmol) and butylamine (2.2g, 30 mmol) were dissolved in acetone at room temperature and stirred for 1hr. A product precipitated out of the solution and was washed with acetone. Product **24** was isolated as a white powder (very hygroscopic). (yield 74%) $^1\text{H NMR}$ (DMSO- d_6): 12.10 (NH), 7.37 (OH), 6.41 (d, 2H), 5.05 (s, 1H), 4.84 (s, 1H), 2.99 (m, 2H), 2.53 (s, 2H), 1.33 (m, 2H), 1.24 (m, 2H), 0.84 (t, 3H).



Equation 10

c) Ring closing (condensation reaction) of **24** (equation 11)

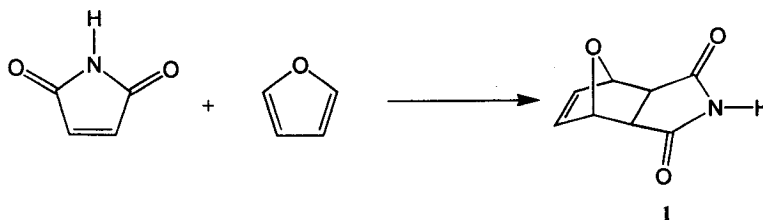
Adduct **24** (3g, 12.5 mmol) and sodium acetate (0.57g, 6.9 mmol) were mixed in acetic anhydride (50 ml) at 80°C . The reaction mixture was stirred for 2hrs. The color of the mixture changed from turbid to colorless to dark yellow. The mixture was poured in water and extracted with 3X 20 ml CHCl_3 . The organic phase was then washed 4X with 10% sodium bicarbonate in water. The final organic phase was dried over MgSO_4 .



Equation 11

Evaporation of the solution yielded a dark brown oil. TLC revealed the presence of at least 4 products. Column chromatography was attempted but the desired product could not be isolated.

4.1 Monomer Synthesis



Equation 12

Monomer **1** can be readily synthesized via a Diels-Alder reaction between furan and maleimide. (Equation 12) The exo isomer, the thermodynamic product, is preferentially formed at high temperature.¹⁷ The formation of a single isomer is necessary if one wants to obtain a well-behaved polymerization. The undesirable endo isomer is much less reactive, due to the fact that the catalyst approach is sterically encumbered. In general, the polymerization of such endo isomers will lead to polymers with broad molecular weight distribution.⁷³ The simple synthesis leads to an extremely versatile functional monomer. Monomer **1** can be considered as a thymine (T)/uracil (U) analog since it possesses the same hydrogen bonding motif. (chart 3)

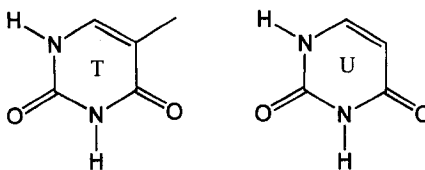
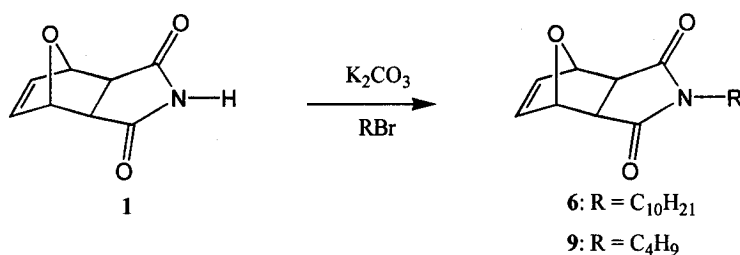


Chart 3

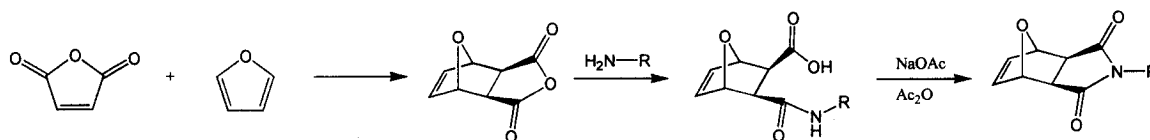
In addition, monomer **1** may act as a building block for the synthesis of comonomers bearing pendant alkyl chains. Two monomers were obtained from monomer **1**, one bearing a pendant 4 carbon-chain while the other possessing a 10 carbon-alkyl chain. The synthesis was achieved by deprotonation of the imide using K_2CO_3 followed by nucleophilic attack on the corresponding alkyl halide (butyl bromide or decyl

bromide). (Equation 13) The monomer bearing the 10 carbon-alkyl chain is previously unreported and its structure was confirmed by ^1H NMR, ^{13}C NMR, as well as elemental analysis. It is of note that a similar monomer bearing an 8 carbon-chain has been reported by Grubbs and coworkers.³³ These monomers were synthesized with the objective of incorporating them into copolymers bearing the thymine/uracyl analog (monomer 1), hopefully leading to the formation of novel nanoscale morphologies.



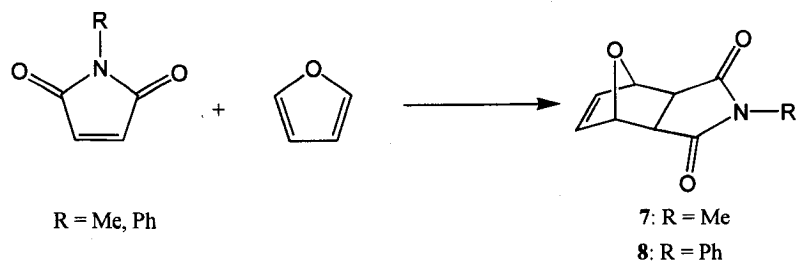
Equation 13

While the synthetic method used for generating these various monomers is straightforward, the cost of maleimide might prove prohibitive for larger scale synthesis. This prompted the design of an alternate (and less costly) synthetic scheme. For instance, inexpensive and readily available maleic anhydride can be used to form an oxanorbornene adduct when reacted with furan. This adduct can be readily synthesized in large scale reactions. Further reaction with the proper amine (butyl amine or decyl amine) followed by a condensation reaction (using a dehydrating agent) would yield the corresponding monomers. (Scheme 27) Unfortunately, various attempts using this procedure did not lead to the desired product, likely due to the high water sensitivity of the final step of the



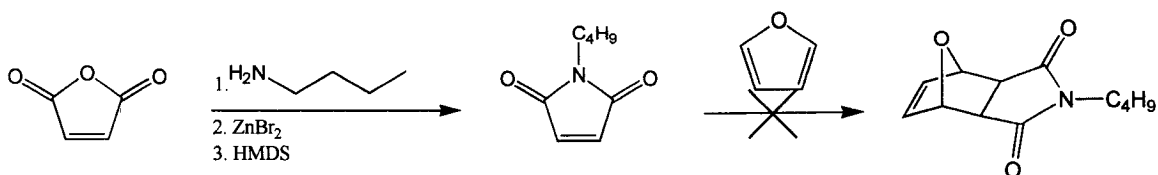
Scheme 27: Synthetic strategy for alkylated monomers

reaction (water is eliminated, therefore trace amounts of water can push the equilibrium to the reagents side).



Equation 14

In contrast, monomers bearing a methyl and phenyl group on the nitrogen are easily accessible via Diels-Alder reactions following analogous conditions used for the synthesis of monomer **1**.⁷⁰ (Equation 14) In addition, large scale synthesis would be possible due to the relatively low cost of the corresponding N-substitutedmaleimides. An analogous synthetic route was explored for the synthesis of N-butylmaleimide for subsequent coupling with furan, to generate monomer **9**. This alternate route would prove less costly (again starting from maleic anhydride) and possibly more appealing for projects involving larger quantities of polymers or copolymers with higher monomer to initiator ratios. N-butylmaleimide was successfully synthesized in a one-step procedure, by reacting maleic anhydride with butylamine in the presence of zinc dibromide and hexamethyldisilazane (HMDS).⁷⁴ (Scheme 28) Unfortunately, the subsequent Diels-Alder reaction with furan failed and monomer **9** could not be synthesized using this pathway.



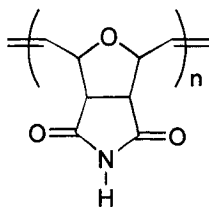
Scheme 28

4.2 Polymer Synthesis and Characterization

4.2.1- Biomimetic Homopolymer

The ring-opening metathesis polymerization of **1** (20 equiv.) was investigated using catalyst **2** in THF at room temperature. Monomer **1** is a thymine/uracyl analog that is expected to exhibit molecular recognition behavior and possibly DNA-like cooperative binding once incorporated into a polymer.¹⁴ In addition, it has shown antitumor activity, and its N-substituted derivatives are potent phosphatase inhibitors.^{11,12}

Upon catalyst addition to the monomer solution, the initially purple solution changed to brown within seconds, indicating catalyst initiation.¹ The reaction mixture was stirred for 10 min. to ensure complete monomer conversion, and then quenched with the addition of ethyl vinyl ether. Polymer **3** was isolated as a light gray solid by precipitation in methanol, and was characterized by ¹H, ¹³C NMR, FTIR and gel permeation chromatography. GPC analysis showed a single peak at $M_n = 4217$ Da (calculated $M_n = 3404$), with a low polydispersity of 1.05, suggesting the living nature of this ROMP reaction.



3

The polymerization of **1** with catalyst **2** was monitored by ¹H NMR in THF-d₈. At room temperature, the reaction was extremely rapid, and both monomer **1** and catalyst **2** were consumed within ca. 3 min. A new ruthenium alkylidene signal appeared at 18.9 ppm, which was assigned to the α -alkylidene proton of the propagating polymer chain

(based on literature precedent).¹ This peak persisted after disappearance of monomer **1**, suggesting the living nature of this polymerization. In addition, the dependence of the polymer molecular weight on monomer conversion was evaluated. The ROMP reaction of monomer **1** (10 equiv.) with catalyst **2** was monitored by ¹H NMR in THF-d₈ at -5°C under inert atmosphere. At this temperature, the kinetics were significantly slower, and monomer conversion was complete after ca. 90 min. The relatively low monomer to initiator ratio (10 equiv.) was necessary, in order to prevent any precipitation of the polymer at -5°C. Analysis of the spectra revealed a clear linear dependence of the average molecular weight of the polymer (obtained by end-group analysis) on monomer conversion, providing strong evidence for the living character of this polymerization.⁷⁵ (Figure 1) The ROMP of **1** generated polymers with remarkably low polydispersities using monomer to initiator ratios in the range of 10-30.⁷⁶

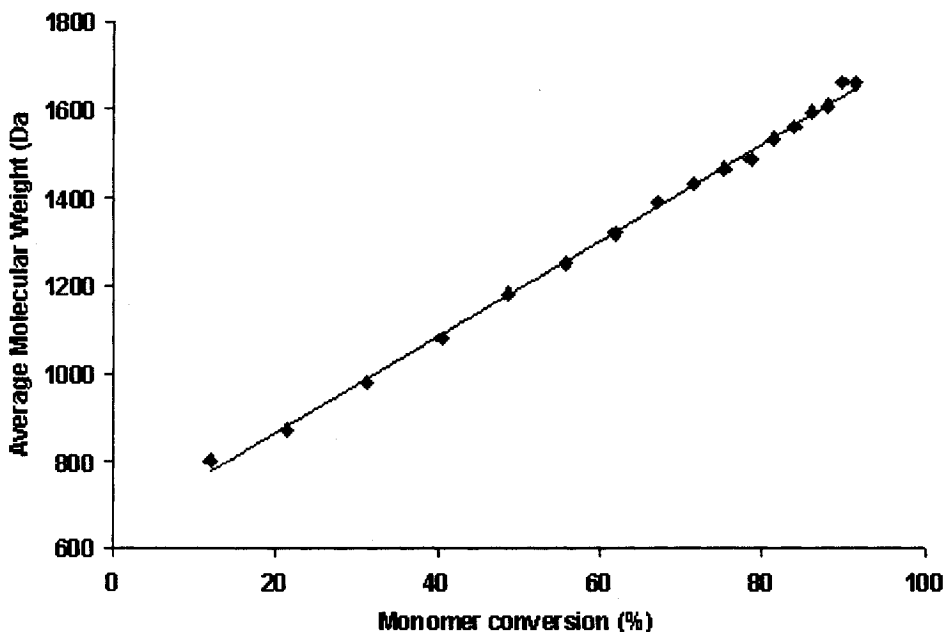
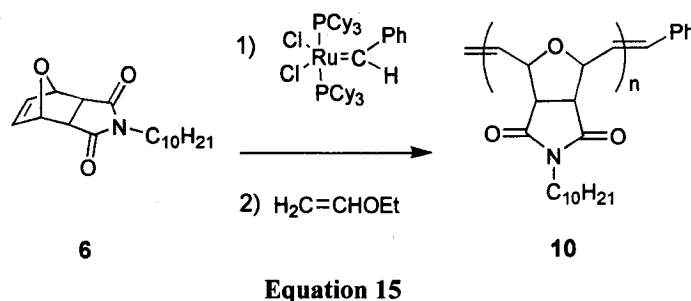


Figure 1: Average molecular weight distribution vs monomer conversion for the polymerization of **1**

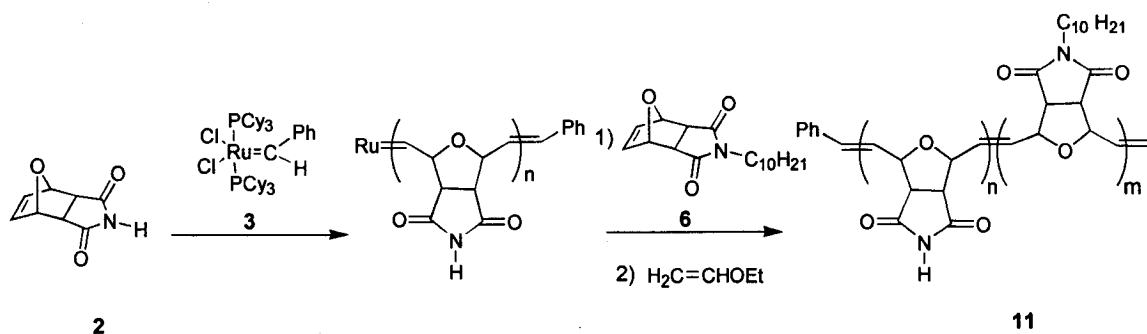
4.2.2- Biomimetic Block Copolymer

Further evidence for the living nature of this ROMP reaction came from the facile generation of a block copolymer containing monomer **1**. We used comonomer **6**, which bears a long alkyl chain (C₁₀) on the imide nitrogen. This monomer was designed specifically to increase the solubility of polymers bearing the molecular recognition motifs and to favor polymer self-assembly. We first established that monomer **6** could be efficiently incorporated into block copolymers by carrying out the homopolymerization using catalyst **2**.³³ (Equation 15) The resulting polymer **10** was isolated as a beige solid and characterized by ¹H, ¹³C NMR, FTIR and GPC. GPC analysis showed a monomodal distribution and a peak located at M_n = 22161 Da (calculated M_n = 18404 Da), with a PDI of 1.08.



The synthesis of block copolymer **11** was carried out by allowing monomer **1** (20 equiv.) to react with catalyst **2** in THF at room temperature for 10 min. Half of the reaction mixture was then removed and quenched with ethyl vinyl ether. The resulting homopolymer of **1** displayed a narrow molecular weight distribution by GPC (M_n = 3404 Da, PDI = 1.09). Monomer **6** (30 equiv.) in THF was then added to the remaining reaction mixture. After an additional 10 min, the polymerization was quenched with ethyl vinyl ether, and **11** was isolated by precipitation in methanol. (Scheme 29) Copolymer **11** was characterized by ¹H, ¹³C NMR, FTIR and GPC. GPC analysis of **11**

showed the disappearance of the homopolymer peak at $M_n = 3404$ Da, and the presence of a single peak at $M_n = 37992$ Da (calc. 21704 Da) and PDI=1.09. (Figure 2)



Scheme 29: Copolymer Synthesis

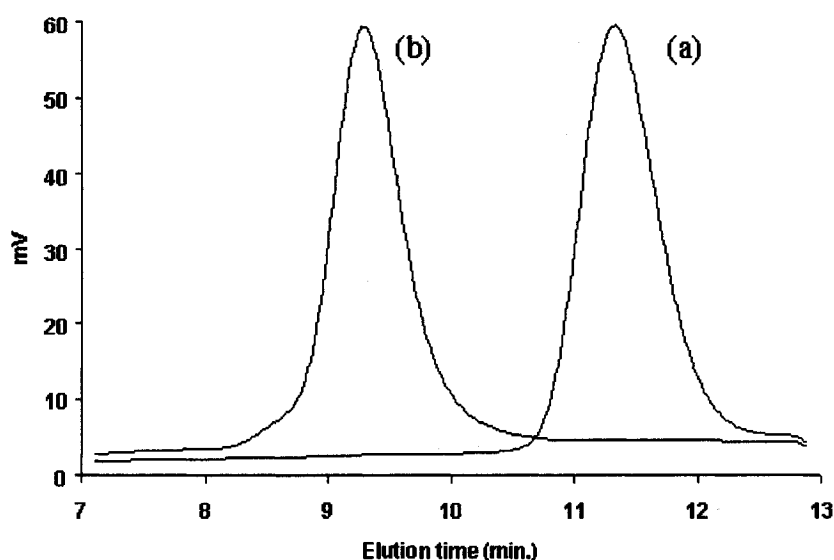


Figure 2: Comparison of GPC traces for (a) homopolymer of 1 and (b) block copolymer 11

The difference between experimental and calculated M_n values may be the result of hydrogen bond mediated folding or aggregation of copolymer 11, thus leading to an increase in its hydrodynamic radius, compared to the linear GPC polystyrene standards. It is of note that the ROMP of monomer 1 results in homopolymers and block copolymers which display some of the lowest polydispersities reported for ROMP polymers using the Grubbs catalyst 2.²⁷ The ease of generation of these polymers (<10 min. at room

temperature), and the readily functionalizable imide moiety (*vide supra*), makes these polymers extremely useful starting materials for conjugation with bioactive molecules,⁷⁷ as well as other functional units.⁷⁸

4.3 Self-Assembly Studies of the Biomimetic Copolymer

4.3.1- Self-Assembly in THF-Water Solvent System

Copolymer **11** is composed of two very distinct blocks. The poly(**6**) block contains long pendant alkyl chains, which confer it with a high degree of hydrophobicity. In contrast, the poly(**1**) block contains the biologically relevant and somewhat hydrophilic dicarboximide units. The presence of two dissimilar blocks in a copolymer can give rise to self-assembly in particular solvent systems. In order to probe for this behavior, copolymer **11** was dissolved in THF, and water was added dropwise until a turbid solution was obtained (17% v/v water content). Light scattering was rapidly observed upon water addition, indicating the onset of aggregation. Dynamic light scattering (DLS), executed at multiple angles (45°, 90°, 135°) confirmed the presence of spherical particles with an average diameter of 200 nm. (Figure 3)

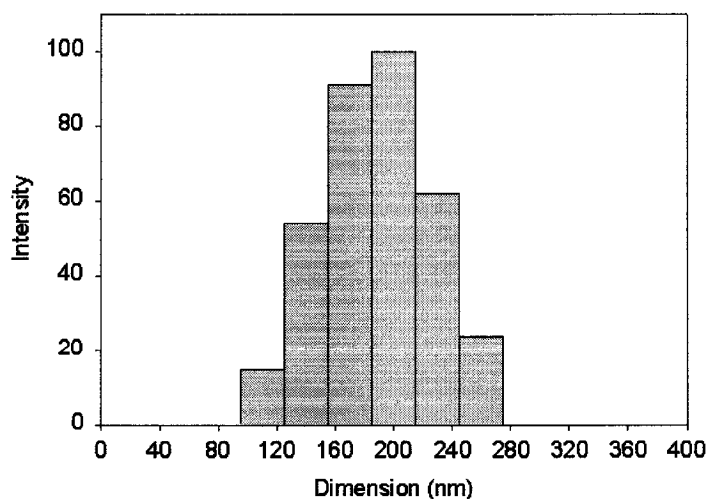


Figure 3: DLS of copolymer **11** in THF / water (17% v/v) (NNLS at 90°)

The morphology of copolymer **11** was further characterized by transmission electron microscopy (TEM). (Figure 4) Samples were prepared by allowing a drop of the turbid solution to evaporate on a carbon-coated copper grid. TEM studies revealed the formation of large micellar aggregates of spherical shape. Image analysis of these particles revealed an average size of 100-300 nm, in agreement with the values obtained by DLS. The particle size is too large for individual micelles, indicating that these spherical aggregates may be large compound micelles (LCM).⁶¹

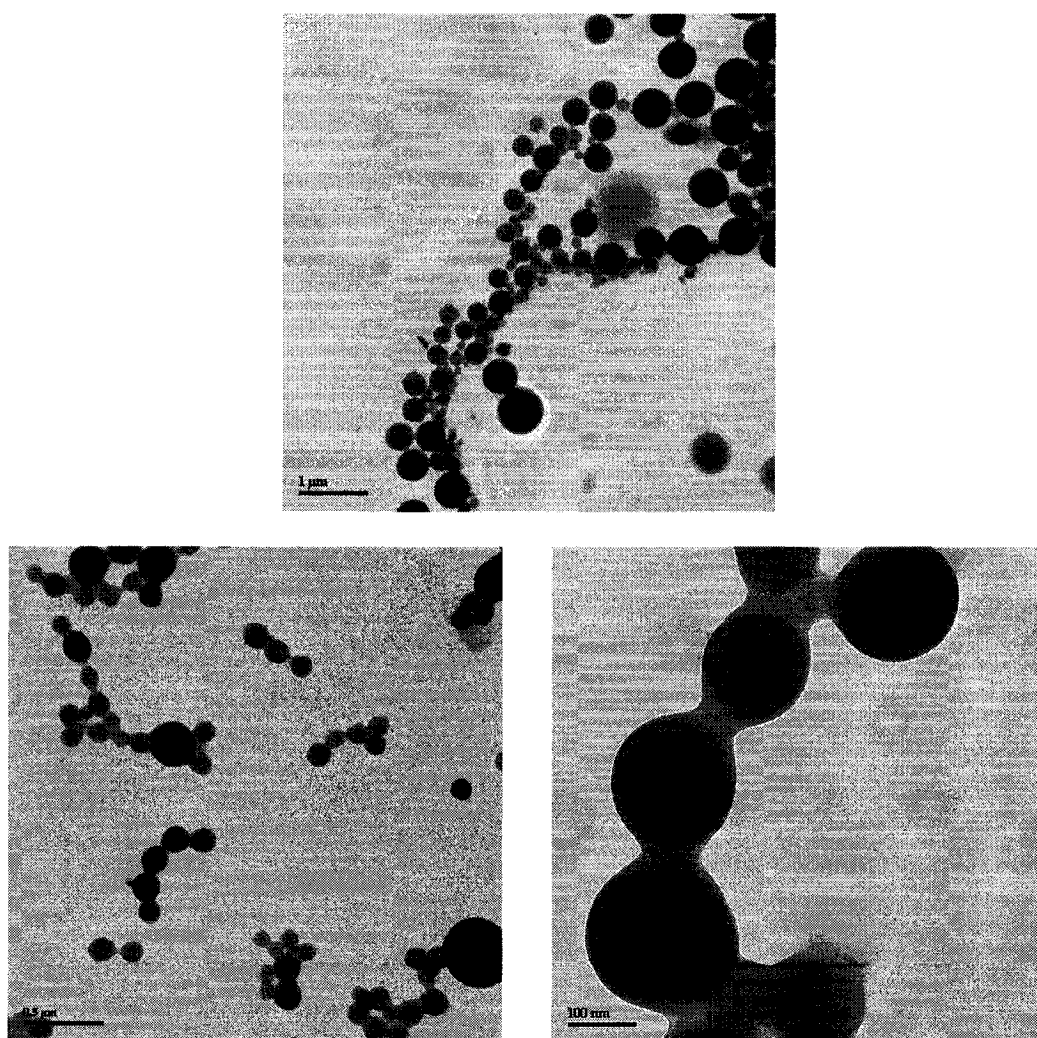
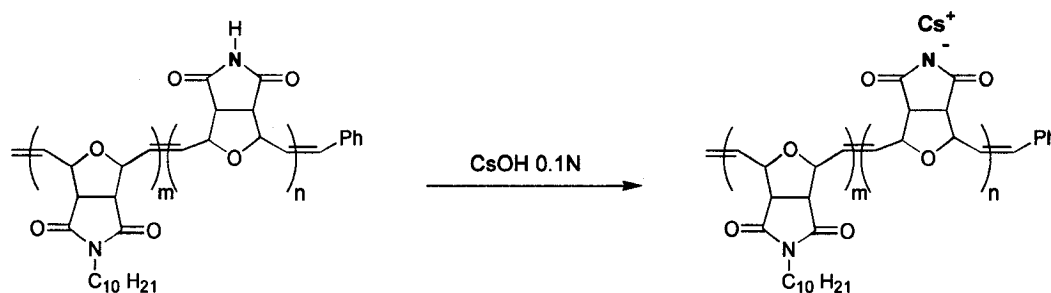


Figure 4: TEM images of copolymer **11** deposited from a THF / water (17% v/v) solution

Interestingly, the observed spherical particles further aggregate into a network of interconnected spheres (commonly referred to as pearl necklaces). The pearl necklace morphology has been previously observed, and has been interpreted as a possible intermediate morphology between spherical and rod-like aggregates.^{63,79}

4.3.2- TEM Staining Experiments



Equation 16

It is expected that in the THF/H₂O mixture, block copolymer **11** aggregates in order to minimize the interaction of the hydrophobic block poly(**6**) with the polar medium, and to expose the more hydrophilic poly(**1**). The dicarboximide units are therefore likely located on the exterior of these nanoscale structures. In order to test this assumption, preliminary TEM studies were carried out using cesium hydroxide as a staining agent. CsOH is expected to deprotonate the dicarboximide moiety, thus providing a preferential staining method for the poly(**1**) block. (Equation 16) The turbid solution containing the micellar aggregates (in THF / water (17% v/v) solution) was deposited onto a TEM grid and allowed to dry. The grid was then immersed into a solution of CsOH (0.1N) for 1 min., and rinsed gently in distilled water, in order to remove any excess CsOH. TEM analysis revealed significant darkening of the spherical aggregates, indicating the likely deprotonation of the imide moieties on the outer surface of the spherical particles.⁸⁰ (Figure 5) This surface localization of the hydrogen bonding

dicarboximide moieties is potentially well suited for molecular recognition studies using block copolymer **11** with complementary receptors.

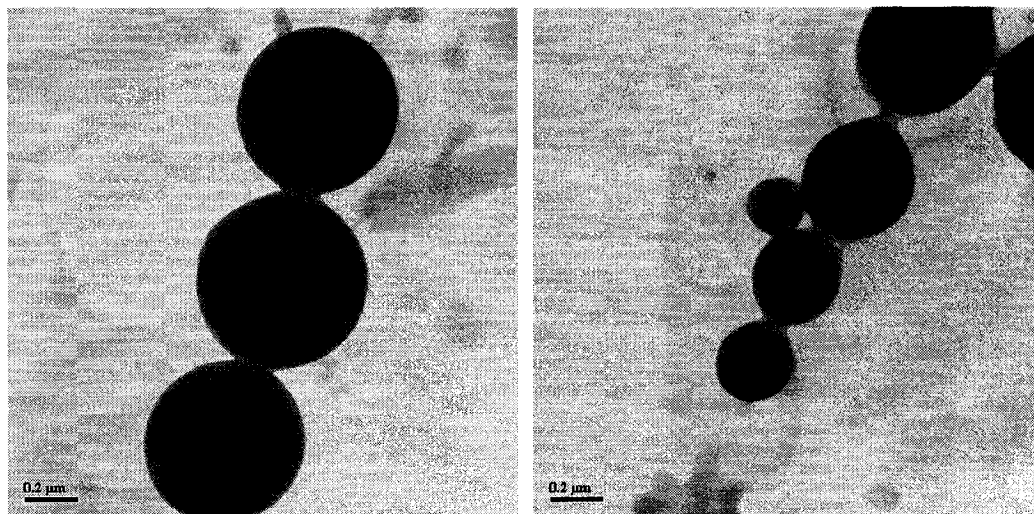


Figure 5: TEM images of copolymer **11** deposited from a THF / water (17% v/v) solution stained with CsOH 0.1N

It is worth mentioning that staining experiments of the hydrophobic block were attempted using uranium acetate. The procedure used is similar to the CsOH staining experiment. However, upon exposure to the staining agent, no noticeable difference was observed by TEM. This could suggest that the hydrophilic surface prevents the diffusion of uranium acetate to the core of the aggregates (where the hydrophobic blocks are likely located), thus strengthening the assumption that LCMs are obtained.

4.3.3- Self-Assembly in Other Solvent Systems

During the exploratory studies leading to the copolymer self-assembly, various solvent systems were tested. While the mixture of THF and water clearly lead to the formation of nanoscale aggregates, other solvents such as CHCl_3 and CH_2Cl_2 did not yield conclusive results. However, we believe that copolymer **11** may form aggregates of micellar nature in CH_2Cl_2 . The corona forming block would be hydrophobic, thus forming reverse micelles. Dynamic light scattering (DLS) studies showed that copolymer

11 could form aggregates in CH_2Cl_2 of ca. 135 nm with a rather large size distribution. Transmission electron microscopy could not confirm the presence of these aggregates (likely due to the nature of the solvent).

In search of a different solvent system that would promote self-assembly, copolymer **11** was dissolved in THF (1mg/ml), and methanol (instead of water) was added in a dropwise fashion until a faint turbidity was observed, indicating the onset of aggregation. A large volume of methanol (as opposed to water) was required to obtain a turbid solution. A ratio of 1:1 THF/methanol was necessary.

This considerably high methanol ratio rendered the identification of the core and corona of the spherical aggregates more problematic. We believe that due to large amount of non-solvent (methanol), the solvent system might yield a variety of nanoscale morphologies which may not be kinetically frozen. Nevertheless, transmission electron micrographs showed that spherical aggregates of considerable size were formed (confirmed by DLS with an average size of 200 nm). (Figure 6) These aggregates are similar (in shape and size) to those formed in the THF/water mixture mentioned earlier.

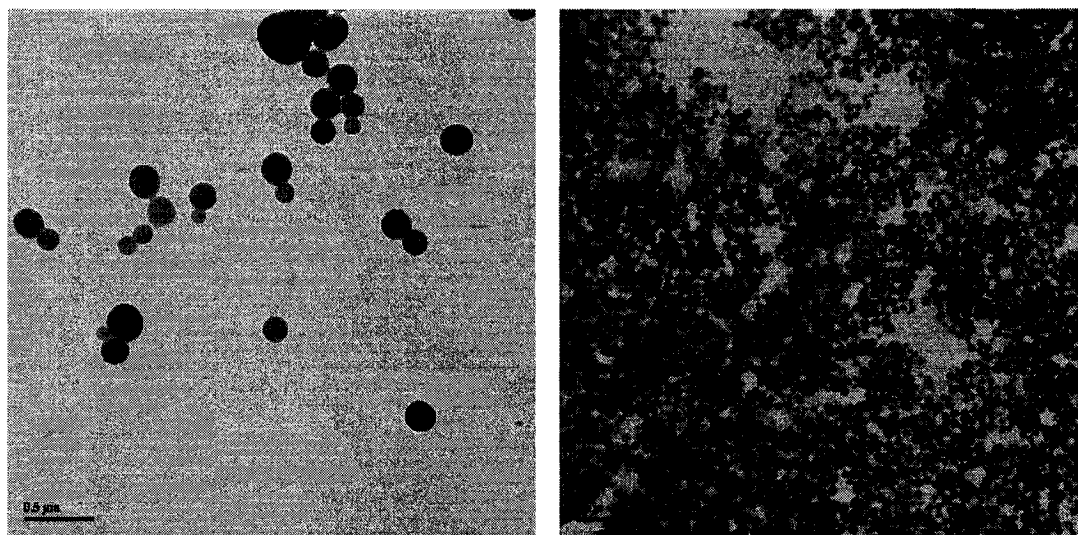
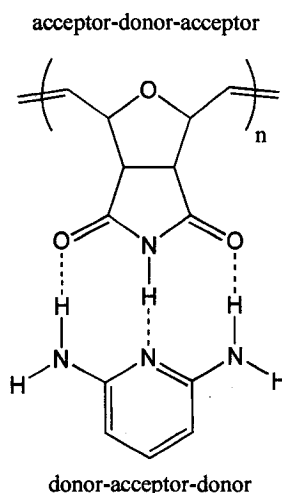


Figure 6: TEM images of copolymer **6** deposited from a THF / MeOH (1:1) solution

4.4 Molecular Recognition Properties

4.4.1- Molecular Recognition between Monomer and Guest Molecules

Our biomimetic polymers are designed to mirror intrinsic DNA properties. Therefore, it is expected that they will be capable of selective hydrogen bonding (i.e. molecular recognition). The three-point hydrogen bonding motif located at the dicarboximide functionality, consists of an acceptor-donor-acceptor (ADA) pattern. This particular binding motif is analogous to the DNA/RNA base thymine (T) and uracil (U), which preferentially bind complementary molecules such as 2,6-diaminopyridine. (Scheme 30)



Scheme 30: Complementary H-bonding

For ease of characterization, initial molecular recognition assays were performed using monomer **1**. Binding studies were conducted using various complementary guests (containing the DAD hydrogen bonding pattern) in CHCl_3 , a non-hydrogen bonding solvent. Although quite polar, chloroform is used because it is the only non-hydrogen bonding solvent capable of dissolving monomer **1** to a sufficient extent (necessary for characterization purposes). Ideally, due to low solvent polarity, benzene or toluene would have been used, thus allowing for stronger hydrogen bonding between host and guest.

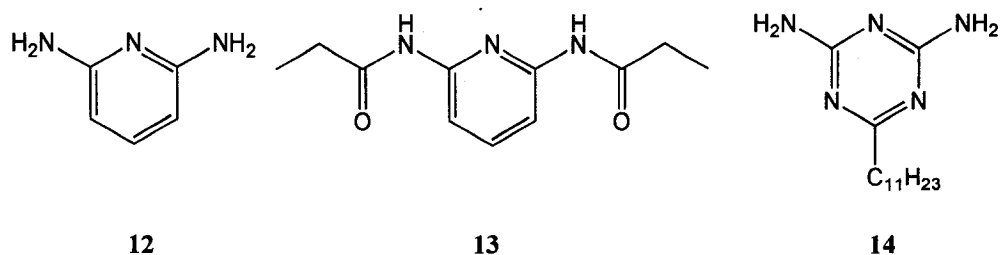


Chart 4

Upon refluxing the host molecule (monomer **1**) and each of the complementary guests (in a 1:1 ratio): 2,6-diaminopyridine (**12**), bis-propionyl-2,6-diaminopyridine (**13**) and undecyl-diaminotriazine (**14**) in CHCl_3 , the solution became increasingly homogeneous. (Chart 4) This behavior is a likely indication of the formation of hydrogen bonded soluble dyads. It is of note that 2,6-diaminopyridine **12** and undecyl-diaminotriazine **14** are both commercially available. On the other hand, the bis-propionyl diaminopyridine **13** was generated following literature procedures.⁴⁹

Following solvent removal, the solids were dissolved in CDCl_3 and ^1H NMR spectra were taken. NMR spectroscopy was chosen since it can easily establish the presence of hydrogen bonding by monitoring any downfield shifts of the protons of interest. Considerable downfield shift of the imide proton of monomer **1** was observed in presence of guest molecules (vs. monomer **1** by itself). (Table 1)

Table 1: ^1H NMR analysis of hydrogen bonded dyad with monomer **1**

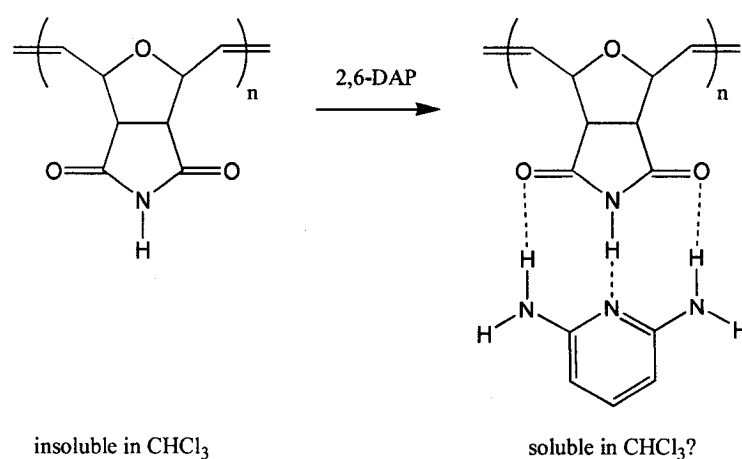
Guest molecule	Observed imide shift of monomer 1
2,6-diaminopyridine (12)	8.2 to 9.4 ppm
Bis-propionyl-2,6-diaminopyridine (13)	8.2 to 9.5 ppm
Undecyl-diaminotriazine (14)	8.2 to 11.3 ppm

The significant downfield shifts are an indication that once incorporated into a polymeric structure, the dicarboximide moiety of monomer **1** is likely to promote molecular recognition. The greater downfield shift resulting from binding of monomer **1** with undecyl-diaminotriazine **14** might be related to a considerable gain in solubility of the resulting dyad. This result indicates that molecular recognition may be partially driven by the dissolution of the non-covalently linked complex, as compared to the unbound molecules. This, in turn, may prove helpful in favoring binding with the polymeric receptor.

4.4.2- Molecular Recognition between Polymers and Guest Molecules

4.4.2.1 Direct NMR characterization

Molecular recognition studies (using ^1H NMR) between monomer **1** and various guest molecules generated conclusive results. Therefore, it was assumed that similar NMR studies could be performed on polymer **3** exposed to guests **12**, **13** and **14**. These studies were expected to reveal significant downfield shifts of the imide proton of the homopolymers (when exposed to complementary guests), thus confirming the presence of molecular recognition.



Equation 17

Unfortunately, unlike monomer **1**, the homopolymers **3a**, **3b**, **3** (with an average of 10, 15 and 20 repeating units) proved completely insoluble in any non-hydrogen bonding solvents such as CHCl_3 , CH_2Cl_2 , toluene and benzene. Nevertheless, some NMR studies were attempted with the hope that binding (between the polymer and guest) could lead to an increase in solubility of the resulting polymer-guest complex. (Equation 17) An increase in solubility could likely be detected by an appearance of new polymer related signals in the NMR spectra.

The experiments were performed using various deuterated non-hydrogen bonding solvents, at room temperature, with additional refluxing and cooling, and with extensive stirring (up to many days). No changes in the NMR spectra were observed, under any of these conditions. Hydrogen bonding involving polymer **3** and any guest molecules could not be characterized due to the lack of solubility of the polymers in non competitive solvents. Consequently, molecular recognition assays involving the dissolution of the polymer could not be performed.

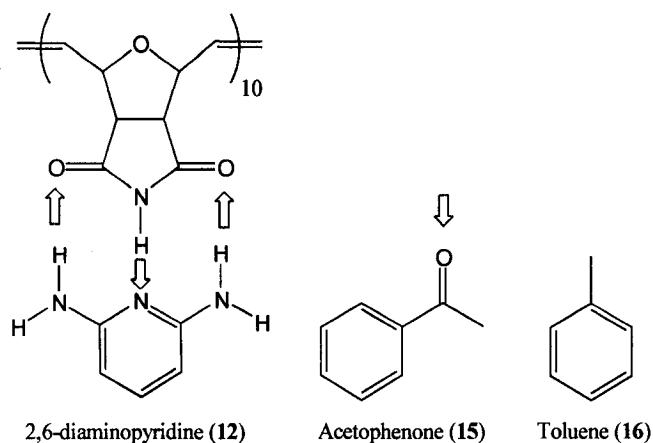
In response to the lack of solubility of the homopolymers, diblock copolymers were designed to overcome this obvious obstacle. A considerable solubility gain was observed in CHCl_3 , CH_2Cl_2 , toluene and benzene for copolymer **11**. This can be simply rationalized by considering the pendant alkyl chains on the new polymer block, which largely contribute to the solubility gain. Such solubility gains prompted us to perform ^1H NMR experiments involving copolymer **11** and various guests, to probe for possible molecular recognition behavior.

Unfortunately, due to the micellar nature of block copolymer **11**, complications quickly arose in the characterization of molecular recognition using ^1H NMR in non-hydrogen bonding solvents (CHCl_3 , CH_2Cl_2 , benzene). It is believed that in an organic

guest as uracil (U) or thymine (T) in the presence of cytosine (C) and pyrimidine could be selectively adsorbed onto the insoluble polymer matrix.

This study leads to the possibility of performing molecular recognition experiments using insoluble polymers. The driving force for such selective adsorption is believed to be due to the presence of complementary multi-point hydrogen bonding coupled with the creation of a hydrophobic microenvironment, a consequence of the nature of the polymer. The selective adsorption studies were conducted using HPLC. However, for initial proof of concept, we decided to design a similar experiment based on NMR spectroscopy.

Polymer **3a** (average of 10 repeating units), which is totally insoluble in benzene- d_6 , was used for selective adsorption studies. Adsorption measurements were taken by referencing against tetramethylsilane (TMS). Due to the presence of many peaks related to various guest molecules, initial studies were conducted with only a single guest molecule exposed to the insoluble polymer per experiment. Competitive binding could not be performed with more than two guest molecules (at a time). Such constraint is due to the large number of signals in the NMR spectra (which can easily overlap). The guest



Scheme 31

molecules used throughout these studies (2,6-diaminopyridine (**12**), acetophenone (**15**) and toluene (**16**)) were individually dissolved in benzene- d_6 in the presence of TMS. (Scheme 31, the arrows signify the presence of a hydrogen bonding acceptor or donor site) An initial spectrum was taken for every guest by measuring the corresponding peak integration (vs. TMS). At that point, the NMR tube was opened briefly and polymer **3a** was quickly added to each guest containing solution.

Upon addition of the insoluble polymer to the guest containing solutions, NMR spectra were collected over approximately 30 min. to allow the system to reach equilibrium. A 1:1 ratio guest/polymer recognition site was used throughout the experiments. Therefore, it was expected that an adsorption percentage of 100% could not be obtained, due to the coiled nature of polymers. We believe that only a fraction of the polymer recognition sites are available for proper guest binding.

Initial experiments revealed a much greater adsorption percentage for 2,6-diaminopyridine. Considering that 2,6-diaminopyridine (**12**) is capable of three-point hydrogen bonding, these results were expected. In addition, acetophenone (**15**) which possess one hydrogen bonding site did bind to a greater extent than toluene (which has no binding sites). (Table 2)

Table 2: Evaluation of selective adsorption of guest on polymer of **1**

Guest molecule	Initial NMR integration ratio guest/TMS	Final NMR integration ratio guest/TMS	Guest adsorption (%)
2,6-diaminopyridine (12)	0.550	0.050	91
Acetophenone (15)	3.66	1.73	53
Toluene (16)	0.637	0.393	38

At first glance, these results seemed reasonable and promising. The different adsorption properties of the guest can be easily rationalized by considering the level of molecular recognition involved. Polymer **3a** and 2,6-diaminopyridine (**12**) are complementary and molecular recognition can be achieved. This leads to a considerably high guest adsorption level (91%). However, the initial ratio of 1:1 (guest-polymer recognition site) would suggest that 9 out of 10 recognition sites are occupied by 2,6-diaminopyridine. We suspect that the coiled nature of the polymer would prevent access to a greater fraction of the binding sites, thus reducing the availability for binding 2,6-diaminopyridine. Consequently, it can be envisioned that indiscriminate adsorption may play a major role in this study.

Acetophenone (**15**) can only act as a single site hydrogen bonding acceptor. The imide proton of the polymer could potentially bind (via hydrogen bonding) with the carbonyl and increase the level of guest adsorption. This might explain the slight difference with toluene (**16**), which would only rely on hydrophobic interactions with the polymer to achieve adsorption. Toluene managed to adsorb to level that we consider significantly high, 38%. We consider this level of adsorption quite surprising because the spectra were measured in benzene- d_6 , which is structurally similar to toluene, and as such could saturate the polymer binding sites in the same manner as toluene could.

This high level of toluene adsorption prompted us to design a selective binding experiment. In order to assess the recognition properties of the polymer, 2,6-diaminopyridine (**12**) and acetophenone (**15**) were both dissolved in benzene- d_6 and mixed in one NMR tube (TMS was again used as a reference). The ratio was 1:1 (guest-polymer recognition site) for both guest molecules. The procedure follows exactly what has been done for the previous experiments. The results are presented in table 3.

Table 3: Selective binding experiments

Guest molecule	Initial NMR integration ratio guest/TMS	Final NMR integration ratio guest/TMS	Guest adsorption (%)
2,6-diaminopyridine (12)	0.085	0.024	72
Acetophenone (15)	0.058	0.021	64

The higher adsorption percentage for 2,6-diaminopyridine (**12**) might suggest the presence of selective binding, promoted by the complementarity between guest and host. However, the 8% difference seems low and might not be significant. In addition, indiscriminate adsorption plays an important role in the interpretation of the final results. Based on the adsorption percentage for both guests, we calculated that each polymer site is occupied by more than one guest molecule. In fact, based on the initial guest ratio and the adsorption percentage, 1.36 guests occupy every polymer recognition site. Consequently, the final result cannot be used to confirm the presence nor the absence of complementary adsorption of guest molecules when exposed to the insoluble polymer.

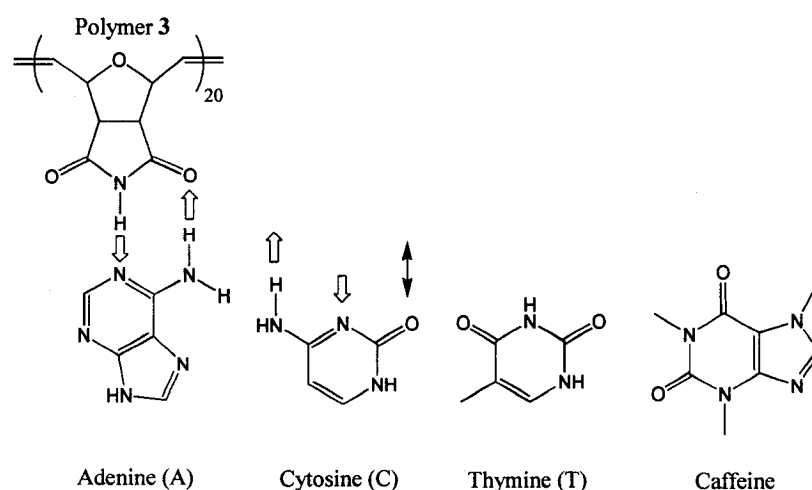
In addition, many uncertainties are related to the NMR technique. Small amounts of guests and polymers were used and the reference (TMS) is extremely volatile. In order to minimize the errors related to the balance accuracy, stock solutions containing the different guests could be generated. However the preparation of such solutions using deuterated solvents such as benzene- d_6 is not very safe and especially costly. On the other hand, TMS could be replaced by tetraphenylsilane, although much less volatile, one has to consider the addition of phenyl peaks in the resulting NMR spectra.

Finally, to promote the hydrophobic interactions between guest and the host microenvironment, the experiment could be run in an aqueous media (D_2O). Although

the hydrogen bonding interactions may be weaker in such solvent, the polymer generated hydrophobic interactions may act as a driving force for the proper complementary binding leading to molecular recognition.

4.4.2.3 Indirect HPLC characterization

Due to the uncertainty of the NMR results, studies were conducted using HPLC methods. We felt that using an additional method for the detection of selective adsorption was required. These studies were conducted to establish that polymers bearing the hydrogen bonding motif were capable of molecular recognition.



Scheme 32

Polymer 3, is a thymine/uracil analog and is expected to preferentially bind adenine in the presence of cytosine, thymine and caffeine. (Scheme 32) Adenine (A) can selectively bind with the polymer molecular recognition site via a two-point hydrogen bonding interaction. As for cytosine (C), it could be considered similar to adenine, and bind via two hydrogen bonding sites, although an unfavorable interaction from the clashing carbonyl would result in steric and electronic repulsions. Consequently, this would lead to lower affinity of the polymer for cytosine (vs. adenine). Since it shares an identical hydrogen bonding motif as polymer 3, thymine (T) cannot favorably interact

with the polymer's recognition sites. Caffeine is added to the system as an internal standard to monitor relative peak integration. No interactions are expected between the polymer and caffeine.

The procedure for establishing the molecular recognition properties of the polymer follows the work of Asanuma.¹⁵ The guest molecules were dissolved in a mixture of THF/water (17% water). Polymer 3, bearing an average of 20 repeating units is insoluble in this solvent mixture. In fact, this particular solvent mixture was chosen because it leads to the self-assembly of copolymer 11. This solvent system was necessary to eventually assess if an increase in the molecular recognition properties was possible when the guests were exposed to nanoscale aggregates of copolymer 11. The initial guest solution was injected in the HPLC without any exposure to the polymer. Peak integration and retention times are summarized in table 4 for the three guests and caffeine (the relative peak integration is calculated vs. caffeine).

Table 4: Guests peak integration prior to polymer exposure

Guest molecule	Retention time (min.)	Peak area	Relative peak integration
Cytosine (C)	3.453	1560.4	86
Thymine (T)	5.885	1867.4	103
Adenine (A)	6.746	3450.8	190
Caffeine	12.920	1818.6	100

Polymer 3 (10 equiv.) was then added to the guest solution and stirred vigorously for 30 min. to reach equilibrium. In order to prevent the injection of particles in the HPLC column, the solution was centrifuged prior to injection. The solution (now exposed to the polymer) was injected again in the HPLC. (Table 5)

Table 5: Guests peak integration prior to polymer exposure

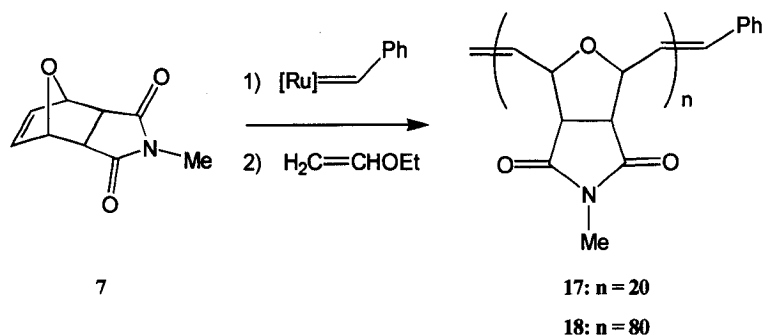
Guest molecule	Retention time (min.)	Peak area	Relative peak integration
Cytosine (C)	3.465	1571.3	84
Thymine (T)	5.932	1880.0	101
Adenine (A)	6.801	3469.5	185
Caffeine	12.941	1877.6	100

By considering the relative peak integration (to caffeine) for the three guest molecules, one obtains an adsorption percentage of approximately 3% for each guest. We believe that such a low adsorption percentage is insignificant. Furthermore, no selectivity due to complementarity is observed based on the adsorption percentage.

In general, HPLC is a more accurate analytical method than NMR when measuring low concentration variations. However, in this particular case, the chosen method might not be the problem. In a similar way to the NMR experiment, the solvent system is mostly organic. It would be quite interesting to use pure water as the solvent system. In an entirely aqueous media, the polymer backbone might form a hydrophobic microenvironment, thus leading to possible hydrophobic interactions (between host polymer and guest molecule) that may drive guest adsorption and recognition. This molecular recognition study involved a solvent system containing a water fraction (17% v/v). However, this water fraction might not be sufficient to promote hydrophobic interactions, thus leading to no considerable guest adsorption on the polymer matrix.

4.5 Additional Polymer Systems

4.5.1- Synthesis and Behavior of N-Methyl Containing Polymers



The methyl containing monomer **7** was initially designed for several reasons: it could be used to generate a control polymer, incapable of molecular recognition, yet structurally similar to polymers of **1** and could increase the solubility of copolymers bearing the dicarboximide moiety.

Polymer **17** bearing an average of 20 repeating units was easily generated by ROMP of **7** (20 equiv.) and catalyst **2**. (Equation 18) As for polymer **18** (average of 80 repeating units), the polymerization was efficient only in CH_2Cl_2 . This can be attributed to the low solubility in THF of the corresponding polymer beyond 20 repeating units. Unfortunately, for characterization and self-assembly, polymers of **7** are not ideal due to their lack of solubility in THF. In fact, the solubility behavior of these polymers closely resembles what is observed with polymers bearing the dicarboximide functionality. Consequently, the copolymerization of the monomer bearing the N-methyl functionality with the molecular recognition unit was not actively pursued due to the copolymers consistently precipitating (in THF) during ROMP reactions.

Nevertheless, polymer **17** and **18** were characterized by ^1H NMR in DMSO-d_6 . Due to obvious solubility issues in THF, GPC analysis was conducted only for polymer

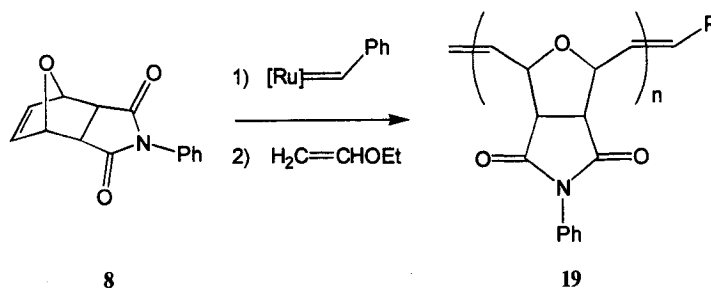
17, bearing an average of 20 repeating units. A peak was observed at $M_n = 4262$ (calculated value is $M_n = 3524$ Da) and with a rather narrow molecular weight distribution (PDI = 1.10).

This particular monomer could be of interest if one wishes to create a copolymer soluble in CH_2Cl_2 bearing the dicarboximide units. It is expected that a considerably high ratio of the N-methyl based monomer would be required to enhance the solubility of the copolymer in non-hydrogen bonding solvents. The advantage of using the N-methyl monomer as opposed to the monomers bearing long alkyl chains resides in the fact that the N-methyl block would not behave as comb-like block, as is the case for polymer 10. Incorporating the N-methyl functionality in block copolymers could lead to different nanoscale morphologies than those obtained with copolymer 11.

4.5.2- Synthesis and Behavior of N-Phenyl Containing Polymers

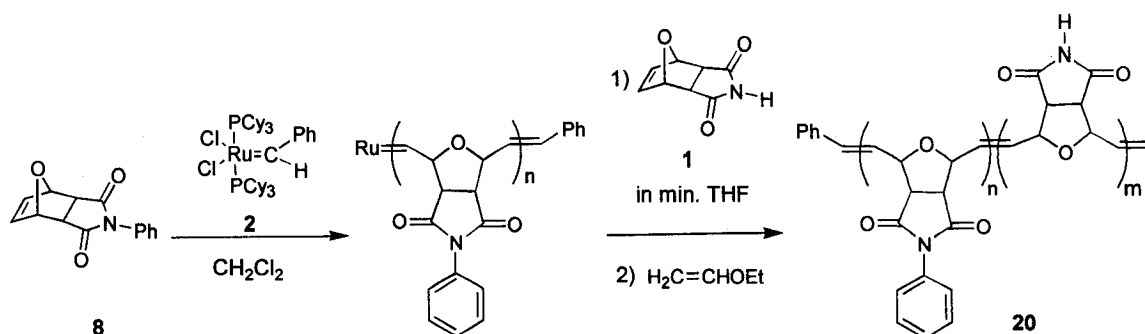
A drawback associated with having structurally similar blocks is that they are often indistinguishable by ^1H NMR. Such is the case for copolymer 11, where the only difference resides in the nitrogen substituent. Therefore, upon micellization in non-hydrogen bonding organic media (e.g. CDCl_3), the dicarboximide proton cannot be located by ^1H NMR. Such behavior is likely indicative of the formation of micellar aggregates where the unsolvated core is not apparent by NMR spectroscopy. While the other signals related to the core forming block could be present, they overlap perfectly with the signals from the corona forming block. Although integration parameters could confirm the disappearance of the signals of the hydrophilic block, the width of the NMR peaks (typical of polymers) can sometimes be misleading. Therefore, a block with distinct ^1H NMR signals could be quite useful in monitoring peak disappearance upon copolymer micellization.

For this current project, the only possible variation resides on the imide nitrogen. Polymer **19** was obtained via living ROMP (in THF) of monomer **8** (20 eq.) using Grubbs catalyst **2**. (Equation 19) The resulting tacky light brown polymer was purified by precipitation in methanol. It was characterized by ^1H NMR and gel permeation chromatography (GPC). Polymer **19** proved insoluble in THF and CHCl_3 beyond 20 repeating units, although it was soluble in CH_2Cl_2 . The insertion of **19** into copolymers was not actively pursued due to poor solubility in THF, likely due to π -stacking between the phenyl rings. Nevertheless, GPC (using THF as the eluent) of the homopolymer bearing an average of 20 repeating units was conducted and a single peak $M_n = 2897$ Da was observed (calculated $M_n = 4924$ Da) with a PDI of 1.26.



Equation 19

Interestingly, polymer **19** bearing the N-phenyl functionality exhibits particular NMR behavior. The presence of the N-phenyl substituent seems to greatly influence the chemical shifts of the repeating unit. Distinct NMR signals became apparent once the N-phenyl substituent was incorporated into a diblock copolymer bearing dicarboximide units (copolymer **20**). Copolymer **20** was obtained using a novel ROMP copolymerization method that, to our knowledge, has not yet been reported. The poor solubility of the N-phenyl monomer in THF forced us to use CH_2Cl_2 as the ROMP solvent. However, this solvent does not dissolve polymers of **1** (containing the



Scheme 33: Copolymer Synthesis

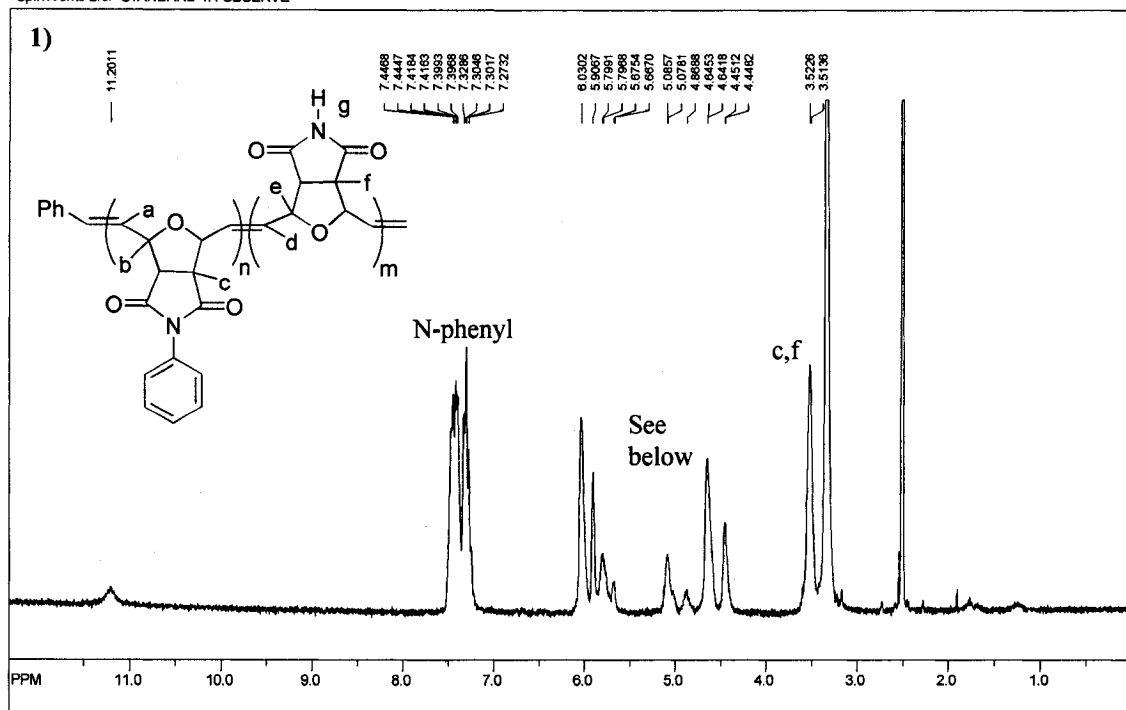
dicarboximide unit). This could prove troublesome if one wants to incorporate the molecular recognition dicarboximide block into copolymers containing the N-phenyl block. Grubbs catalyst **2** was dissolved in CH_2Cl_2 and monomer **8** (40 equiv.) was polymerized. At that point, monomer **1** (20 equiv.) was added to the reaction mixture in minimum THF. A slight turbidity appeared (and quickly faded away) upon addition of monomer **1** to the reaction mixture in CH_2Cl_2 . (Scheme 33) The solution remained homogeneous throughout the reaction. Unfortunately, the block copolymer could not be characterized by GPC, due to insolubility in THF and CHCl_3 .

This novel polymerization method could be used to design ROMP block copolymers (diblock and triblock) that possess blocks with extremely different solubility parameters. It could allow for the design of new copolymers by bypassing the lack of solubility of certain blocks (e.g. poly(**1**)) that one wishes to incorporate into particular copolymers.

^1H NMR of **20** revealed a significant downfield shift of the N-Phenyl block (vs. the signals for the dicarboximide block), for a majority of the repeating unit's protons. (Figure 9) This interesting behavior could prove helpful due to the challenges of the NMR characterization of diblock copolymers that exhibit micellar aggregation in non-hydrogen bonding solvents. Such NMR characteristics could solve the problematic

assessment of copolymer behavior in different solvents, as well as the assessment of molecular recognition properties.

SpinWorks 2.0: STANDARD 1H OBSERVE



SpinWorks 2.0: STANDARD 1H OBSERVE

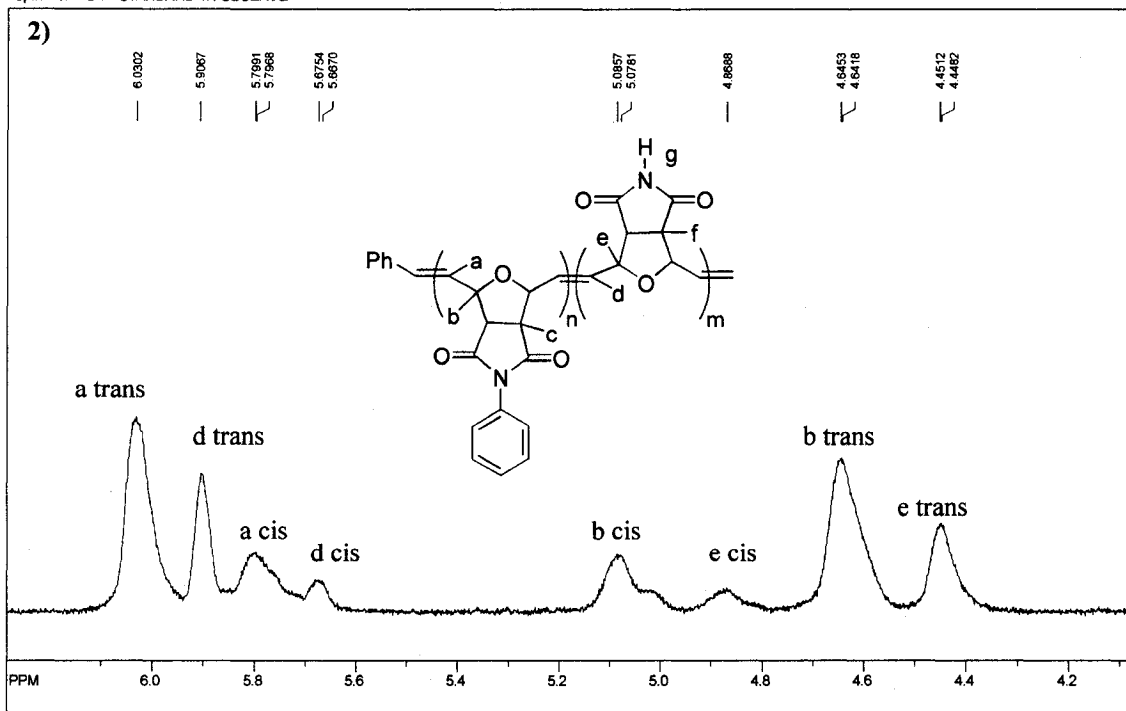
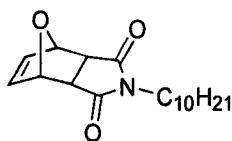


Figure 9: 1) Copolymer 20 NMR spectra in DMSO-d₆ 2) zoom on region of interest of NMR spectra

4.5.3- Synthesis and Behavior of N-Alkyl Containing Polymers

Comonomer **6** bearing the pendant 10 carbon-alkyl chain has been extensively used during this research project with the objective to generate asymmetric diblock copolymers that would undergo self-assembly when exposed to certain solvent conditions. While this monomer highly contributes to the increase in solubility of polymers containing the dicarboximide units, we believe that it could dictate the morphology adopted by the self-assembled copolymer. It can be envisioned that this block acts as a comb-polymer and that the nature of the shorter block plays a minor role in dictating the final morphology.

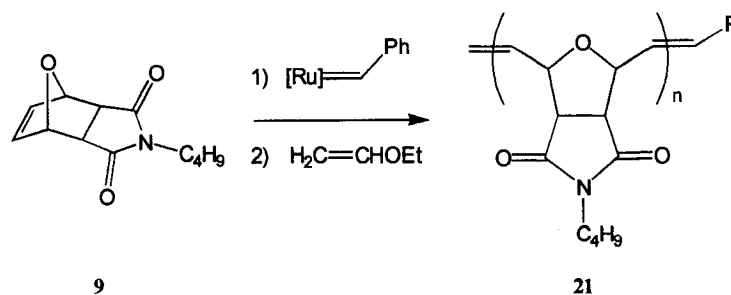


6

In addition, in non-hydrogen bonding solvents such as CH₂Cl₂ and CHCl₃, the comb-like nature of the hydrophilic block renders NMR characterization of the dicarboximide containing block difficult. Micellization in non-hydrogen bonding solvents of the block copolymer prevents the detection of the signals related to the dicarboximide block by ¹H NMR. In fact, we believe that the long alkyl chains may play a role in effectively shielding the imide proton.

In order to minimize the shielding effect and with the hope of creating new self-assembled morphologies, monomer **9** bearing a much shorter carbon chain was synthesized. Polymer **21** containing this new monomer was first generated (bearing an average of 60 repeating units) and possessed some interesting properties. It showed good solubility in common organic solvents, and exhibited solubility in DMSO to a much

greater extent than polymer **10** (bearing the 10 carbon alkyl chains). Polymer **21** was easily obtained by ROMP using catalyst **2** and monomer **9** (60 equiv.) in THF and characterized by ^1H NMR and GPC. (Equation 20) The GPC analysis displayed a peak at $M_n = 16258$ Da (calculated $M_n = 13364$ Da) and PDI = 1.20.



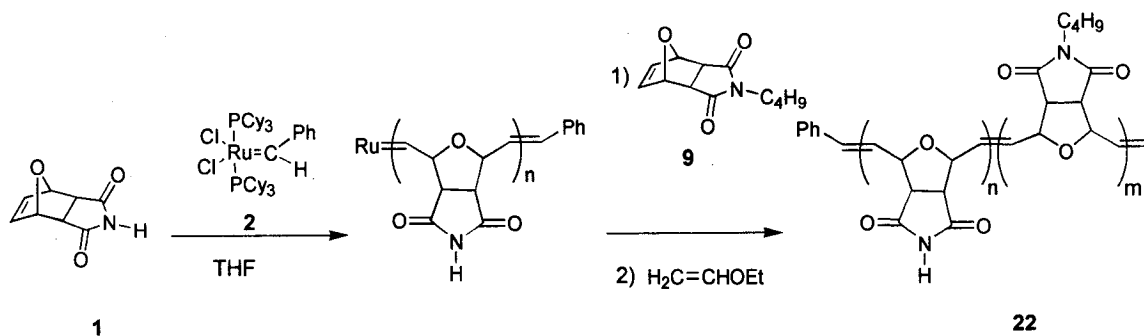
Equation 20

As opposed to polymers bearing the 4 carbon-alkyl chains, homopolymers of **6** cannot be generated via ROMP in a controlled manner (in THF). On the other hand, a polymer with a very narrow molecular weight distribution (PDI=1.08) can be easily obtained in CH_2Cl_2 . This striking behavior is likely related to the coordinating nature of THF combined with the possible steric hindrance of monomer **6**. Consequently, the copolymerization must inevitably be initiated using the dicarboximide monomer **1**, followed by the copolymerization of monomer **6**. By doing so, a copolymer with an extremely narrow molecular weight distribution is readily obtained. While not as well-behaved as monomer **1**, monomer **9** seems to properly initiate and polymerize in THF (based on GPC analysis). Therefore, it can be used as the initial block in copolymer synthesis, thus increasing the flexibility of the copolymerization method.

It was envisioned that by increasing the length of the hydrophobic block (i.e. increasing the number of repeating units) would result in a copolymer capable of molecular recognition with increased solubility in non-hydrogen bonding solvents. A

new copolymer with a different behavior than copolymer **11** in non-hydrogen bonding solvent could be obtained by making use of monomer **9**.

Copolymer **22** was synthesized by ROMP of monomer **1** (20 equiv.) followed by the removal of half of the reaction mixture and by the addition of monomer **9** (75 equiv.). (Scheme 34) The resulting copolymer bears an average of 20 molecular recognition units (dicarboximide functionality) and a hydrophobic block containing an average of 150 repeating units designed to greatly enhance copolymer solubility. Copolymer **22** was characterized by ^1H NMR and GPC. The homopolymer of **1** gave a peak of $M_n = 3572$ (calculated $M_n = 3404$ Da) and a PDI of 1.09; while the copolymer generated a peak at $M_n = 83681$ Da (calculated $M_n = 36554$ Da) and PDI of 1.14. The considerable difference between experimental and calculated average molecular weight for copolymer **17** could be attributed to the standards (polystyrene) and might also be attributed to copolymer aggregation (in THF, the GPC eluent) caused by the extremely long hydrophobic chain of the copolymer.



Scheme 34: Copolymer Synthesis

While copolymer **11** has been shown to undergo self-assembly in selective solvents, its molecular recognition properties were difficult to establish. During solubility tests, it was clear that the new copolymer (**22**) had much greater solubility in CHCl_3 . In fact, upon stirring the copolymer in CHCl_3 , a homogeneous solution could be formed

within 1-2 hrs. This copolymer should be ideally suited for molecular recognition studies, as well as self-assembly in non-hydrogen bonding solvent systems.

5. Conclusion

In summary, we have used living ring-opening metathesis polymerization to generate a new class of homopolymers and block copolymers of narrow molecular weight distributions, which contain biologically relevant and readily functionalizable dicarboximide moieties. Self-assembly of these block copolymers leads to the formation of nanoscale spherical micellar aggregates with surface localization of the dicarboximide units. These polymers and copolymers could find direct applications as biosensors as well as drug delivery vectors.^{45,46} The molecular recognition patterns incorporated within the polymers could allow for the selective binding of drugs and other biologically relevant molecules.

Molecular recognition studies have been conducted with success at the monomer level. Simple ^1H NMR characterization allowed for examination of the molecular recognition properties of monomer **1**. Unfortunately, the various binding experiments conducted on polymer **3** and copolymer **11** yielded no conclusive results. Direct and indirect ^1H NMR characterization of molecular recognition properties were attempted on the polymers and copolymers and demonstrated the presence of both molecular recognition, as well as indiscriminate binding. HPLC studies measuring selective adsorption did not reveal any significant molecular recognition properties of polymer **3** when exposed to complementary and non-complementary nucleic acid bases in polar media.

An exploratory study of polymer solubility was conducted by synthesizing a library of polymer and copolymers bearing different functional groups. Various monomers derived from monomer **1** were used with the objective of generating new copolymers that could self-assemble and form different morphologies than those obtained

with copolymer **11**. In addition, solubility issues regarding the determination of molecular recognition properties of copolymer **11** were confronted by synthesizing a new copolymer bearing a much longer hydrophobic block (copolymer **22**). These exploratory studies allowed for the determination of new polymeric systems which possess interesting potential for further studies regarding self-assembly, and more importantly DNA-like molecular recognition. Future studies will probe the guest-induced response of the self-assembled polymer nanoparticles to molecules containing complementary hydrogen bonding moieties, such as adenine and adenine-containing oligonucleotides.

6. References

1. Schwab, P.; Grubbs, R. H.; Ziller, J. W. *J. Am. Chem. Soc.*, **1996**, *118*, 100.
2. a) Buchmeiser, M. R. *Chem. Rev.*, **2000**, *100*, 1565. b) Trnka, T. M.; Grubbs, R. H. *Acc. Chem. Res.*, **2001**, *34*, 18.
3. a) Mortell, K. H.; Weatherman, R. V.; Kiessling, L. L. *J. Am. Chem. Soc.*, **1996**, *118*, 2297. b) Kanai, M.; Mortell, K. H.; Kiessling, L. L. *J. Am. Chem. Soc.*, **1997**, *119*, 9931. c) Kiessling, L. L.; Strong, L. E. *Top. Organomet. Chem.*, **1998**, *1*, 199. d) Cairo, C. W.; Gestwicki, J. E.; Kanai, M.; Kiessling, L. L. *J. Am. Chem. Soc.*, **2002**, *124*, 1615.
4. Meier, S.; Reisinger, H.; Haag, R.; Mecking, S.; Mülhaupt, R.; Stelzer, F. *Chem. Commun.*, **2001**, 855.
5. a) Maynard, H. D.; Okada, S. Y.; Grubbs, R. H. *Macromolecules*, **2000**, *33*, 6239. b) Maynard, H. D.; Okada, S. Y.; Grubbs, R. H. *J. Am. Chem. Soc.*, **2001**, *123*, 1275.
6. a) Gibson, V. C.; Marshall, E. L.; North, M.; Robson, D. A.; Williams, P. J. *Chem. Commun.*, **1997**, 1095. b) Davies, R. G.; Gibson, V. C.; Hursthouse, M. B.; Light, M. E.; Marshall, E. L.; North, M.; Robson, D. A.; Tompson, I.; White, A. J. P.; Williams, D. J.; Williams, P. J. *J. Chem. Soc., Perkin Trans 1*, **2001**, 3365.
7. Watson, K. J.; Anderson, D. R.; Nguyen, S. T. *Macromolecules*, **2001**, *34*, 3507
8. Watson, K. J.; Park, S.-J.; Im, J.-H.; Nguyen, S. T.; Mirkin, C. A. *J. Am. Chem. Soc.*, **2001**, *123*, 5592.
9. a) Gratt, J.; Cohen, R. E. *Macromolecules*, **1997**, *30*, 3137. b) Matzger, A. J.; Lawrence, C. E.; Grubbs, R. H.; Lewis, N. S. *J. Comb. Chem.*, **2000**, *2*, 301. c) Liaw, D.-J.; Huang, C.-C.; Wu, P.-L. *Polymer*, **2001**, 9371. d) Bazzi, H. S.; Sleiman, H. F. *Macromolecules*, **2002**, *35*, 624.

10. a) Halperin, A.; Tirrell, M.; Lodge, T. P. *Adv. Polym. Sci.*, **1992**, *100*, 31. b) Zhang, L.; Barlow, R. J.; Eisenberg, A. *Macromolecules*, **1995**, *28*, 6055. c) Zhang, L.; Eisenberg, A. *Science*, **1995**, *268*, 1728.
11. Kim, G.-C.; Jeong, J.-G.; Lee, N.-J.; Ha, C.-S.; Cho, W.-J. *J. Appl. Polym. Sci.*, **1997**, *64*, 2605.
12. McCluskey, A.; Walkom, C.; Bowyer, M. C.; Ackland, S. P.; Gardiner, E.; Sakoff, J. *A. Bioorg. Med. Chem. Lett.*, **2001**, *11*, 2941.
13. Park, T. K.; Schroeder, J.; Rebek Jr., J. *J. Am. Chem. Soc.*, **1991**, *113*, 5125.
14. Molecular recognition units incorporated in synthetic polymers: a) Aponte, M. A.; Butler, G. B. *J. Polym. Sci.: Polym. Chem. Ed.*, **1984**, *22*, 3715. b) Lange, R. F. M.; Meijer, E. W. *Macromolecules*, **1995**, *28*, 782. c) Wada, T.; Inaki, Y.; Takemoto, K. "Nucleic acid Analogs", in: *Polymeric Materials Encyclopedia*, Salamone, J. C., Ed., CRC Press, Boca Raton 1996, Vol. 6, p. 4640. d) Ilhan, F.; Galow, T. H.; Gray, M.; Clavier, G.; Rotello, V. M. *J. Am. Chem. Soc.*, **2000**, *122*, 5895. e) Ilhan, F.; Gray, M.; Rotello, V. M. *Macromolecules*, **2001**, *34*, 2597. f) Frankamp, B. L.; Uzun, O.; Ilhan, F.; Boal, A. K.; Rotello, V. M. *J. Am. Chem. Soc.*, **2002**, *124*, 892. g) Boal, A. K.; Gray, M.; Ilhan, F.; Clavier, G. M.; Kapitzky, L.; Rotello, V. M. *Tetrahedron*, **2002**, 765.
15. Examples of interaction between nucleic acids and synthetic polymers: a) Asanuma, H.; Ban, T.; Gotoh, S.; Hishiya, T.; Komiyama, M. *Macromolecules*, **1998**, *31*, 371. b) Asanuma, H.; Hishiya, T.; Ban, T.; Gotoh, S.; Komiyama, M. *J. Chem. Soc., Perkin Trans. 2*, **1998**, 1915. c) Asanuma, H.; Ban, T.; Gotoh, S.; Hishiya, T.; Komiyama, M. *Supramolecular Science*, **1998**, *5*, 405.

16. Polymers for DNA delivery: Kabanov, A. V. *Pharmaceutical Science & Technology Today*, **1999**, 2, 365.
17. a) T. Viswanathan, J. Jethmalani, *J. Appl. Polym. Sci.*, 1993, 48, 1289. b) Cooley, J. H.; Williams, R. V. *J. Chem. Edu.*, **1997**, 74, 582.
18. Ivin, K. J.; Mol, J. C. *Olefin Metathesis and Metathesis Polymerization*; Academic Press, London, 1997.
19. a) Schrock, R. R. *J. Organomet. Chem.*, **1986**, 300, 249. b) Schrock, R. R.; Murdzek, J. S.; Bazan, G. C.; Robbins, M.; Dimare, M.; O'Regan, M. *J. Am. Chem. Soc.*, **1990**, 112, 3875. c) Schrock, R. R. *Acc. Chem. Res.*, **1990**, 23, 158.
20. Katz, T. J. et al., *Tetrahedron Lett.*, **1976**, 4247.
21. a) Wagener, K. B.; Boncella, J. M.; Nel, J. G. *Macromolecules* **1991**, 24, 2649. b) Lehman Jr., S. E.; Wagener, K. B. *Macromolecules*, **2002**, 35, 48.
22. Scholl, M.; Ding, S.; Lee, C. W.; Grubbs, R. H. *Org. Lett.*, **1999**, 1, 953.
23. Hérisson, J. L.; Chauvin, Y. *Makromol. Chem.*, **1970**, 141, 161.
24. a) Dias, E. L.; Nguyen, S. T.; Grubbs, R. H. *J. Am. Chem. Soc.*, **1997**, 119, 3887. b) Sanford, M. S.; Ulman, M.; Grubbs, R. H. *J. Am. Chem. Soc.*, **2001**, 123, 749. c) Sanford, M. S.; Love, J. A.; Grubbs, R. H. *J. Am. Chem. Soc.* **2001**, 123, 6543.
25. Matyjaszewski, K. *Macromolecules*, **1993**, 26, 1787.
26. Campbell, I. M. *Introduction to Synthetic Polymers*, Oxford Press, New York, 2000.
27. Bielawski, C. W.; Grubbs, R. H. *Macromolecules*, **2001**, 34, 8838.
28. Bielawski, C. W.; Grubbs, R. H. *Angew. Chem. Int. Ed.*, **2000**, 39, 2903.
29. Kirkland, T. A.; Grubbs R. H., *J. Org. Chem.*, **1997**, 62, 7310.
30. Weskamp, T.; Kohl, F. J.; Hieringer, W.; Gliuch, D.; Herrmann, W.A. *Angew. Chem. Int. Ed.*, **1999**, 38, 2416.

31. Chatterjee, A. K.; Morgan, J. P.; Grubbs, R. H. *J. Am. Chem. Soc.*, **2000**, *122*, 3783.
32. Bazzi, H. S.; Sleiman, H. F. *Macromolecules*, manuscript submitted.
33. Weck, M.; Schwab P.; Grubbs, R. H. *Macromolecules*, **1996**, *29*, 1789.
34. Strong, L. E.; Kiessling, L. L. *J. Am. Chem. Soc.*, **1999**, *121*, 6193.
35. Gibson, V. C.; Marshall, E. L.; North, M.; Robson, D. A.; Williams, P. J. *Chem. Commun.*, **1997**, 1095.
36. Duncan, R. *Pharm. Sci. Technol. Today*, **1999**, *2*, 441.
37. Perchar, M.; Ulbrich, K.; Subr, V.; Seymour, L. W.; Schacht, E. H. *Bioconjugate Chem.*, **2000**, *11*, 131.
38. Biagini, S. C. G.; Gibson, V. C.; Giles, M. R.; Marshall, E. L.; North, M. *Chem. Commun.*, **1997**, 1097.
39. Lindoy, L. F.; Atkinson, I.M. *Self-Assembly in Supramolecular Systems*, Monographs in Supramolecular Chemistry, Stoddart, J. F., Ed., RSC, Cambridge, 2000.
40. Jeffrey, G. A., *An Introduction to Hydrogen Bonding*, Oxford University Press, New York, 1997.
41. Watson, J.D.; Crick, F. H. C. *Nature (London)*, **1953**, *171*, 737.
42. a) Senear, D. F.; Ross J. B. A.; Laue, T. M. *Methods: Acompanion to Methods in Enzymology*, **1998**, *16*, 3. b) Amouyal, M.; Perez, N.; Rolland, S. *Comptes Rendus de l'Académie des Sciences-série III, Science de la Vie*, **1998**, 877. c) Williams, D. H.; Calderone, C. T.; O'Brien, D. P.; Zerella, R. *Chem. Commun.*, **2002**, *12*, 1266.
43. a) Vaillancourt, L.; Simard, M.; Wuest, J. D. *J. Org. Chem.*, **1998**, *63*, 9746. b) Kimizuka, N.; Kawasaki, T.; Hirata, K.; Kunitake, T. *J. Am. Chem. Soc.*, **1998**, *120*, 4094. c) Corbin, P. S.; Zimmerman, S. C. *J. Am. Chem. Soc.*, **2000**, *122*, 3779. d) Fenniri, H.; Mathivanan, P.; Vidale, K. L.; Sherman, D. M.; Hallenga, K.; Wood, K.

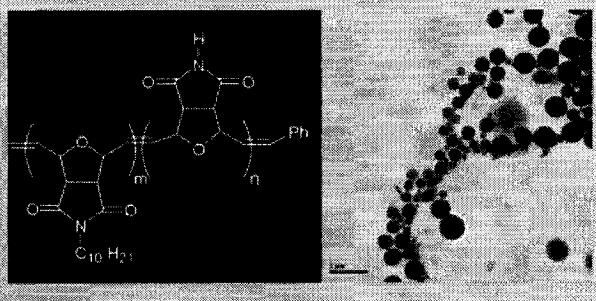
- V.; Stowell, J. G. *J. Am. Chem. Soc.*, **2001**, *123*, 3854. e) Rispens, M. T.; Sanchez, L.; Knol, J.; Hummelen, J. C. *Chem. Commun.*, **2001**, 161.
44. a) Ruokolainen, J.; Tanner, J.; Ikkala, O.; ten Brinke, G.; Thomas, E. L. *Macromolecules*, **1998**, *31*, 3532. b) Schenning, A. P. H. J.; Jonkheijm, P.; Peters, E.; Meijer, E. W. *J. Am. Chem. Soc.*, **2001**, *123*, 409.
45. Wang, J. *Nucleic Acid Research*, **2000**, *28*, 3011.
46. Takakura, Y.; Nishikawa, M.; Yamashita, F.; Hashida, M. *Eur. J. Pharm. Sci.*, **2002**, *13*, 71.
47. Rebek Jr., J.; Askew, B.; Ballester, P.; Buhr, C.; Jones, S.; Nemeth, D.; Williams, K. *J. Am. Chem. Soc.*, **1987**, *109*, 5033.
48. a) Hamilton, A. D.; Engen, D. V. *J. Am. Chem. Soc.*, **1987**, *109*, 5035. b) Hirst, S. C.; Hamilton, A. D. *Tetrahedron Lett.*, **1990**, *31*, 2401.
49. Yu, L.; Schneider, H.-J. *Eur. J. Org. Chem.*, **1999**, 1619.
50. Mammen, M.; Choi, S.-K.; Whitesides, G. M. *Angew. Chem. Int. Ed.*, **1998**, *37*, 2754.
51. a) Deans, R.; Ilhan, F.; Rotello, V. M. *Macromolecules*, **1999**, *32*, 4956. b) Galow, T. H.; Ilhan, F.; Cooke, G.; Rotello, V. M. *J. Am. Chem. Soc.*, **2000**, *122*, 3595.
52. Beijer, F. H.; Sijbesma, R. P.; Vekemans, J. A. J. M.; Meijer, E. W.; Kooijman, H.; Spek, A. L. *J. Org. Chem.*, **1996**, *61*, 6371.
53. a) Cowie, J. M. G.; Cocton, D. *Polymer*, **1998**, 227. b) Cowie, J. M. G.; Love, C. *Polymer*, **2001**, 4783.
54. Michaels, A. S.; Miekka, R. G. *J. Phys. Chem.*, **1961**, *65*, 1765.
55. Smith, P.; Eisenberg, A. *J. Polym. Sci. Polym. Lett. Ed.*, **1983**, *21*, 22.

56. a) Guerra, G.; Choe, S.; Williams, D. J.; Karasz, F. E.; MacKnight, W. J. *Macromolecules*, **1988**, *21*, 231. b) Shonaike, G. O.; Simon G. P. *Polymer Blends and Alloys*; Marcel Dekker, New York, 1999.
57. Nowick, J. S.; Chen, J. S. *J. Am. Chem. Soc.*, **1992**, *114*, 1107.
58. a) Xu, R.; Winnik, M.A. *Macromolecules*, **1991**, *24*, 87. b) Wilhelm, M.; Zhao, C. L.; Wang, Y.; Xu, R.; Winnik, M. A. *Macromolecules*, **1991**, *24*, 1033. c) Prochazka, K.; Kiserow, D.; Ramireddy, C.; Tuzar, Z.; Munk, P.; Webber, S. E. *Macromolecules*, **1992**, *25*, 454. d) Astafieva, I.; Zhong, Z. F.; Eisenberg, A. *Macromolecules*, **1993**, *26*, 7339. e) Qin, A.; Tian, M.; Ramireddy, C.; Webber, S. E.; Munk, P. *Macromolecules*, **1994**, *27*, 120.
59. Gao, Z.; Varshney, S.K.; Wong, S.; Eisenberg, A. *Macromolecules*, **1994**, *27*, 7923.
60. Allen, C.; Maysinger, D.; Eisenberg, A. *Colloids and Surfaces: Biointerfaces*, **1999**, *16*, 3.
61. Zhang, L.; Eisenberg, A. *J. Am. Chem. Soc.*, **1996**, *118*, 3168.
62. Terreau O.; Eisenberg, A. *Langmuir*, manuscript to be submitted.
63. Zhang, L.; Eisenberg, A. *Science*, **1996**, *272*, 1777.
64. Zhang, L.; Eisenberg, A. *Journal of Polymer Science : Part B : Polymer Physics*, **1999**, *37*, 1469.
65. Yu, Y.; Zhang, L.; Eisenberg, A. *Macromolecules*, **1998**, *31*, 1144.
66. Zhong, X-F.; Varshniy, S. K.; Eisenberg, A. *Macromolecules*, **1992**, *25*, 7160.
67. Yu, K.; Eisenberg, A. *Macromolecules*, **1996**, *29*, 6359.
68. Lee, J. H.; Lee, B. H.; Andrade, J. D. *Prog. Polym. Sci.*, **1995**, *20*, 1043.
69. Baines, F. L.; Billingham, N. C.; Armes, S. P. *Macromolecules*, **1996**, *29*, 3416.
70. Kwart, H.; Burchuk, I. *J. Am. Chem. Soc.*, **1952**, *74*, 3094.

71. Clevenger, R. C.; Turnbull, K. D. *Synth. Comm.*, **2000**, *30*, 1379.
72. Hillmyer, M. A.; Lepetit, C.; McGrath, D. V.; Novak, B. M.; Grubbs, R. H. *Macromolecules*, **1992**, *13*, 3345.
73. a) Seehof, N.; Grutke, S.; Risse, W. *Macromolecules*, **1993**, *26*, 695. b) Khosravi, E.; Feast, W. J.; Al-Hajaji, A. A.; Leejarkpai, T. *Journal of Molecular Catalysis A: Chemical*, **2000**, *160*, 1. c) Rule, J. D.; Moore, J. S. *Macromolecules*, **2002**, *35*, 7878.
74. Reddy, P. Y.; Kondo, S.; Toru, T.; Ueno, Y. *J. Org. Chem.*, **1997**, *62*, 2652.
75. The absence of data points below ca. 10% monomer conversion is due to the fact that the polymerization reaction had already started prior to the first ^1H NMR acquisition (at -5°C).
76. Higher monomer to initiator ratios resulted in precipitation of the homopolymers from THF solution.
77. Park, J.-G.; Ha, C.-S.; Cho, W.-J. *J. Polym. Sci.; Part A: Polym. Chem.*, **1999**, *37*, 2113.
78. Gangadhara; Noel, C.; Thomas, M.; Reyx, D. *J. Polym. Sci.; Part A: Polym. Chem.*, **1998**, *36*, 2531.
79. Resendes, R.; Massey, J. A.; Temple, K.; Cao, L.; Power-Billard, K. N.; Winnik, M. A.; Manners, I. *Chem. Eur. J.*, **2001**, *7*, 2414.
80. The unstained particles (fig. 4) showed higher optical density in their central region, compared to their outer shell (TEM). On the other hand, the CsOH stained particles (fig. 5) showed uniform darkening, both within their center and outer shells. These two qualitative results suggest preferential staining of the CsOH on the outer surface of these particles.

81. a) Desjardins, A.; Eisenberg, A. *Macromolecules*, **1991**, *24*, 5779. b) Desjardins, A.;
Van de Ven, T. G. M.; Eisenberg, A. *Macromolecules*, **1992**, *25*, 2412. c) Honda, C.;
Sakaki, K.; Nose, T. *Polymer*, **1994**, *35*, 5309.

Full Paper: Polymers with narrow molecular weight distributions and controlled architectures were generated by living ring-opening metathesis polymerization of *exo*-7-oxabicyclo[2.2.1]hept-5-ene-2,3-dicarboximide. The dicarboximide units have been previously shown to exhibit biological activity, can selectively bind to the nucleic acid base adenine by hydrogen-bonding, and are readily functionalizable. Block copolymers containing these moieties were generated, and underwent self-assembly into nanoscale spherical aggregates, with surface localized molecular recognition motifs.



Synthesis and Self-Assembly of Polymers Containing Dicarboximide Groups by Living Ring-Opening Metathesis Polymerization

Jake Dalphond, Hassan S. Bazzi, Kenza Kahrim, Hanadi F. Sleiman*

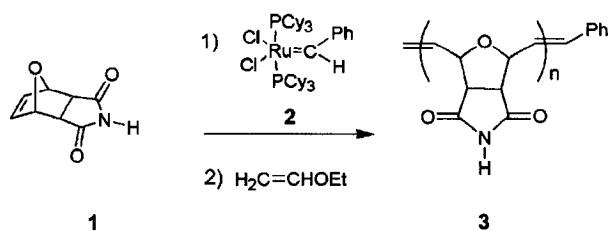
Department of Chemistry, McGill University, 801 Sherbrooke St. West, Montreal, Quebec, H3A 2K6 Canada
E-mail: hanadi.sleiman@mcgill.ca

Keywords: block copolymers; micelles; molecular recognition; ROMP; self-assembly

Introduction

The ring-opening metathesis polymerization (ROMP) currently occupies a central role as an efficient method to generate functional polymers of narrow molecular weight distribution.^[1,2] In particular, with the development of highly active and functional group-tolerant ruthenium catalysts (e.g., Grubbs catalyst **2**^[11]), the scope of this reaction has recently been extended to biologically relevant polymers with increasingly complex functionalities, such as carbohydrates,^[3,4] peptides,^[5] nucleic acid bases,^[6] anti-tumor compounds,^[7] and oligonucleotides.^[8] Importantly, due to the living nature of the ROMP reaction, this method has also been employed to give efficient access to a wide range of block copolymers.^[2a,9] When containing incompatible blocks, these polymers can undergo self-organization into nanometer-scale micellar aggregates of spherical, lamellar, cylindrical, vesicular and other morphologies, with the functional blocks located in segregated domains.^[10] Combining the above two strategies, through the synthesis of ROMP block copolymers containing biologically active units, can lead to nanoscale aggregates which are able to efficiently interface with biological systems. However, to our knowledge, this strategy has not been systematically investigated.^[5,7]

A particularly attractive molecule for incorporation into ROMP polymers and block copolymers is *exo*-7-oxabicyclo[2.2.1]hept-5-ene-2,3-dicarboximide **1** (Scheme 1). As a monomer, this molecule has shown antitumor activity, and its *N*-substituted derivatives are potent phosphatase inhibitors.^[11,12] Importantly, addition polymers of this molecule have also exhibited significant antitumor activity, and have been demonstrated to be less cytotoxic than the monomer **1**.^[11] In addition, the dicarboximide moiety in **1** possesses the same specific hydrogen-bonding characteristics as the nucleic acid bases thymine and uracil.^[13,14] This imide unit can selectively bind adenine, and thus it has the potential to interface efficiently with nucleic acids.^[15,16] Finally, the imide functionality can be readily functionalized by facile deprotonation, followed by nucleophilic substitution



Scheme 1.

(vide infra), thus allowing the incorporation of a variety of other bioactive units into polymers of **1**.

Dicarboximide **1** has been previously polymerized using non-living methods.^[11,17] On the other hand, the synthesis of poly(**1**) using living ring-opening metathesis polymerization would result in polymers with controlled molecular weights and narrow molecular weight distributions, thus providing biologically relevant polymers with precisely known compositions and architectures. Importantly, it would also provide ready access to block copolymers. We here report the use of living ring-opening metathesis polymerization to construct a new class of polymers containing **1**, where the dicarboximide units are arranged on a regular polymer backbone of narrow molecular weight distribution. In addition, we report the synthesis of block copolymers containing these dicarboximide units, and their self-assembly into novel nanoscale morphologies.

Experimental Part

Materials

Reagents were purchased from Aldrich and used as received. The Grubbs catalyst **2** was obtained from Strem Chemicals. Deuterated solvents were obtained from Cambridge Isotope Laboratories and used without further purification. Tetrahydrofuran (THF) was freshly distilled from sodium/benzophenone, dichloromethane (CH₂Cl₂) was freshly distilled from CaH₂. All polymerization reactions were carried out under a dry nitrogen atmosphere using standard Schlenk techniques.

Characterization

¹H NMR and ¹³C NMR spectra were recorded on a Varian M300 spectrometer operated at 300.076 MHz and 75.459 MHz, respectively. Chemical shifts are reported in ppm relative to the deuterated solvent resonances. IR spectra were recorded on an Avatar 360 FT-IR spectrophotometer in the range of 4000 and 400 cm⁻¹ with a resolution of 2 cm⁻¹. GPC spectra were recorded using a Waters 510 pump equipped with two polystyrene-packed Styragel columns (HR4 and HR1, 7.8 × 300 mm) in series and in-line Waters 2410 refractive index detector. THF was used as the eluent at a flow rate of 0.6 mL/min, and the instrument was calibrated with polystyrene standards from Aldrich. TEM images were recorded on a JEOL 2000FX electron microscope operating at 80 kV, using 400 mesh carbon coated grids purchased from Electron Microscopy Sciences. DLS experiments were performed on a Brookhaven Instruments Corporation system equipped with a BI-200SM goniometer, a BI-9000AT digital correlator and a Compass 315-150 CW laser light source from Coherent Inc. operating at 532 nm (150 mW).

NMR Monitoring of the ROMP of **1**

Monomer **1** (0.020 g, 0.12 mmol, 10 equiv.) and catalyst **2** (0.010 g, 0.012 mmol) were weighed and transferred to an NMR tube under inert atmosphere. Degassed THF-*d*₈ was

cooled to -30 °C to prevent any premature polymerization, and then added to the above reagents. ¹H NMR spectra were immediately recorded at 5 min intervals for 90 min (-5 °C, inert atmosphere). Monomer conversion values were obtained by integration of the vinyl peaks of the polymer and monomer. The average molecular weight of the formed polymer was determined by end-group analysis of the vinyl peak of the polymer vs. the phenyl signal of the polymer chain.

Synthesis of *exo*-7-Oxabicyclo[2.2.1]hept-5-ene-2,3-dicarboximide **1**

Monomer **1** was prepared according to literature methods (yield 97%).^[18] ¹H NMR spectroscopy reveals that the isolated product is pure *exo*.^[17]

¹H NMR (DMSO-*d*₆): δ = 11.40 (s, 1H, NH), 6.52 (s, 2H, CH=CH), 5.10 (s, 2H, CH-O), 2.83 (s, 2H, CH-C(O)).

¹³C NMR (DMSO-*d*₆): δ = 178.4, 137.1, 81.0, 49.2.

Synthesis of *exo*-N-Dodecyl-7-oxabicyclo[2.2.1]hept-5-ene-2,3-dicarboximide **4**

Monomer **4** was prepared following a modification of literature procedure.^[19] Monomer **1** (1 g, 6 mmol) and bromodecane (1.3 g, 6 mmol) were dissolved in anhydrous DMF (50 ml). Potassium carbonate (4 g, 40 mmol) was added to the reaction mixture at 50 °C and stirred for 1.5 h under N₂. The resulting mixture was poured in water (100 ml) and extracted (4 ×) with ethyl acetate (200 ml). The organic phase was collected, dried over MgSO₄ and evaporated to yield a yellow oil. Silica gel chromatography (5% MeOH/CH₂Cl₂) yielded a beige oil that quickly solidified (yield 65%).

¹H NMR (CDCl₃): δ = 6.45 (s, 2H, CH=CH), 5.20 (s, 2H, CH-O), 3.40 (t, 2H, N-CH₂), 2.77 (s, 2H, CH-C(O)), 1.48 (m, 2H, alkyl), 1.18 (m, 14H, alkyl), 0.81 (t, 3H, CH₃).

¹³C NMR (CD₂Cl₂): δ = 176.59, 136.83, 81.29, 47.76, 39.11, 32.24, 29.85, 29.82, 29.64, 29.47, 27.91, 27.00, 23.04, 14.24.

(C₁₈H₂₇NO₃) (305.41): Calcd. C 70.78, H 8.91, N 4.59; Found: C 70.49, H 9.25, N 4.62.

Synthesis of Polymer **3**

A solution of catalyst **2** (0.015 g, 0.018 mmol) in THF (2.5 ml) was sonicated for 5 min. The catalyst solution was transferred to monomer **1** (0.060 g, 0.36 mmol, 20 equiv.) in THF (2.5 ml). Initiation was apparent by the change of color from purple to brown. The reaction mixture was vigorously stirred for 10 min and quenched with ethyl vinyl ether (600 equiv.). The resulting light gray polymer was purified by precipitation in methanol (yield 80%).

¹H NMR (DMSO-*d*₆): δ = 11.20 (s, br, NH), 5.89 (s, br, CH=CH, trans), 5.66 (s, br, CH=CH, cis), 4.86 (s, br, CH-O, cis), 4.44 (s, br, CH-O, trans).

¹³C NMR (DMSO-*d*₆): δ = 178.30, 131.78, 80.51, 53.99.

IR (KBr): 3207 (NH), 3080, 2864, 2767, 1775 and 1712 (C=O), 1344, 1272, 1182, 1037, 972, 892, 755, 633.

GPC (THF, polystyrene standards): a peak at $\bar{M}_n = 4217$ Da (calculated $\bar{M}_n = 3404$ Da) and PDI = 1.05. (trans 80%, determined by ¹H NMR).

Synthesis of Polymer 5

Polymer **5** was obtained following the same procedure as for polymer **3** using monomer **4** (0.334 g, 1.095 mmol, 60 equiv.) in dichloromethane. The resulting beige polymer was purified by precipitation in methanol (yield 67%).

^1H NMR (CDCl_3): $\delta = 6.08$ (s, br, $\text{CH}=\text{CH}$, trans), 5.79 (s, br, $\text{CH}=\text{CH}$, cis), 5.10 (s, br, $\text{CH}-\text{O}$, cis), 4.45 (s, br, $\text{CH}-\text{O}$, trans), 3.45 (s, br, $\text{N}-\text{CH}_2$), 3.31 (s, br, $\text{CH}-\text{C}(\text{O})$), 1.54 (s, br, alkyl), 1.25 (s, br, alkyl), 0.87 (t, br, CH_3).

^{13}C NMR (CDCl_3): $\delta = 175.81, 131.10, 81.24, 53.64, 52.54, 39.21, 32.10, 29.77, 29.73, 29.52, 29.41, 27.90, 27.07, 22.90, 14.35$.

IR (KBr): 2924, 2854, 1776 and 1701 ($\text{C}=\text{O}$), 1437, 1397, 1367, 1267, 1162, 1138, 1035, 968, 918, 770, 722, 635.

GPC (THF, polystyrene standards): a peak at $\bar{M}_n = 22161$ Da (calculated $\bar{M}_n = 18404$ Da) and $\text{PDI} = 1.08$ (trans 71%, determined by ^1H NMR).

Synthesis of Copolymer 6

A solution of catalyst **2** (0.015 g, 0.018 mmol) in THF (2.5 ml) was sonicated for 5 min. The catalyst solution was transferred to monomer **1** (0.060 g, 0.36 mmol, 20 equiv.) in THF (2.5 ml) and vigorously stirred for 10 min. At that point, half of the reaction mixture was removed from the Schlenk flask, and a solution of monomer **4** (0.167 g, 0.548 mmol, 30 equiv.) in THF (2.5 ml) was added. The reaction mixture was stirred for an additional 10 min and quenched with ethyl vinyl ether (600 equiv.). The resulting solution was concentrated by evaporation and precipitated in methanol, yielding a white polymer (71%).

^1H NMR (C_6D_6): $\delta = 6.70$ (s, br, $\text{CH}=\text{CH}$, trans), 5.86 (s, br, $\text{CH}=\text{CH}$, cis), 5.26 (s, br, $\text{CH}-\text{O}$, cis), 4.41 (s, br, $\text{CH}-\text{O}$, trans), 3.45 (s, br, $\text{N}-\text{CH}_2$), 2.96 (s, br, $\text{CH}-\text{C}(\text{O})$), 1.59 (s, br, alkyl), 1.28 (s, br, alkyl), 0.93 (s, br, CH_3).

^{13}C NMR (C_6D_6): $\delta = 175.31, 131.33, 81.35, 52.68, 39.50, 32.34, 30.05, 29.81, 29.61, 28.19, 27.73, 23.17, 14.47$.

IR (KBr): 3195 (NH), 2923, 2855, 1775 and 1705 ($\text{C}=\text{O}$), 1437, 1398, 1364, 1269, 1163, 1137, 1037, 969, 918, 773, 721, 638.

GPC (THF, polystyrene standards): the homopolymer gave a peak of $\bar{M}_n = 3632$ (calculated $\bar{M}_n = 3404$ Da) and a $\text{PDI} = 1.09$, the copolymer peak $\bar{M}_n = 37992$ Da (calculated $\bar{M}_n = 21704$ Da) and $\text{PDI} = 1.09$. (trans 85%, determined by ^1H NMR).

Results and Discussion

The ring-opening metathesis polymerization of **1** (20 equiv.) was investigated using catalyst **2** in THF at room temperature. Upon catalyst addition to the monomer solution, the initially purple solution changed to brown within seconds, indicating catalyst initiation.^[11] The reaction mixture was stirred for 10 min to ensure complete monomer conversion, and then quenched with the addition of ethyl vinyl ether. Polymer **3** was isolated as a light gray solid by precipitation in methanol, and was characterized by ^1H ,

^{13}C NMR, FTIR and gel permeation chromatography. GPC analysis showed a single peak at $\bar{M}_n = 4217$ Da (calculated $\bar{M}_n = 3404$), with a low polydispersity of 1.05, suggesting the living nature of this ROMP reaction.

The polymerization of **1** with catalyst **2** was monitored by ^1H NMR in THF- d_8 . At room temperature, the reaction was extremely rapid, and both monomer **1** and catalyst **2** were consumed within ca. 3 min. A new ruthenium alkylidene signal appeared at 18.9 ppm, which was assigned to the α -alkylidene proton of the propagating polymer chain.^[11] This peak persisted after disappearance of monomer **1**, suggesting the living nature of this polymerization. In order to evaluate the dependence of the polymer molecular weight on monomer conversion, the ROMP reaction of monomer **1** (10 equiv.) with catalyst **2** was monitored by ^1H NMR in THF- d_8 at -5°C under inert atmosphere. At this temperature, the kinetics were significantly slower, and monomer conversion was complete after ca. 90 min. The relatively low monomer to initiator ratio (10 equiv.) was necessary, in order to prevent any precipitation of the polymer at -5°C . Analysis of the spectra revealed a clear linear dependence of the average molecular weight of the polymer (obtained by end-group analysis) on monomer conversion, providing strong evidence for the living character of this polymerization (Figure 1).^[20] The ROMP of **1** generated polymers with remarkably low polydispersities using monomer to initiator ratios in the range of 10–30.^[21]

Further evidence for the living nature of this ROMP reaction came from the facile generation of a block copolymer containing monomer **1** (Scheme 2). We used comonomer **4**, which bears a long alkyl chain (C_{10}) on the imide nitrogen. This monomer was readily synthesized by deprotonation of **1** using K_2CO_3 , followed by reaction with decyl bromide. We first established that monomer **4** can be efficiently incorporated into block copolymers, by carrying out the homopolymerization using catalyst **2**.^[22] The resulting polymer **5** was isolated as a beige solid and

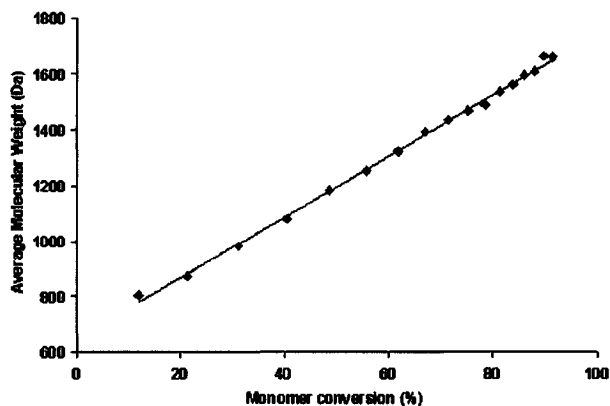


Figure 1. Average molecular weight of the polymer vs. monomer conversion for the ROMP of **1**.

characterized by ^1H , ^{13}C NMR, FTIR and GPC. GPC analysis showed a monomodal distribution and a peak located at $\bar{M}_n = 22\,161$ Da (calculated $\bar{M}_n = 18\,404$ Da), with a PDI of 1.08.

The synthesis of block copolymer **6** was carried out by allowing monomer **1** (20 equiv.) to react with catalyst **2** in THF at room temperature for 10 min. Half of the reaction mixture was then removed and quenched with ethyl vinyl ether. The resulting homopolymer of **1** displayed a narrow molecular weight distribution by GPC ($\bar{M}_n = 3\,404$ Da, PDI = 1.09). Monomer **4** (30 equiv.) in THF was then added to the remaining reaction mixture. After an additional 10 min, the polymerization was quenched with ethyl vinyl ether, and **6** was isolated by precipitation in methanol. Copolymer **6** was characterized by ^1H , ^{13}C NMR, FTIR and GPC. GPC analysis of **6** showed the disappearance of the homopolymer peak at $\bar{M}_n = 3\,404$ Da, and the presence of a single peak at $\bar{M}_n = 37\,992$ Da (calc. $21\,704$ Da) and PDI = 1.09 (Figure 2). The observed difference between experimental and calculated \bar{M}_n values may be the result of hydrogen-bond mediated folding or aggregation of copolymer **6**, thus leading to an increase in its hydrodynamic radius, compared to the linear GPC polystyrene standards. It is of note that the ROMP of monomer **1** results in homopolymers and block copolymers which display some of the lowest polydispersities reported for ROMP polymers using the Grubbs catalyst **2**.^[23] The ease of generation of these polymers (< 10 min at room temperature), and the readily functionalizable imide moiety (vide supra), makes these polymers extremely useful starting materials for conjugation with bioactive molecules,^[24] as well as other functional units.^[25]

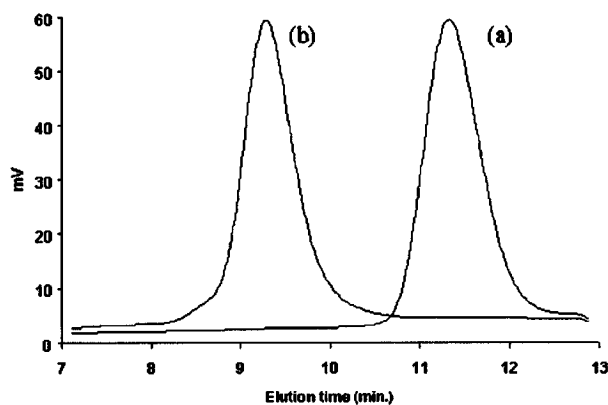
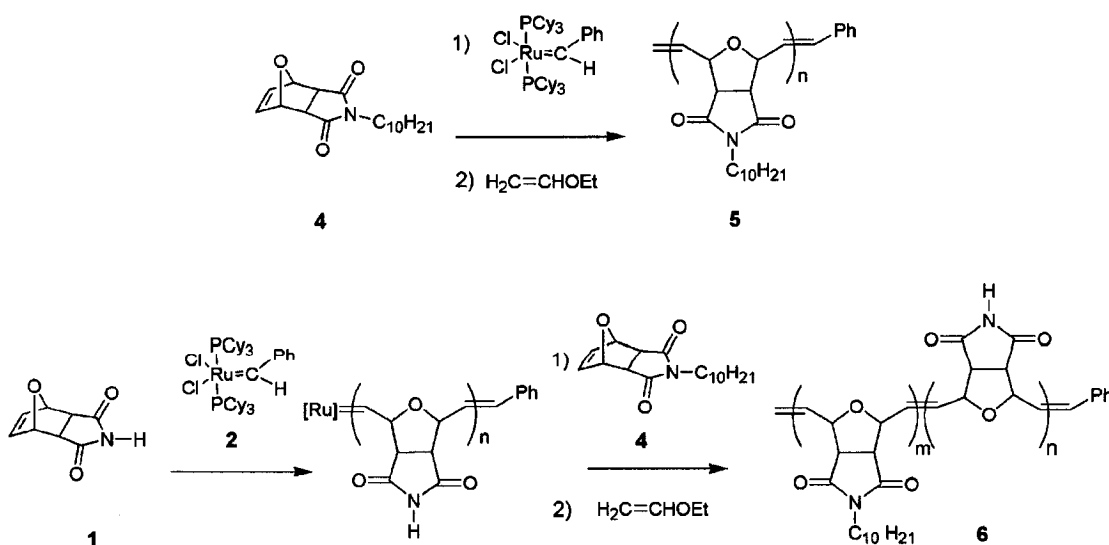


Figure 2. Comparison of GPC traces for (a) homopolymer of **1** and (b) block copolymer **6**.

Copolymer **6** is composed of two very distinct blocks. The poly(**4**) block contains long pendant alkyl chains, which confer it with a high degree of hydrophobicity. In contrast, the poly(**1**) block contains the biologically relevant and hydrophilic dicarboximide units. The presence of two dissimilar blocks in a copolymer can give rise to self-assembly in particular solvent systems. In order to probe for this behavior, copolymer **6** was dissolved in THF, and water was added dropwise until a turbid solution was obtained (17% v/v water content). Light scattering was rapidly observed upon water addition, indicating the onset of aggregation. Dynamic light scattering (DLS), executed at multiple angles (45° , 90° , 135°) confirmed the presence of spherical particles with an average diameter of 200 nm (Figure 3).



Scheme 2.

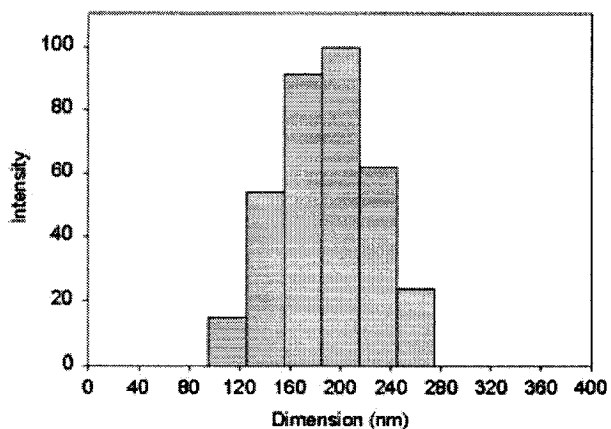


Figure 3. DLS of copolymer **6** in THF/water (17% v/v) (NLS at 90°).

The morphology of copolymer **6** in the above solvent mixture was further characterized by transmission electron microscopy (TEM) (Figure 4). Samples were prepared by allowing a drop of the turbid solution to evaporate on a carbon-coated copper grid. TEM studies revealed the formation of large micellar aggregates of spherical shape. Image analysis of these particles revealed an average size of 100–300 nm, in agreement with the values obtained by DLS. The particle size is too large for individual micelles, indicating that these spherical aggregates may be large compound micelles (LCM).^[26] Interestingly, the observed spherical particles further aggregate into a network of interconnected spheres (“pearl necklaces”). The pearl necklace morphology has been previously observed, and has been interpreted as a possible intermediate morphology between spherical and rod-like aggregates.^[27]

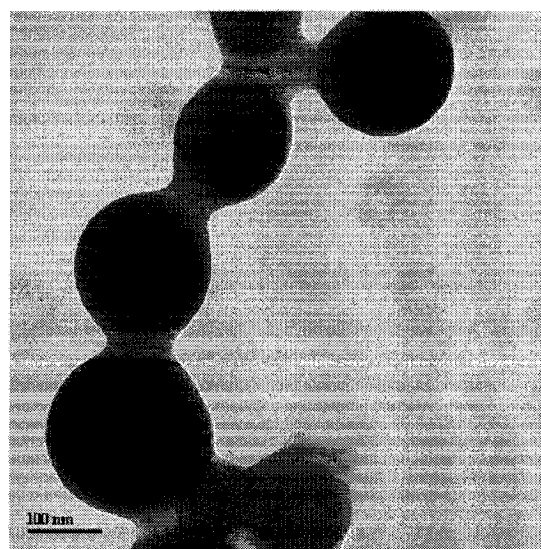
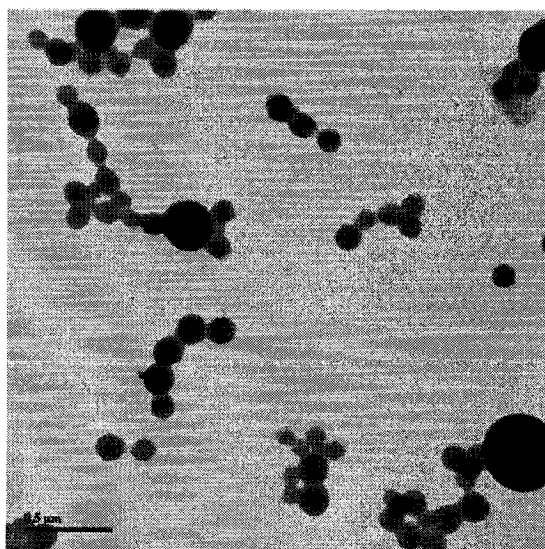
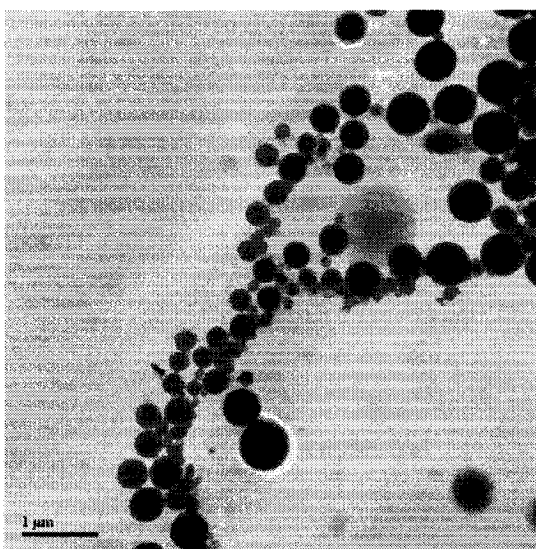


Figure 4. TEM images of copolymer **6** deposited from a THF/water (17% v/v) solution.

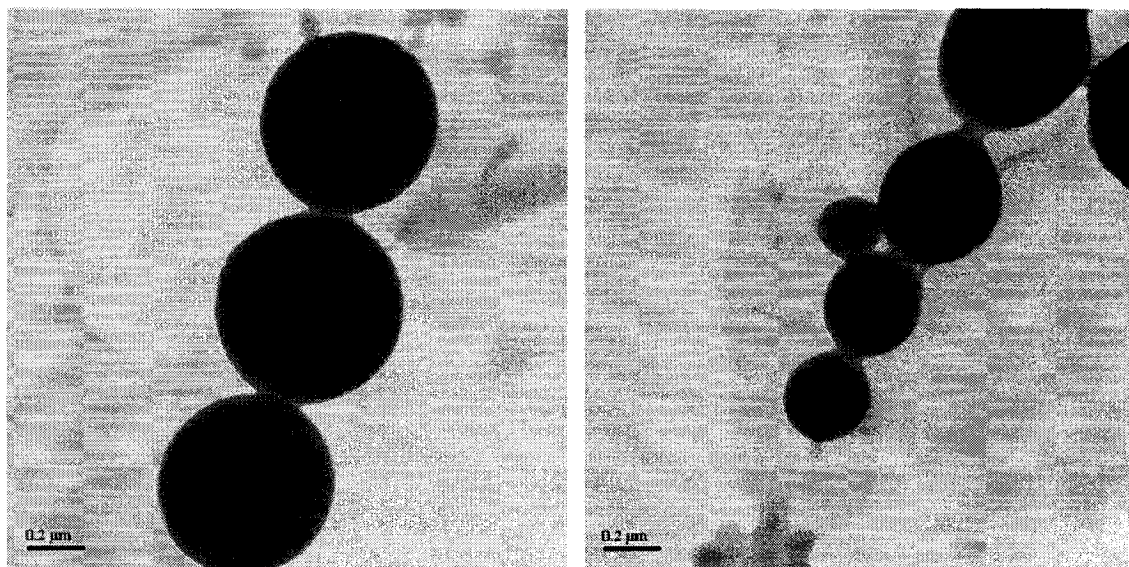


Figure 5. TEM images of copolymer **6** deposited from a THF/water (17% v/v) solution stained with CsOH 0.1 N.

It is expected that in the THF/H₂O mixture, block copolymer **6** aggregates in order to minimize the interaction of the hydrophobic block poly(**4**) with the polar medium, and to expose the more hydrophilic poly(**1**). The dicarboximide units are therefore likely located on the exterior of these nanoscale structures. In order to test this assumption, preliminary TEM studies were carried out using cesium hydroxide as a staining agent. CsOH is expected to deprotonate the dicarboximide moiety, thus providing a preferential staining method for the poly(**1**) block. The turbid solution containing the micellar aggregates (in THF/water (17% v/v) solution) was deposited onto a TEM grid and allowed to dry. The grid was then immersed into a solution of CsOH (0.1 N) for 1 min, and rinsed gently in distilled water, in order to remove any excess CsOH. TEM analysis revealed significant darkening of the spherical aggregates, indicating the likely deprotonation of the imide moieties on the outer surface of the spherical particles (Figure 5).^a This surface localization of the hydrogen bonding dicarboximide moieties is potentially well suited for molecular recognition studies of this block copolymer with complementary receptors.

Conclusion

In summary, we have used living ring-opening metathesis polymerization to generate a new class of homopolymers

and block copolymers of narrow molecular weight distributions, which contain biologically relevant, and readily functionalizable dicarboximide moieties. Self-assembly of these block copolymers leads to the formation of nanoscale spherical micellar aggregates with surface localization of the dicarboximide units. Future studies will probe the bioactivity of these polymers (e.g., as antitumor agents), and their further substitution with other functional units. Work is also currently underway to assess the guest-induced response of the self-assembled polymer nanoparticles to molecules containing complementary hydrogen bonding moieties, such as adenine and adenine-containing oligonucleotides.

Acknowledgement: We thank the *Natural Science and Engineering Research Council of Canada (NSERC)*, the *Fonds pour la Formation de Chercheurs et l'Aide à la Recherche (FCAR, Quebec)*, the *Canada Foundation for Innovation (CFI)* and *McGill University* for financial support. The authors wish to acknowledge Dr. *H. Vali* for help in TEM studies.

Received: April 18, 2002

Revised: May 29, 2002

Accepted: June 7, 2002

^a The unstained particles (Figure 4) showed higher optical density in their central region, compared to their outer shell (TEM). On the other hand, the CsOH stained particles (Figure 5) showed uniform darkening, both within their center and outer shells. These two qualitative results suggest preferential staining of the CsOH on the outer surface of these particles.

- [1] P. Schwab, R. H. Grubbs, J. W. Ziller, *J. Am. Chem. Soc.* **1996**, *118*, 100.
- [2] [2a] M. R. Buchmeiser, *Chem. Rev.* **2000**, *100*, 1565; [2b] T. M. Trnka, R. H. Grubbs, *Acc. Chem. Res.* **2001**, *34*, 18.
- [3] [3a] K. H. Mortell, R. V. Weatherman, L. L. Kiessling, *J. Am. Chem. Soc.* **1996**, *118*, 2297; [3b] M. Kanai, K. H. Mortell, L. L. Kiessling, *J. Am. Chem. Soc.* **1997**, *119*, 9931; [3c] L. L. Kiessling, L. E. Strong, *Top. Organomet. Chem.* **1998**, *1*,

- 199; [3d] C. W. Cairo, J. E. Gestwicki, M. Kanai, L. L. Kiessling, *J. Am. Chem. Soc.* **2002**, *124*, 1615.
- [4] S. Meier, H. Reisinger, R. Haag, S. Mecking, R. Mülhaupt, F. Stelzer, *Chem. Commun.* **2001**, 855.
- [5] [5a] H. D. Maynard, S. Y. Okada, R. H. Grubbs, *Macromolecules* **2000**, *33*, 6239; [5b] H. D. Maynard, S. Y. Okada, R. H. Grubbs, *J. Am. Chem. Soc.* **2001**, *123*, 1275.
- [6] [6a] V. C. Gibson, E. L. Marshall, M. North, D. A. Robson, P. J. Williams, *Chem. Commun.* **1997**, 1095; [6b] R. G. Davies, V. C. Gibson, M. B. Hursthouse, M. E. Light, E. L. Marshall, M. North, D. A. Robson, I. Tompson, A. J. P. White, D. J. Williams, P. J. Williams, *J. Chem. Soc. Perkin Trans.* **2001**, *1*, 3365.
- [7] K. J. Watson, D. R. Anderson, S. T. Nguyen, *Macromolecules* **2001**, *34*, 3507.
- [8] K. J. Watson, S.-J. Park, J.-H. Im, S. T. Nguyen, C. A. Mirkin, *J. Am. Chem. Soc.* **2001**, *123*, 5592.
- [9] [9a] J. Gratt, R. E. Cohen, *Macromolecules* **1997**, *30*, 3137; [9b] A. J. Matzger, C. E. Lawrence, R. H. Grubbs, N. S. Lewis, *J. Comb. Chem.* **2000**, *2*, 301; [9c] D.-J. Liaw, C.-C. Huang, P.-L. Wu, *Polymer* **2001**, *42*, 9371; [9d] H. S. Bazzi, H. F. Sleiman, *Macromolecules* **2002**, *35*, 624.
- [10] [10a] A. Halperin, M. Tirrell, T. P. Lodge, *Adv. Polym. Sci.* **1992**, *100*, 31; [10b] L. Zhang, R. J. Barlow, A. Eisenberg, *Macromolecules* **1995**, *28*, 6055; [10c] L. Zhang, A. Eisenberg, *Science* **1995**, *268*, 1728.
- [11] G.-C. Kim, J.-G. Jeong, N.-J. Lee, C.-S. Ha, W.-J. Cho, *J. Appl. Polym. Sci.* **1997**, *64*, 2605.
- [12] A. McCluskey, C. Walkom, M. C. Bowyer, S. P. Ackland, E. Gardiner, J. A. Sakoff, *Bioorg. Med. Chem. Lett.* **2001**, *11*, 2941.
- [13] T. K. Park, J. Schroeder, J. Rebek, Jr., *J. Am. Chem. Soc.* **1991**, *113*, 5125.
- [14] Molecular recognition units incorporated in synthetic polymers: [14a] M. A. Aponte, G. B. Butler, *J. Polym. Sci.: Polym. Chem. Ed.* **1984**, *22*, 3715; [14b] R. F. M. Lange, E. W. Meijer, *Macromolecules* **1995**, *28*, 782; [14c] T. Wada, Y. Inaki, K. Takemoto, "Nucleic acid Analogs", in: *Polymeric Materials Encyclopedia*, J. C. Salamone, Ed., CRC Press, Boca Raton 1996, Vol. 6, p. 4640; [14d] F. Ilhan, T. H. Galow, M. Gray, G. Clavier, V. M. Rotello, *J. Am. Chem. Soc.* **2000**, *122*, 5895; [14e] F. Ilhan, M. Gray, V. M. Rotello, *Macromolecules* **2001**, *34*, 2597; [14f] B. L. Frankamp, O. Uzun, F. Ilhan, A. K. Boal, V. M. Rotello, *J. Am. Chem. Soc.* **2002**, *124*, 892.
- [15] Examples of interaction between nucleic acids and synthetic polymers: [15a] H. Asanuma, T. Ban, S. Gotoh, T. Hishiyama, M. Komiyama, *Macromolecules* **1998**, *31*, 371; [15b] H. Asanuma, T. Hishiyama, T. Ban, S. Gotoh, M. Komiyama, *J. Chem. Soc., Perkin Trans.* **1998**, *2*, 1915.
- [16] Polymers for DNA delivery: A. V. Kabanov, *Pharm. Sci. Technol. Today* **1999**, *2*, 365.
- [17] T. Viswanathan, J. Jethmalani, *J. Appl. Polym. Sci.* **1993**, *48*, 1289.
- [18] H. Kwart, I. Burchuk, *J. Am. Chem. Soc.* **1952**, *74*, 3094.
- [19] R. C. Clevenger, K. D. Turnbull, *Synth. Comm.* **2000**, *30*, 1379.
- [20] The absence of data points below ca. 10% monomer conversion is due to the fact that the polymerization reaction had already started prior to the first ^1H NMR acquisition (at -5°C).
- [21] Higher monomer to initiator ratios resulted in precipitation of the homopolymers from THF solution.
- [22] M. Weck, P. Schwab, R. H. Grubbs, *Macromolecules* **1996**, *29*, 1789.
- [23] C. W. Bielawski, R. H. Grubbs, *Macromolecules* **2001**, *34*, 8838.
- [24] [24a] L. E. Strong, L. L. Kiessling, *J. Am. Chem. Soc.* **1999**, *121*, 6193; [24b] J.-G. Park, C.-S. Ha, W.-J. Cho, *J. Polym. Sci.; Part A: Polym. Chem.* **1999**, *37*, 2113.
- [25] Gangadhara, C. Noel, M. Thomas, D. Reyx, *J. Polym. Sci.; Part A: Polym. Chem.* **1998**, *36*, 2531.
- [26] L. Zhang, A. Eisenberg, *J. Am. Chem. Soc.* **1996**, *118*, 3168.
- [27] [27a] L. Zhang, K. Yu, A. Eisenberg, *Science* **1996**, *272*, 1777; [27b] R. Resendes, J. A. Massey, K. Temple, L. Cao, K. N. Power-Billard, M. A. Winnik, I. Manners, *Chem. Eur. J.* **2001**, *7*, 2414.